

CO₂ Hydrogenation to Formate and Methanol as an Alternative to Photo- and Electrochemical CO₂ Reduction

Wan-Hui Wang,^{a,} Yuichiro Himeda,^{b,c,*} James T. Muckerman,^d Gerald F. Manbeck,^d
and Etsuko Fujita^{d,*}*

^a School of Petroleum and Chemical Engineering, Dalian University of Technology, Panjin
124221, China.

^b National Institute of Advanced Industrial Science and Technology, Tsukuba Central 5-1, 1-1-1
Higashi, Tsukuba, Ibaraki 305-8565, Japan.

^c JST, ACT-C, 4-1-8 Honcho, Kawaguchi, Saitama, 332-0012, Japan.

^d Chemistry Department, Brookhaven National Laboratory, Upton, NY 11973-5000, USA.

Email: Chem_wangwh@dlut.edu.cn, himeda.y@aist.go.jp, fujita@bnl.gov

Contents

1. Introduction
2. Recent developments in CO₂ hydrogenation to formate
 - 2.1. Catalysts with phosphine ligands
 - 2.2. Catalysts with pincer ligands.
 - 2.3. Catalysts with *N*-heterocyclic carbene ligands
 - 2.4. Half-sandwich catalysts with/without proton-responsive ligands
 - 2.4.1. *Electronic effects*
 - 2.4.2. *Second coordination sphere effects*
 - 2.4.3. *Mechanistic investigations*
 - 2.4.4. *pH-dependent solubility and catalyst recovery*
3. Formic Acid Dehydrogenation with Various Metal Complexes
 - 3.1. Catalysts with phosphine ligands
 - 3.1.1. *Organic solvent systems*
 - 3.1.2. *Aqueous solvent systems*
 - 3.2. Catalysts with pincer-type ligands
 - 3.3. Catalysts with bidentate *C,N-/N,N*-ligands
 - 3.4. Half-sandwich catalysts with/without proton-responsive ligands
 - 3.4.1. *Electronic effects*
 - 3.4.2. *Pendent-base effect changing RDS of formic acid dehydrogenation*
 - 3.4.3. *Solution pH changing RDS of formic acid dehydrogenation*
 - 3.5. Non-precious metals

4. Interconversion of CO₂ and Formic acid
 - 4.1. Background
 - 4.2. Reversible H₂ storage controlled by temperature or pressure
 - 4.3. Reversible H₂ storage controlled by pH
5. Recent developments in CO₂ hydrogenation to methanol
 - 5.1. Hydrogenation of formate, carbonate, carbamate, and urea derivatives to MeOH
 - 5.2. Catalytic disproportionation of formic acid to MeOH
 - 5.3. Cascade catalysis of CO₂ to MeOH
 - 5.4. Direct hydrogenation of CO₂ to MeOH
6. Summary and Future Outlook

Abbreviations

acac	acetylacetonate
BIH	1,3-dimethyl-2-phenyl-2,3-dihydro-1 <i>H</i> -benzo[d]imidazole
Bmim	1-butyl-3-methylimidazol-2-ylidene
Bpm	2,2'-bipyrimidine
Bpy	2,2'-bipyridine
Cod	1,5-cyclooctadiene
Cyclam	1,4,8,11-tetraazacyclotetradecane
DBU	1,8-diazabicyclo[5,4,0]undec-7-ene
dcpm	1,1-bis(dicyclohexylphosphino)methane

DHPT	4,7-dihydroxy-1,10-phenanthroline
diphos	Ph ₂ PCH ₂ CH ₂ PPh ₂
DMOA	dimethyloctylamine
dmpe	1,2-bis(dimethylphosphino)ethane
dppb	1,2-bis(diphenylphosphino)butane
dppe	1,2-bis(diphenylphosphino)ethane
dppm	1,1-bis(diphenylphosphino)methane
EMIM	1-ethyl-3-methylimidazolium
FA	Formic acid
HMD	5,7,7,12,14,14-hexamethyl-1,4,8,11-tetraazacyclotetradeca-4,11-diene
H4MPT	tetrahydromethanopterin
HER	hydrogen evolution reaction
IL	ionic liquid
KIE	kinetic isotope effect
methallyl	(CH ₂ C(CH ₃)CH ₂ -)
MSA	methanesulfonic acid
N-N'	pyridinylazolato
NADH	reduced nicotinamide adenine dinucleotide
NBD	norbornadiene
nDHBP	n,n'-dihydroxy-2,2'-bipyridine
NHC	<i>N</i> -heterocyclic carbene
NP3	tris[2-(diphenylphosphino)ethyl]amine
NTf ₂	bis(trifluoromethylsulfonyl)imide

PC	propylene carbonate
PEI	polyethyleneimine
Phen	1,10-phenanthroline
^{Ph} I ₂ P	phenyl-substituted bis(imino)pyridine
PP ₃	P(CH ₂ CH ₂ PPh ₂) ₃
PTA	1,3,5-triaza-7-phosphaadamantane
pz	1-phenylpyrazole
RDS	rate-determining step
^R PN ^H P	HN{CH ₂ CH ₂ (PR ₂) ₂ } ₂ ; R = <i>i</i> Pr or Cy
SDS	sodium dodecylsulfate
TaON	N-doped Ta ₂ O ₅ semiconductor
THBPM	4,4',6,6'-tetrahydroxy-2,2'-bipyrimidine
TMM	trimethylenemethane
TOF	turnover frequency
TON	turnover number
tos	<i>p</i> -toluene sulfonate
tppms	3-sulfonatophenyldiphenylphosphine
tppts	tris(3-sulfonatophenyl)phosphine
tpy	2,2':6',2''-terpyridine
triphos	1,1,1-tris-(diphenylphosphinomethyl)ethane

1. Introduction

Carbon dioxide is one of the end products of combustion, and is not a benign component of the atmosphere. The concentration of CO₂ in the atmosphere has reached unprecedented levels and continues to increase owing to an escalating rate of fossil fuel combustion, causing concern about climate change and rising sea levels.¹⁻⁶ In view of the inevitable depletion of fossil fuels, a possible solution to this problem is the recycling of carbon dioxide, possibly captured at its point of generation, to fuels.^{5,7-12} Researchers in this field are using solar energy for CO₂ activation and utilization in several ways: (i) so-called artificial photosynthesis using photo-induced electrons; (ii) bulk electrolysis of a CO₂ saturated solution using electricity produced by photovoltaics; (iii) CO₂ hydrogenation using solar-produced H₂; and (iv) the thermochemical reaction of metal oxides at extremely high temperature reached by solar collectors. Since the thermodynamics of CO₂ at high temperature (> 1000 °C) are quite different from those near room temperature, only chemistry below 200 °C is discussed in this review.

The one-electron reduction of CO₂ to CO₂^{•-} (eq 1) has the standard potential of -1.90 V vs. NHE,¹³ and is highly unfavorable owing in part to the geometric rearrangement from linear to bent. The potentials for proton assisted multi-electron reductions at pH 7 (eqs 2 – 4) are substantially lower;¹⁴⁻¹⁶ however, catalysts are necessary to mediate the multi-proton, multi-electron reductions when we use methods (i) to (iii) listed above.



Researchers in this field have investigated photochemical and electrochemical CO₂ reduction to CO or formate, even to methanol, using transition metal electrodes, metal complexes, semiconductors and also organic molecules, and the details of these achievements can be found in many reviews recently published.¹⁴⁻³¹ While recent progress in this field is quite remarkable in photochemical CO₂ reduction using semiconductors or heterogeneous systems, most experiments have not been confirmed using labeled CO₂ (i.e., ¹³CO₂) and H₂O (i.e., H₂¹⁸O and/or D₂O). When quantum yields of product formation are relatively low, carbon sources in the photochemical reaction must be carefully investigated. Since CO₂ is more stable than any other carbon-containing contaminants, these systems may be decomposing carbon-containing impurities attached to the surfaces of the semiconductors leading to an overestimation of the real catalytic activity. As a case study, Mul and coworkers investigated ¹³CO₂ photoconversion over Cu(I)TiO₂ and found significant amounts of ¹²CO product implicating surface residues as the source of CO.³² The photo-Kolbe reaction (CH₃CO₂H → CH₄ + CO₂) is catalyzed by TiO₂,^{33,34} and is a significant source of CH₄ during photolysis of TiO₂ under CO₂ due to the approximately 1 nano-mol/mg content of acetic acid adsorbed on TiO₂ as reported by Ishitani.^{32,35} Complete removal of acetic acid and therefore suppression of CH₄ production required calcination at 350 °C and thorough washing with deionized water.

The homogeneous photochemical reduction of CO₂ is inherently difficult due to the multi-electron requirement of reduction limited by single-photon, single-electron-transfer reactions. A classical approach to photocatalysis employs a catalyst, photosensitizer, and sacrificial reductant with a low oxidation potential as a substitute for the oxidation of water which must ultimately complement the production of solar fuels. For example, CO is produced by irradiation of [Ru(bpy)₃]²⁺ (bpy = 2,2'-bipyridine), [Ni(cyclam)]²⁺ (cyclam = 1,4,8,11-

tetraazacyclotetradecane) and ascorbic acid in pH 4 aqueous solution.³⁶ In most cases, the reaction is driven by reductive quenching of the photosensitizer excited state by the electron donor which is present in large excess (upwards of 25-50% solvent by volume). Transfer of an electron from the reduced photosensitizer to the catalyst precursor initiates catalysis. It follows logically that a competent sensitizer/catalyst pair requires stability in a variety of oxidation states and appropriately aligned redox potentials for favorable electron transfer between the pair. Further electron transfer steps are inherently difficult to analyze because they likely involve reactive intermediates, and any such system requires careful control experiments since the sensitizer itself may decompose and catalyze CO₂ reduction.³⁷ Because multi-electron reactions are needed, researchers have developed creative methods for accumulation of multiple photo-induced redox equivalents.³⁸ One approach is to use catalysts that can change the formal oxidation state by 2 such as M(I) to M(III). The detection of key intermediates in photochemical CO₂ reduction is rather difficult. However, using transient UV-vis spectroscopy, [Co^{III}(HMD)(CO₂²⁻)S]⁺ (HMD = 5,7,7,12,14,14-hexamethyl-1,4,8,11-tetraazacyclotetradeca-4,11-diene, S = solvent) has been observed in photochemical CO₂ reduction in CH₃CN/MeOH (v/v = 4/1) with *p*-terphenyl as a photosensitizer and trimethylamine as an electron donor.³⁹ It should be noted that a XANES study clearly indicates that the photo-reduced Co(I) species donates two electrons to the bound CO₂ to facilitate 2-electron reduction of CO₂ to CO.⁴⁰ The second approach to the multi-electron problem is to choose catalysts that undergo disproportionation after 1e⁻ reduction while a third approach employs catalysts, such as [Re(bpy)(CO)₃Cl], that react in a 2:1 stoichiometry with CO₂ after a single reduction.⁴¹

The multicomponent photochemical reduction of CO₂ is also limited by the requirement of bimolecular electron transfer which is diffusion controlled and concentration dependent. Recent

efforts have focused on multinuclear systems in which the sensitizer and catalyst are covalently linked through a bridging ligand.^{19,22} Ideally, the supramolecules are designed to minimize the interaction of the sensitizer and catalyst (which can lead to an inactive system) while promoting vectorial intramolecular electron transfer. Supramolecular Ru-Re complexes with a Ru trisdiimine moiety linked to a Re(I)(diimine)(CO)₂ catalyst are remarkable examples of this approach, and current results have shown that by using the more powerful electron donor 1,3-dimethyl-2-phenyl-2,3-dihydro-1*H*-benzo[d]imidazole (BIH) instead of the more common 1-benzyl-1,4-dihyronicotinamide the efficiency, durability and reaction rate are improved significantly ($\Phi_{\text{CO}} = 0.45$, $\text{TON}_{\text{CO}} = 3029$, and $\text{TOF}_{\text{CO}} = 35.5 \text{ min}^{-1}$).⁴² However, we are still far from a practical system that overcomes numerous limitations including: (i) low turnover numbers and low turnover frequencies with the more frequently used electron donors such as triethanolamine or trimethylamine; (ii) product selectivity (i.e., CO, formate, H₂, and other minor products such as methanol and hydrocarbons); (iii) use of precious metal catalysts; (iv) use of organic solvents and sacrificial reagents; (v) controlling the pH; and (vi) the requirement of coupling oxidative and reductive half-reactions. Furthermore, it is difficult to compare photocatalytic results from different laboratories because the efficiencies are dependent on various factors such as light intensity, light wavelength, catalyst concentration, electron donors, solvents, proton donors, etc. that are often not the same.¹⁶

It should be noted that the photoelectrochemical reduction of CO₂ with 70% selectivity for formate using the so-called Z-scheme was successfully demonstrated by Sato et al.⁴³⁻⁴⁵ The system was constructed using *p*-type InP modified with a combination of electropolymerized and covalently bound ruthenium catalysts as the photo-cathode. Anatase TiO₂ was the photo-anode, and the estimated -0.5 V difference between the conduction band of TiO₂ and the valance band

of InP was sufficient to drive electron transfer between the two electrodes without application of an external bias. Under AM1.5 solar simulation, the turnover number for formic acid was 17 after 24 h, and the conversion efficiency determined as the energy content in formic acid relative to the integrated solar simulation was 0.03-0.04%. While yet inefficient, this is a significant achievement for combining the reductive and oxidative half-reactions to remove a sacrificial reagent in aqueous solution while realizing photo-electrochemical CO₂ reduction without the often unavoidable external potential. They confirmed that water and CO₂ are the proton donor and carbon source, respectively, by labeling experiments (i.e., formation of ¹⁸O₂, H¹³CO₂⁻ and DCO₂⁻). In the mechanistic study, the electron transfer rate from N-doped Ta₂O₅ semiconductor (i.e., TaON) to the ruthenium catalyst was measured on the ultrafast timescale of 12 ps which was faster than the internal trapping of charge carriers within the semiconductor (24 ps).⁴⁵

Ishitani's group constructed an artificial Z-scheme using Ag/TaON with a Ru dinuclear complex to couple the two-electron reduction of CO₂ to formate to the two-electron oxidation of methanol to formaldehyde in a single vessel without compartmentalizing oxidative and reductive half reactions (Figure 1).⁴⁶ This photosystem was designed such that photoexcitation of the semiconductor and the [Ru(bpy)₃]²⁺ moiety (Ru_{photo}) of the dinuclear complex was required. The best turnover number for formate after 9 h was 41, and isotope labeling experiments verified ¹³CH₃OH and ¹³CO₂ as the sources of H¹³COH and H¹³COOH, respectively. Consideration of redox potentials of the TaON conduction band, the Ru_{photo} (excited and ground states), and the Ru catalyst (Ru_{cat}) led the authors to conclude that electron transfer from TaON to Ru_{photo} could occur in the Ru_{photo} excited state or one-electron oxidized state but not to the ground state. The Ru_{cat} reduction potential of -1.6 V implies electron transfer from the reduced Ru_{photo} (-1.85V) is possible, but oxidative quenching of the excited state (-1.3V) is unfavorable.

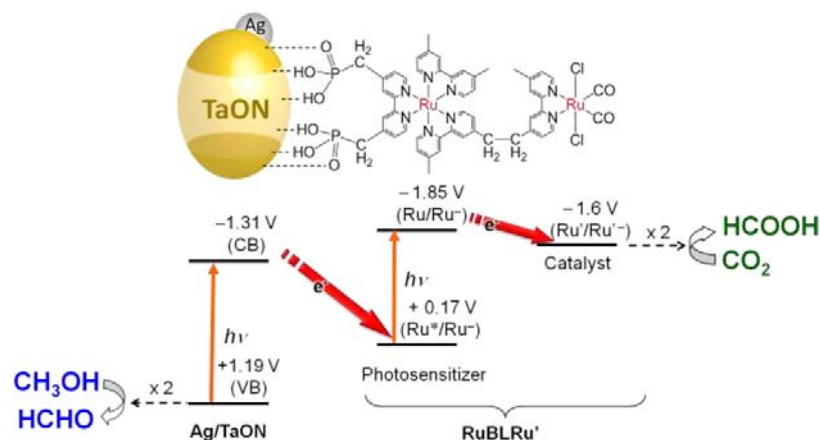


Figure 1. Z-Scheme for photocatalytic CO₂ reduction coupled to methanol oxidation. Reference 46. Copyright 2013 American Chemical Society.

The electrochemical reduction of CO₂ overcomes the problem of photo-induced multielectron transfer reactions since the electrode source is simply a cathode upon which the applied potential can be adjusted. Recently, dramatic improvements in efficiencies and overpotentials (the difference between the applied potential of the catalyst and the thermodynamic reduction potential of CO₂ i.e., eqs. 1-4) have been demonstrated by electrode surface engineering,⁴⁷⁻⁴⁹ the use of electrocatalysts that have second-coordination-sphere bases,^{17,21,50,51} and the use of ionic liquids that might directly interact with CO₂.⁵²⁻⁵⁴ Mechanistic and kinetic investigations of electrochemical CO₂ reduction using molecular catalysts and organic proton sources, mainly in CH₃CN, point toward formation of metallocarboxylate species, followed by a protonation to form a metallocarboxylic acid (M = Co, Ni, Ru, Re, etc.) as precursors for CO production while metal formate complexes generated via insertion of CO₂ into a metal hydride bond are suspected precursors to formate. However, the detection of these intermediates is rather difficult.^{39,55} Reports on electrochemical CO₂ reduction with molecular catalysts in water are rare since reduction of protons competes with CO₂ reduction and carbon dioxide solubility is much lower in water compared to organic media. Exceptions are the well-

known Ni-cyclam and related catalysts.⁵⁶⁻⁵⁸ The active catalyst is an adsorbed Ni(I) species on a mercury pool electrode. Product selectivity is largely a consequence of the pK_a of the adsorbed Ni(III)(H) species being < 2 , thereby preventing H_2 formation via protonation of the adsorbed Ni(I) species under experimental conditions (pH 5).^{21,58}

Hydrogen is a clean fuel with a high gravimetric energy density and potentially zero contribution to the global carbon cycle. Ironically, the reforming of natural gas (primarily methane) currently used to produce hydrogen on an industrial scale requires harsh temperatures and emits as much CO_2 into the atmosphere as burning the natural gas.⁵⁹ If hydrogen is to be an important alternative fuel, its source must be water. Ideally, this could be accomplished by the electrolysis of water using solar energy as the power source (i.e., photovoltaic electricity) or direct solar water splitting (i.e., artificial photosynthesis). The details of the achievements on electrochemical H_2 production using both heterogeneous and homogeneous catalysts can be found in recent articles and reviews.⁶⁰⁻⁹⁰ For example, our group developed biomass-derived electrocatalysts (Mo_xSoy , $x = 0.1-1.0$ with x being the weight ratio of the Mo precursor to soybean powder) from soybeans and $(NH_4)_6Mo_7O_{24}\cdot 4H_2O$ that is a compound of an earth-abundant metal, molybdenum, with an environmentally benign, straightforward synthesis.^{71,91} The catalyst Mo_1Soy , composed of a catalytic β - Mo_2C phase and an acid-proof γ - Mo_2N phase, drives the hydrogen evolution reaction (HER) with remarkably low overpotentials, and is highly durable in a corrosive acidic solution over a period exceeding 500 hours. When supported on graphene sheets, the Mo_1Soy catalyst exhibits very fast charge transfer kinetics, and its performance almost reaches that of noble-metal catalysts such as Pt for hydrogen production.

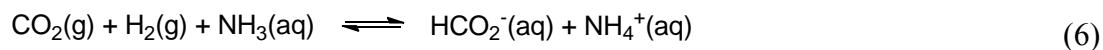
Despite the potential for production of solar-generated hydrogen, the problems of storage and transport remain. Here we present another approach to solar fuels generation based on CO_2

hydrogenation using catalysts for recycling CO₂ combined with the use of solar-generated H₂. In our review, we will focus our presentation on the use of molecular catalysts in recent developments in: (1) CO₂ hydrogenation to formate; (2) formic acid (FA) dehydrogenation; (3) interconversion of CO₂ and formic acid; and (4) CO₂ hydrogenation to methanol. While formic acid is not a perfect hydrogen storage medium owing to its relatively small hydrogen content (4.4 wt%), it is currently still one of the best among liquid storage and transport media for H₂.⁹² Also, formic acid can be used in a formic acid fuel cell,⁹³ or as a substrate for further reduction to a carbon-based fuel. Compared to FA, methanol has a higher hydrogen density (12.6 wt%) as a hydrogen storage material. Although currently reversible hydrogen storage using methanol derived from CO₂ is a great challenge,⁹⁴⁻⁹⁶ methanol is a viable fuel which can be used directly in fuel cells, burned alone, or mixed with gasoline. Research pertaining to CO₂ hydrogenation to methanol is of fundamental importance to the development of a methanol economy.⁸

The hydrogenation of CO₂ primarily produces formic acid, formaldehyde, methanol, and methane which are all entropically disfavored compared to CO₂ and H₂ (eqs. 5-7). Therefore, selection of a proper solvent is important because it affects the entropy difference of reactants and product via solvation. Although hydrogenation of CO₂ to formic acid is endergonic in the gas phase (eq. 5, $\Delta G^{\circ}_{298} = +32.8 \text{ kJ mol}^{-1}$), the reaction is exergonic in the aqueous phase ($\Delta G^{\circ}_{298} = -4.0 \text{ kJ mol}^{-1}$).⁹⁷ Another strategy is the use of additives, such as a base (eq. 6) to improve the enthalpy of CO₂ hydrogenation. For the reaction in water, hydroxides, bicarbonates, and carbonates are commonly used. In organic solvent, amines such as inexpensive Et₃N, amidine, guanidine, or DBU (1,8-diazabicyclo[5,4,0]undec-7-ene) are utilized. Reaction rates are often correlated to the strength of the base. Strongly basic Verkade's base (2,8,9-triisopropyl-2,5,8,9-tetraaza-1-phoshabicyclo[3,3,3]undecane) is highly effective although not inexpensive.



$$\Delta G^\circ = 32.8 \text{ kJ mol}^{-1} \quad \Delta H^\circ = -31.5 \text{ kJ mol}^{-1} \quad \Delta S^\circ = -216 \text{ J mol}^{-1} \text{ K}^{-1}$$

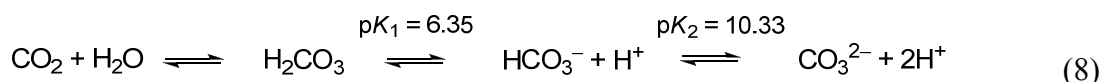


$$\Delta G^\circ = -9.5 \text{ kJ mol}^{-1} \quad \Delta H^\circ = -84.3 \text{ kJ mol}^{-1} \quad \Delta S^\circ = -250 \text{ J mol}^{-1} \text{ K}^{-1}$$



$$\Delta G^\circ = -9.5 \text{ kJ mol}^{-1} \quad \Delta H^\circ = -131 \text{ kJ mol}^{-1} \quad \Delta S^\circ = -409 \text{ J mol}^{-1} \text{ K}^{-1}$$

Furthermore, CO₂ hydrogenation in water is complicated owing to the acid/base equilibria of CO₂ in aqueous solutions as shown in eq. 8.^{98,99} Hydrogenation of bicarbonate into formate is exergonic and favorable in water (eq. 9) as thermochemical calculations predicted.¹⁰⁰ The real substrate of the hydrogenation should be carefully specified because the CO₂/bicarbonate/carbonate equilibrium is influenced by many factors such as the temperature, solution pH, and CO₂ pressure etc. Despite the term “hydrogenation of CO₂” being frequently used in this review and elsewhere, such reactions in basic aqueous solutions, may involve HCO₃⁻ or CO₃²⁻ as substrates. In some cases “hydrogenation of CO₂” can be carried out in a HCO₃⁻ or CO₃²⁻ solution in the absence of added CO₂, but such reactions are not always successful and are often used as control experiments to prove CO₂ as a reaction substrate. Finally, we note that the “hydrogenation of CO₂” is, in fact, the thermal reduction of CO₂ by H₂, and differs from the electrochemical (or photo-electrochemical) reduction of CO₂ versus the normal hydrogen electrode only by combining the two half-reactions into an overall net reaction.





While several reviews have been published previously on CO₂ hydrogenation to formate,^{97,101,102} reversible interconversion of CO₂ and formic acid,^{103,104} and CO₂ hydrogenation to methanol¹⁰⁵⁻¹⁰⁷ using homogeneous molecular catalysts, here we describe the remarkable recent progress toward efficient and selective CO₂ hydrogenation using molecular catalysts with and without bio-inspired ligands. We focus on the rational design of catalysts, and aim at a fundamental understanding of processes that might lead to a practical scheme for recycling CO₂ when combined with the use of solar-generated H₂ as an alternative for direct conversion of CO₂ by photo-induced electrons and/or protons. We also describe the indispensable interconversion of formic acid and CO₂ in water with the goal of using formic acid as an H₂ storage medium or in formic acid fuel cells. We hope to demonstrate new design principles that greatly improve the catalytic activity.

2. Recent developments in CO₂ hydrogenation to formate

Considering that carbon dioxide is an economical, safe, abundant C1 source,¹⁰⁸ the hydrogenation of CO₂ to formic acid is a promising way to utilize CO₂ that not only contributes to the mitigation of climate change caused by the increase in CO₂ emissions, but also provides a sustainable method for making essential organic chemicals or materials. Homogeneous hydrogenation of CO₂ to formate or formic acid has attracted increasing attention and a number of reviews have summarized significant progress in the last two decades.^{97,101,108-111} In this section we introduce the development of CO₂ hydrogenation to formate, and highlight the most efficient catalytic systems (Table 1).

Table 1. Hydrogenation of CO₂ to formic acid/formate.^{a,b}

Catalyst precursor	Solvent	Additive	P(H ₂ /CO ₂) / MPa	T / °C	Reac. time / h	TON	TOF ^c / h ⁻¹	Ref.
Phosphine Ligand								
RuH ₂ (PPh ₃) ₄	C ₆ H ₆	Et ₃ N/H ₂ O	2.5/2.5	rt	20	87	4	112
Ni(dppe) ₂	C ₆ H ₆	Et ₃ N/H ₂ O	2.5/2.5	rt	20	7	0.35	112
Pd(dppe) ₂	C ₆ H ₆	Et ₃ N/H ₂ O	2.5/2.5	rt	20	12	0.6	112
RhCl(PPh ₃) ₃	DMSO	Et ₃ N	2/4	25	20	2500	125	113
[Rh(cod)Cl] ₂ /dppb	DMSO	Et ₃ N	2/2	rt	22	1150	30-47	114
RhCl(tppts) ₃	H ₂ O	NHMe ₂	2/2	81	0.5	-	7300	110
RhCl(tppts) ₃	H ₂ O	NHMe ₂	2/2	rt	12	3440	290	115,110
[RhCl(tppms) ₃]/tppms	H ₂ O	HCO ₂ Na	1/1	50	20	120	-	116
RuH ₂ (PMe ₃) ₄	scCO ₂	Et ₃ N	8.5/12	50	-	3700	1400	117
RuCl ₂ (PMe ₃) ₄	scCO ₂	Et ₃ N	8.5/12	50	-	7200	1040	117
RuCl(OAc)(PMe ₃) ₄	scCO ₂	Et ₃ N / C ₆ F ₅ OH	7/12	50	0.33	32,000	95,000	118
[RuCl ₂ (tppms) ₂] ₂	H ₂ O	NaHCO ₃	6/3.5	80	0.03	-	9600	119
[RuCl ₂ (tppms) ₂] ₂	H ₂ O	NaHCO ₃	1/0	50	6	180	50	119
RuCl ₂ (PTA) ₄	H ₂ O	NaHCO ₃	6/0	80	-	-	345	120
[RuCl ₂ (C ₆ H ₆)]/dppm	H ₂ O	NaHCO ₃	5/0	130	2	1600	800	121
[RuCl ₂ (C ₆ H ₆)]/dppm	H ₂ O	NaHCO ₃	5/3.5	70	2	2520	1260	121
Fe(BF ₄) ₂ /PP ₃	MeOH	NaHCO ₃	6/0	80	20	610	30	122
Co(BF ₄) ₂ /PP ₃	MeOH	NaHCO ₃	6/0	120	20	3900	200	123
IrH ₃ (P1)	H ₂ O/THF	KOH	4/4	200	2	300,000	150,000	124,125
IrH ₃ (P1)	H ₂ O/THF	KOH	4/4	120	48	3,500,000	73,000	124,125
FeH ₂ (CO)(P3)	H ₂ O/THF	NaOH	0.67/0.33	80	5	790	156	126
IrH ₃ (P2)	H ₂ O	KOH	2.8/2.8	185	24	348,000	14,500	127
IrH ₃ (P2)	H ₂ O	KOH	2.8/2.8	125	24	3820	160	127
Ru(PNNP)(CH ₃ CN)(Cl)	toluene	DBU	70/70	100	4	1880		128
Co(dmpe) ₂ H	THF	Verkade's base	0.05/0.05	21	<1	2000	3400	129

[Rh(PN ^{Me} P) ₂] ⁺	THF	Verkade's base	20/20	21	-	280	920	130
RuH(Cl)(CO)(P3)	DMF	DBU	2/2	70	2	38,600	-	131
RuH(Cl)(CO)(P3)	DMF	DBU	3/1	120			1,100,000	132
Ru(P6)CO(H)	diglyme	K ₂ CO ₃	3/1	200	48	23,000	2200	133
RuCl ₂ (PMe ₃) ₄	scCO ₂	DBU/ C ₆ F ₅ OH	7/10	100	4	7600	1900	134
(N-N')RuCl(PMe ₃) ₃	scCO ₂	DBU/ C ₆ F ₅ OH	7/10	100	4	4800	1200	134
[Rh(cod)(methallyl) ₂]/ PBu ₄ tppms	scCO ₂ / EMIM NTf ₂	Et ₃ N	5/5	50	20	310	630	135
[Rh(cod)(methallyl) ₂]/ PBu ₄ tppms	scCO ₂ / EMIM NTf ₂	Et ₃ N /EMIMCl	5/5	50	20	545	1090	135
[Rh(cod)(methallyl) ₂]/ PBu ₄ tppms	scCO ₂ / EMIM HCO ₂ (flow system)		5/5	50	20	1970	>295	135
[RuCl ₂ (P(OMe) ₃) ₄]	scCO ₂	DBU/ C ₆ F ₅ OH	7/10	100	4	6630	1660	136
RuCl ₂ (PTA) ₄	DMSO	-	5/5	60	-	750		137
Nitrogen Ligand								
K[RuCl(EDTA-H)]	H ₂ O	-	1.7/8.2	40	0.5	-	3750	138
[Ru(6,6'-Cl ₂ bpy) ₂ - (OH ₂) ₂](CF ₃ SO ₃) ₂	EtOH	Et ₃ N	3/3	150	8	5000	625	139
[Cp*Ir(4DHBP)Cl] ⁺	H ₂ O	KOH	3/3	120	57	190,000	(42,000)	140
[Cp*Ir(4DHBP)Cl] ⁺	H ₂ O	KOH	0.5/0.5	80	30	11,000	(5100)	141
[Cp*Ir(4DHBP)Cl] ⁺	H ₂ O	NaHCO ₃	0.05/0.05	25	24	92	(7)	142
[Cp*Ir(6DHBP)(OH ₂) ₂] ²⁺	H ₂ O	KHCO ₃	0.5/0.5	120	8	12,500	(25,200)	143
[Cp*Ir(6DHBP)(OH ₂) ₂] ²⁺	H ₂ O	NaHCO ₃	0.5/0.5	80	9	9020	(8050)	143
[Cp*Ir(6DHBP)(OH ₂) ₂] ²⁺	H ₂ O	NaHCO ₃	0.05/0.05	25	33	330	(27)	143
[Cp*Ir(3DHBP)(OH ₂) ₂] ²⁺	H ₂ O	KHCO ₃	0.5/0.5	50	1	0.30	0.30	144
[Cp*Ir(5DHBP)(OH ₂) ₂] ²⁺	H ₂ O	KHCO ₃	0.5/0.5	50	1	1.1	1.1	144
[Cp*Ir(DHPT)Cl] ⁺	H ₂ O	KOH	3/3	120	48	222,000	(33,000)	140
[Cp*Ir(DHPT)Cl] ⁺	H ₂ O	K ₂ CO ₃	0.05/0.05	30	30	80	(3.5)	140
[(Cp*IrCl) ₂ (THBPM)] ²⁺	H ₂ O	KHCO ₃	0.05/0.05	25	336	7200	(65)	142
[(Cp*IrCl) ₂ (THBPM)] ²⁺	H ₂ O	KHCO ₃	2/2	50	8	153,000	(15,700)	142

$[(Cp^*IrCl)_2(THBPM)]^{2+}$	H ₂ O	KHCO ₃	2.5/2.5	80	2	79,000	(53,800)	142
$[Cp^*Ir(N1)(OH_2)]^+$	H ₂ O	K ₂ CO ₃	0.05/0.05	30	15	100	6.8	145
$[Cp^*Ir(N2)(OH_2)]^{2+}$	H ₂ O	KHCO ₃	1.5/1.5	80	8	34,000	(33,300)	146
$[Cp^*Ir(N2)(OH_2)]^{2+}$	H ₂ O	KHCO ₃	0.05/0.05	25	24	190	65	146
$[Cp^*Ir(N2)(OH_2)]^{2+}$	H ₂ O	NaHCO ₃	0.5/0.5	50	24	28,000	(3060)	146
$[Cp^*Ir(N8)(OH_2)]^{2+}$	H ₂ O	KHCO ₃	0.5/0.5	50	1	388	388	147
$[Cp^*Ir(N9)(OH_2)]^{2+}$	H ₂ O	KHCO ₃	0.5/0.5	50	1	440	440	147
$[Cp^*Ir(N10)(OH_2)]^{2+}$	H ₂ O	KHCO ₃	0.5/0.5	50	1	637	637	147
Carbon Ligand								
$IrI_2(AcO)(bis-NHC)$	H ₂ O	KOH	3/3	200	75	190,000	2500	148

^a Insignificant digits are rounded. ^b Abbreviations are the following: diphos = Ph₂PCH₂CH₂PPh₂, cod = 1,5-cyclooctadiene, dppb = Ph₂P(CH₂)₄PPh₂, tppts = tris(3-sulfonatophenyl)phosphine, tppts = 3-sulfonatophenyldiphenylphosphine, PP₃ = P(CH₂CH₂PPh₂)₃, PTA = 1,3,5-triaza-7-phosphaadamantane, dppe = 1,2-bis(diphenylphosphino)ethane, dppm = 1,1-bis(diphenylphosphino)methane, dmpe = 1,2-bis(dimethylphosphino)ethane, N-N' = pyridinylazolato, methallyl = CH₂C(CH₃)CH₂-. See Chart 2 for P1-P6. See Chart 4 for nDHBP (n = 3,4,5,6), DHPT, THBPM, N1-2, and N8-10. ^c The data in the parenthesis are initial TOFs.

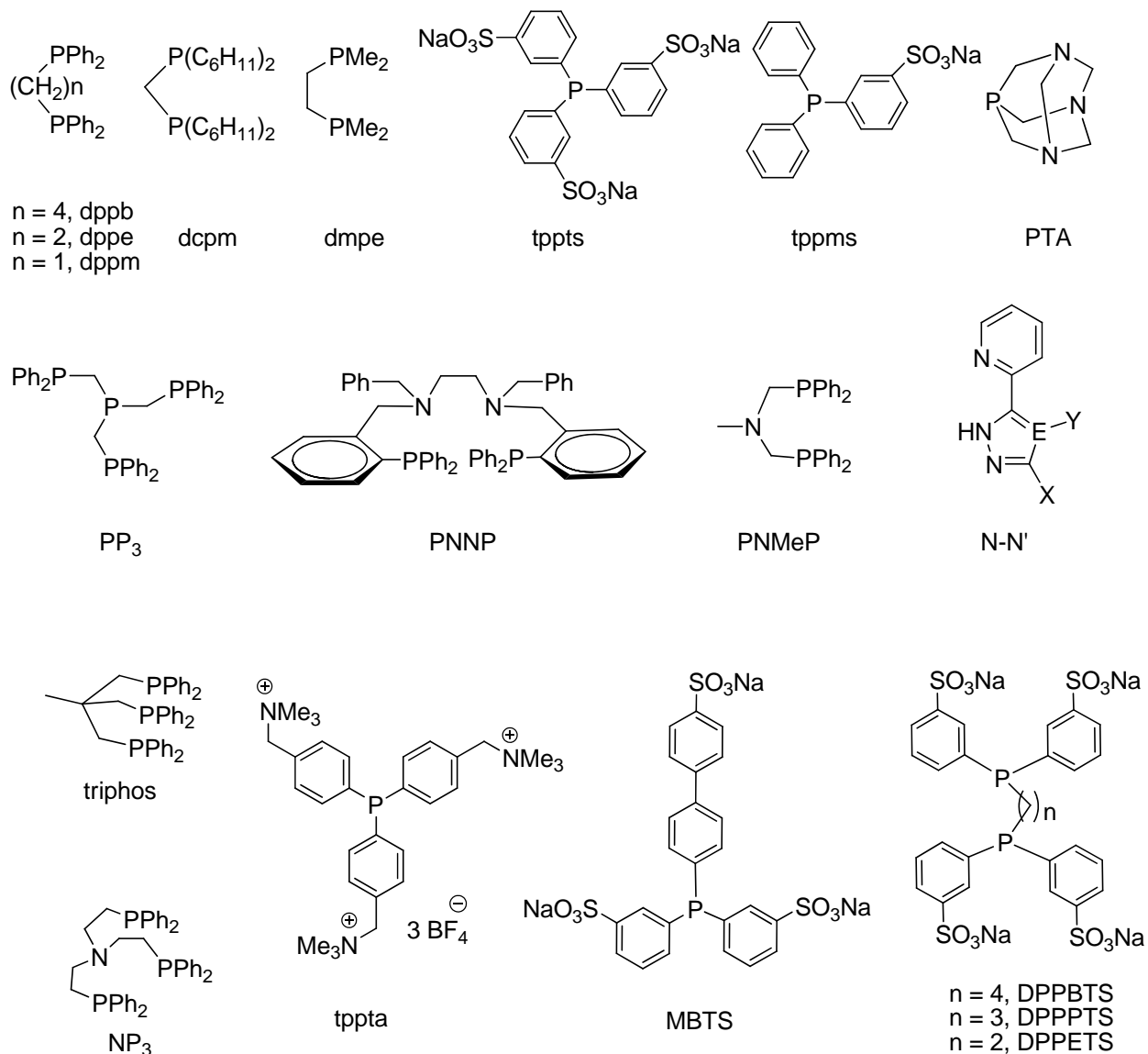
2.1. Catalysts with phosphine ligands

The pioneering work by Inoue et al. in 1976 using triphenylphosphine (PPh₃) complexes of Ru, Rh, Ir, etc. laid the foundation for the previously uncharted homogeneous catalytic hydrogenation of CO₂ to formic acid.¹¹² They carried out the reaction using a mixture of 2.5 MPa CO₂ and 2.5 MPa H₂ in benzene containing a catalyst, a small amount of water and a base at room temperature. Following on that research, the class of hydrogenation catalysts was extended to incorporate a variety of transition metals such as Pd, Ni, etc. with diphos (Ph₂PCH₂CH₂PPh₂) ligands. The nature of the solvent can also significantly affect the catalytic performance by stabilizing the catalytic intermediate or by exerting an influence on the entropy difference between reactants and product via solvation. Ezhova et al. demonstrated that the hydrogenation reaction proceeded with higher rates in polar solvents (e.g., DMSO and MeOH) with Wilkinson's complex.¹¹³ Moreover, Noyori and Jessop et al. carried out hydrogenation of CO₂ to formate in Et₃N and MeOH dissolved in scCO₂, in which hydrogen is highly miscible, with

$\text{RuH}_2(\text{PMe}_3)_4$ or $\text{RuCl}_2(\text{PMe}_3)_4$ as a catalyst to obtain high initial rates of 1400 h^{-1} or 1040 h^{-1} , respectively, at $50 \text{ }^\circ\text{C}$.¹¹⁷ Later Jessop et al. developed a remarkable catalytic system with $\text{RuCl}(\text{OAc})(\text{PMe}_3)_4$ (TOF up to $95,000 \text{ h}^{-1}$) by testing a variety of amines and alcohols in scCO_2 .¹¹⁸ Supercritical CO_2 could act as both reactant and solvent, and led to better mass transport and heat transfer properties as well as high solubility of H_2 .¹¹⁸ The study also illuminated an accelerating effect on the rate of the hydrogenation reaction by utilizing appropriate amine and alcohol adducts.^{118,149} While Lewis bases are required for formate generation by CO_2 hydrogenation, the role of alcohol is not well known. Alcohol may not generate carbonic acids or protonated amines, but it could be involved as a proton donor and hydrogen bond donor.¹¹⁸

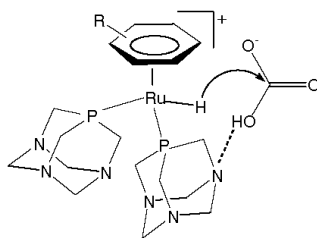
Initially, phosphine complexes were widely used in organic solvents for CO_2 hydrogenation. Nevertheless, the addition of a small amount of water is favorable for catalytic capability in rhodium catalysed hydrogenation of CO_2 in THF.¹⁵⁰ A detailed mechanistic investigation by Tsai and Nicholas revealed that a precatalyst $[\text{Rh}(\text{NBD})(\text{PMe}_2\text{Ph})_3]\text{BF}_4$ (NBD = norbornadiene) converts to $[\text{H}_2\text{Rh}(\text{PMe}_2\text{Ph})_3(\text{OH}_2)]\text{BF}_4$ by the addition of H_2 in wet THF (4% H_2O), and produces formate more than twice as fast than in dry THF. They speculated that the transition state for CO_2 insertion could be stabilized by improved electrophilicity of carbon caused by the formation of a hydrogen-bond between the bound H_2O molecule and an oxygen atom of CO_2 . This was an auspicious result because water is abundant, inexpensive, and environmentally friendly, and, as mentioned above, hydrogenation of CO_2 in water is considerably favored thermodynamically compared to the reaction in the gas phase. In this section, we briefly introduce the development of CO_2 hydrogenation using phosphine ligands with an emphasis on the most recent studies involving water.^{101,111,151}

Chart 1. Phosphine containing ligands and N-N' ligands (E = C, N; X = H, CH₃, C₂H₅, C₆H₅, C₆H₄OCH₃; Y = H, Br, NO₂).



In 1993, Leitner et al. first reported water-soluble rhodium-phosphine complexes that can catalyze the hydrogenation of CO₂ to formic acid in water-amine mixtures. Among the catalysts examined, RhCl(tppts)₃ (tppts: tris(3-sulfonatophenyl)phosphine) exhibited the high TON of

3440 at room temperature and 4 MPa H₂/CO₂.¹¹⁵ Joó et al. investigated a series of rhodium and ruthenium complexes including [RuCl₂(tppms)₂]₂ (tppms: 3-sulfonatophenyldiphenylphosphine), [RhCl(tppms)₃], [RuCl₂(PTA)₄] (PTA: 1,3,5-triaza-7-phosphaadamantane) in aqueous solutions without amines.^{100,119,152-155} The high TOF of 9600 h⁻¹ was obtained at 80 °C and 9.5 MPa when using [RuCl₂(tppms)₂]₂.¹¹⁹ They found aqueous suspensions of CaCO₃ were also hydrogenated with CO₂/H₂ gas mixtures. Laurency et al. reported reaction mechanisms with iridium and ruthenium catalysts incorporating the water-soluble PTA ligand.^{120,156-158} They demonstrated the formation of [η⁶-(C₆H₆)RuH(PTA)₂]⁺ as the major hydride species, and proposed a mechanism involving hydride transfer to bicarbonate as shown in Scheme 1. TOFs of 237 and 409 h⁻¹ were obtained at 70 and 80 °C, respectively, with 10 MPa of H₂ and 1 M HCO₃⁻.¹⁵⁶



Scheme 1. Possible catalyst and substrate interaction during the hydrogenation of HCO₃⁻ in aqueous solution. Ref. 156.

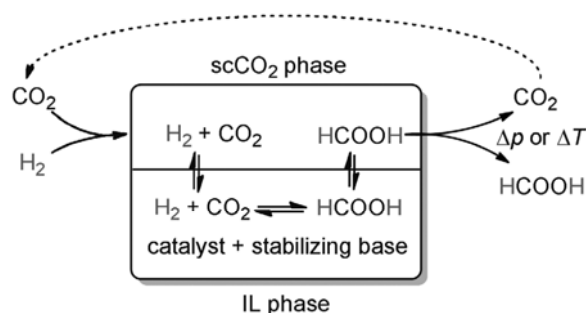
Subsequently, Beller and Laurency et al. reported a [RuCl₂(C₆H₆)₂] complex that acted as a catalyst precursor for hydrogenation in aqueous NaHCO₃ by incorporating one of a series of phosphine ligands including PPh₃, 1,1-bis(dicyclohexylphosphino)methane (dcpm), 1,2-bis(diphenylphosphino)ethane (dppe), 1,1-bis(diphenylphosphino)methane (dppm), and others (Chart 1). When dppm was used as a ligand, the high TOFs of 800 h⁻¹ and 1260 h⁻¹ were obtained in 2 h at 130 °C under 5 MPa of H₂ and at 70 °C under 8.5 MPa of H₂/CO₂ (5/3.5),

respectively.¹²¹ Although the catalyst system produced a high initial reaction rate, it became deactivated after the first few hours.

In 2012, Beller and co-workers investigated non-precious-metal catalysts for the hydrogenation of bicarbonate and CO₂.^{123,159} They obtained the high TON of 3877 by using Co(BF₄)₂·6H₂O and the PP₃ (PP₃: P(CH₂CH₂PPh₂)₃) ligand. This catalyst remarkably improved the catalytic activity compared to other non-precious-metal based catalysts and some precious-metal systems. They subsequently reported a thermally stable and more active iron catalyst, iron(II) fluoro-tris[2-(diphenylphosphino)phenyl]phosphino]tetrafluoroborate, which produced a TON over 7500 at 100 °C under 6 MPa H₂. Linehan et al. reported a Co complex, Co(dmpe)₂H (dmpe: 1,2-bis(dimethylphosphino)ethane), for the hydrogenation of CO₂ in THF.¹²⁹ In the presence of a very strong base, Verkade's base, at room temperature, the high TOFs of 3400 h⁻¹ and 74,000 h⁻¹ were achieved under 1 atm and 20 atm of CO₂/H₂ (1:1), respectively. While this is a significant result, a drawback is the requirement of Verkade's base (pK_a = 33.6)¹⁶⁰ for regeneration of Co(dmpe)₂H from [Co(dmpe)₂(H)₂]⁺. A mechanistic study using DFT calculations suggested a probable reaction pathway beginning with the binding of CO₂ through its carbon to Co to produce a six-coordinate Co(dmpe)₂(H)(CO₂) precursor, which undergoes intramolecular hydride transfer from the Co center to the electrophilic carbon of CO₂.¹⁶¹ The direct hydride transfer from cobalt hydride to approaching CO₂ is also possible since the energy barrier of this pathway is only 1.4 kcal mol⁻¹ higher. The direct hydride pathway is consistent with the calculations of Baiker et al. for CO₂ hydrogenation with [Ru(dmpe)₂H₂].¹⁶²

Leitner et al. proposed a new concept that applies continuous-flow hydrogenation of scCO₂ to produce pure formic acid in a single process unit as shown in Scheme 2.¹³⁵ They first identified a suitable combination of catalysts and ionic liquid (IL) matrices in batch reactions and

achieved the high initial TOF of 627 h^{-1} by using a ruthenium catalyst $[\text{Ru}(\text{cod})(\text{methallyl})_2]/\text{PBu}_4\text{tppms}$ ($\text{cod} = 1,5\text{-cyclooctadiene}$, $\text{methallyl} = \text{CH}_2\text{C}(\text{CH}_3)\text{CH}_2\text{-}$) and IL as the stationary phase (with dissolved non-volatile bases) at $50 \text{ }^\circ\text{C}$ under 10 MPa of H_2/CO_2 (1/1). By adding EMIMCl (1-ethyl-3-methylimidazolium chloride) as an additive, the TOF increased to 1090 h^{-1} . A variation of anions of ILs showed an increase in TONs and TOFs with the order $\text{NTf}_2^- < \text{OTf}^- < \text{HCO}_2^-$. While they obtained a high TON (1970) and TOF ($> 295 \text{ h}^{-1}$) in a continuous-flow system using the amine-free IL EMIM(HCO_2), formic acid extraction from the non-volatile amine-functionalized ionic liquid was found to be the limiting factor under the continuous-flow conditions.



Scheme 2. Direct continuous-flow hydrogenation of CO_2 to formic acid based on a biphasic reaction system consisting of scCO_2 as mobile phase and an IL such as EMIM(NTf_2) as a stationary phase containing a catalyst and a stabilizing base such as $[\text{Ru}(\text{cod})(\text{methallyl})_2]/\text{PBu}_4\text{tppms}$ and triethylamine, respectively. Reprinted with permission from Ref. 135, Copyright (2014) WILEY-VCH Verlag GmbH & Co, KGaA, Weinheim.

A series of pyridinylazolato (N-N') ruthenium(II) complexes with PMe_3 $[(\text{N-N}')\text{RuCl}(\text{PMe}_3)_3]$ (Chart 1) with various electron-withdrawing and -donating substituents were investigated to probe the structure-reactivity relationships in the hydrogenation of CO_2 under supercritical conditions.¹³⁴ In a comparison of catalytic capability, the triazolato system with an

unsubstituted ligand offered the best performance (TON 4800) under relatively mild conditions. Under supercritical carbon dioxide conditions, Thiel et al. reported the simple ruthenium complexes with commercially available and low-cost phosphine ligands P(OMe)₃, P(OEt)₃, P(OiPr)₃ and P(OPh)₃ together with DBU and C₆F₅OH that catalyze CO₂ hydrogenation.¹³⁶ High activity was obtained for *trans*-[RuCl₂{P(OMe)₃}₄] (TON = 6630, TOF = 1660 h⁻¹) similar to those of one of the landmark catalysts [RuCl₂(PMe₃)₄] (TON = 7630, TOF = 1910 h⁻¹) under their experimental conditions. Zhao and Joó studied CO₂ hydrogenation with inorganic additives such as CaCO₃, NaHCO₃, Na₂CO₃ and HCO₂Na with [RhCl(tppps)₃] in aqueous solutions. Interestingly, HCO₂Na as an additive produced the best yield of FA and afforded a highly concentrated FA of 0.13 M at 50 °C for 20 h under 100 bar H₂/CO₂ (1/1).¹¹⁶ Byers and co-workers investigated inexpensive additives for the CO₂ hydrogenation process with a variety of noble-metal and non-noble-metal catalysts, such as RuCl₂(PPh₃)(*p*-cymene) and the *in-situ* catalyst prepared from Fe(BF₄)₂ and PP₃ in DMSO or MeOH.¹⁶³ Comparison of catalytic performance with various catalysts suggested that the addition of KHCO₃ or other similar inorganic additives such as KOAc and KNO₃, etc., improved CO₂ hydrogenation activity by up to 510%. These studies promoted the design of catalytic systems inclusive of cheap additives to enhance catalytic activity.

Some novel protocols have been established by He and his group based on the capture of CO₂ as carbamate using PEI (polyethyleneimine) and simultaneous *in-situ* hydrogenation with RhCl₃·3H₂O with a monophosphine ligand.¹⁶⁴ These catalytic systems with RhCl₃·3H₂O/CyPPh₂ could capture CO₂ with PEI and sequentially hydrogenate it to formate, providing a maximum TON of 852. Hicks and co-workers synthesized several mesoporous organic-inorganic hybrid silica-tethered Ir-complexes shown in Figure 2. Ir-PN/SBA-15 containing a bidentate

iminophosphine ligand can heterogeneously catalyze CO₂ hydrogenation to formic acid.¹⁶⁵ Under moderate conditions (60 °C, 4 MPa H₂/CO₂ (1/1)), the catalyst provided a TON of 2800 after 20 h.

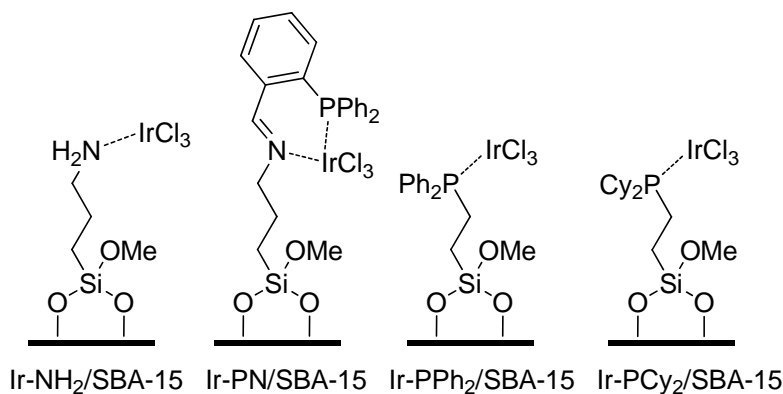


Figure 2. Structures of the SBA-15 tethered Ir complexes (Ph = phenyl, Cy = cyclohexyl). Ref. 165.

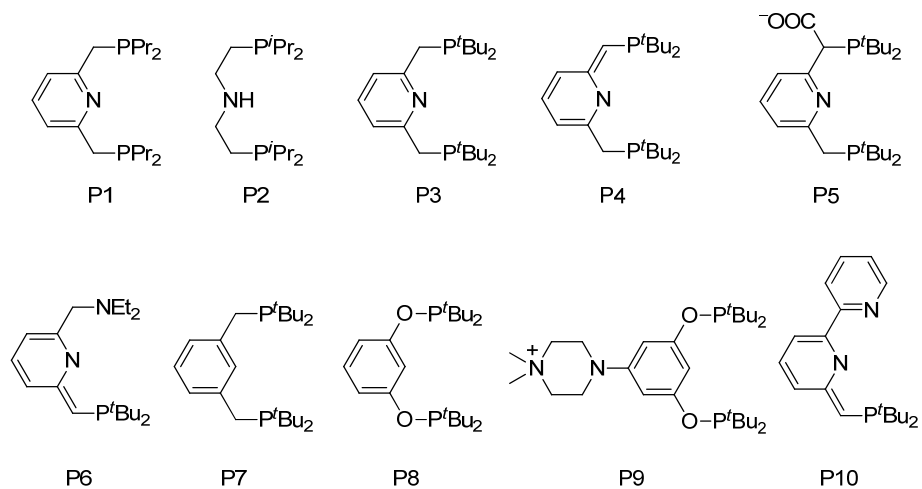
Most recently, Laurency et al. described the direct hydrogenation of CO₂ to produce formic acid using [RuCl₂(PTA)₄] in acidic media.¹³⁷ In an aqueous solution (pH 2.7), 0.2 M formic acid can be obtained at 60 °C under 20 MPa H₂/CO₂ (3/1), corresponding to a TON of 74. In DMSO under 10 MPa H₂/CO₂ (1/1), the ruthenium phosphine catalyst provided 1.9 M formic acid at 60 °C after 120 h, and achieved a total TON of 749 after the fourth cycle in recyclability tests. Although the TON is similar to that in basic aqueous solution, the product is FA and the catalyst operates in the absence of base or any other additives. It is also highly stable and can be recycled and reused multiple times without loss of activity.

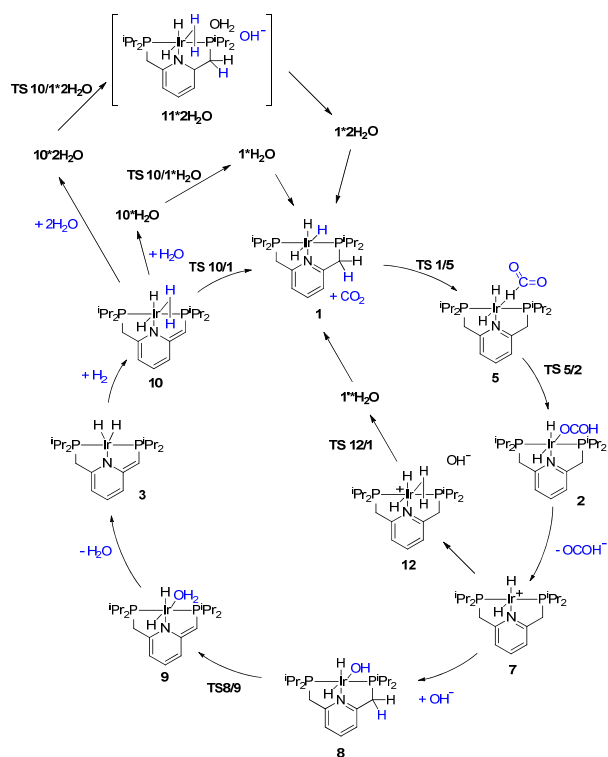
2.2. Catalysts with pincer ligands.

In 2009, Nozaki and co-workers synthesized a new Ir(III) trihydride complex, IrH₃(P1), (P1 = 2,6-bis-(di-isopropylphosphinomethyl)pyridine, Chart 2) for CO₂ hydrogenation in basic aqueous solution, and achieved the highest activity to that date at high temperature and high

pressure. The use of THF as a co-solvent was necessary owing to the low water solubility of the complex. The IrH₃(P1) complex exhibited a TOF of 150,000 h⁻¹ at 200 °C and a TON of 3,500,000 at 120 °C over a period of 48 h under 8 MPa H₂/CO₂ (1/1) in H₂O/THF (5/1).^{124,125} This excellent catalytic performance soon attracted considerable attention, and led to related research.

Chart 2. Pincer ligands for complexes used in CO₂ hydrogenation to formate and formic acid dehydrogenation.



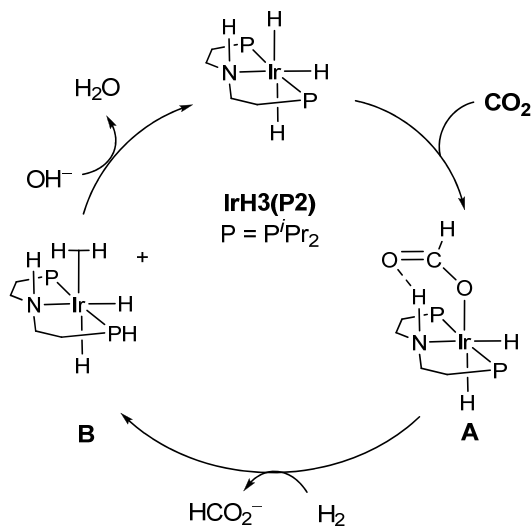


Scheme 3. Proposed mechanism for the hydrogenation of CO₂ by IrH₃(P1) based on Ref. 125.

Using the P1-ligated iridium(III) trihydride complex as a catalyst,¹²⁵ DFT calculations on the hydrogenation of CO₂ have been used to explain the dependence of the catalytic cycle on the strength of the base and hydrogen pressure. Two competing reaction pathways were identified with either the deprotonative dearomatization step (via TS8/9) or the hydrogenolysis step (via TS12/1) as being rate determining (see Scheme 3). The calculated free-energy profiles were consistent with the experimental data. Analogous Co and Fe hydride complexes incorporating the PNP ligand were investigated in DFT studies that predicted only slightly higher enthalpic barriers (entropic effects were neglected) than for Ir.^{166,167} Also, Ni and Pd hydride complexes with related PCP or PSiP ligands were investigated for catalyzing CO₂ insertion reactions in both experimental and computational studies.^{166,167} DFT calculations predicted that the pathway for

CO₂ insertion involves a four-centered transition state, the free energy of which decreases as the *trans* influence of the anionic donor of the pincer ligand increases.

The importance of secondary coordination sphere interactions has been documented in the field of [Fe-Fe] and [Fe-Ni] hydrogenases^{168,169} and molecular catalysts for H₂ production and CO₂ reduction.¹⁷⁰⁻¹⁷³ For synthetic catalytic systems, Crabtree¹⁷⁴ and others¹⁷⁵⁻¹⁷⁷ have published excellent reviews on ligand design with additional functional groups including: (1) proton-responsive ligands that are capable of changing their chemical properties upon gaining or losing one or more protons; (2) electro-responsive ligands that can gain or lose one or more electrons; (3) ligands that can provide a hydrogen bonding functionality; (4) photo-responsive ligands that exhibit a useful change in properties upon irradiation; (5) NADH-type ligands that can work as a hydride source; and (6) hemilabile ligands that provide a vacant coordination site.



Scheme 4. Proposed mechanism for CO₂ hydrogenation using IrH₃(P2) with the displacement of formate by H₂ as the rate determining step based on Ref. 127.

In 2011, Hazari and co-workers reported an air stable, water-soluble catalyst IrH₃(P2) (P2 = (di-isopropylphosphinoethyl)amine, Chart 2) containing an N–H group in the secondary

coordination sphere for CO₂ hydrogenation.¹²⁷ This hydrogen bond donor (Scheme 4, complex A), upon reaction with CO₂, facilitated the formation of the stable complex Ir(OCHO)H₂(P2), which was effective for CO₂ hydrogenation with a maximum TON of 348,000 and TOF up to 18,780 h⁻¹.¹²⁷ Their DFT calculations indicated that CO₂ insertion was more thermodynamically favorable by means of stabilization of an N–H–O hydrogen bond through an outer sphere interaction. Their proposed mechanism for CO₂ hydrogenation (Scheme 4) involves the displacement of coordinated formate by H₂ to generate the dihydrogen complex, deprotonation of the coordinated H₂ to form the trihydride IrH₃(P2), and CO₂ insertion to form the η¹-formate species stabilized by the N–H hydrogen bond to the other formate O atom. Detailed DFT calculations suggested that the insertion of CO₂ leads to an H-bound formate intermediate that dissociates and reforms as an O-bound species, with both stabilized by a N–H–O outer sphere hydrogen bond.

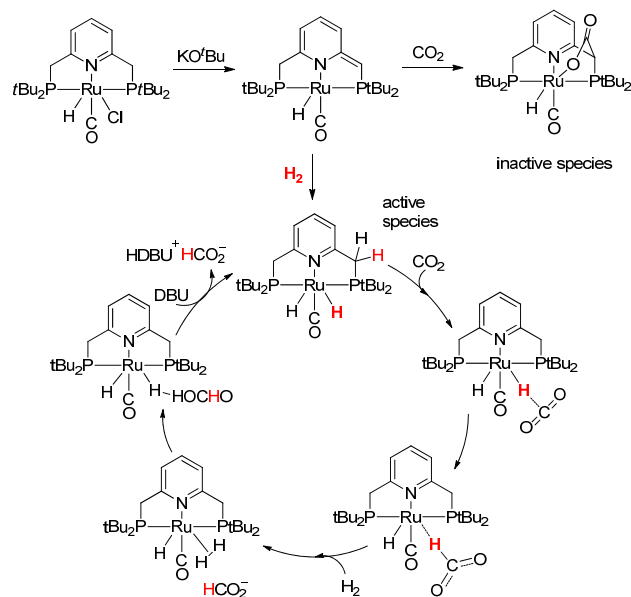
With regard to using an earth-abundant metal instead of a noble transition metal with a pincer ligand, Milstein and co-workers focused attention on the active iron complex *trans*-[FeH₂(CO)(P3)] (P3 = 2,6-bis-(di-*tert*-butylphosphinomethyl)pyridine), Chart 2), which was capable of hydrogenating CO₂ with a TON of up to 780 and a TOF of up to 160 h⁻¹ at 80 °C under low pressure (0.6 – 1.0 MPa) in H₂O/THF (10/1).¹²⁶ Almost simultaneously, Milstein and Sanford published the crystal structures of a Ru(PNP) complex [RuH(CO)(P4)] (P4: the dearomatized ligand of P3, Chart 2) and a Ru(PNN) complex [RuH(CO)(P6)] (P6 = 6-(di-*tert*-butylphosphinomethylene)-2-(*N,N*-diethylaminomethyl)-1,6-dihydropyridine, Chart 2), which both activate CO₂ through an aromatization/dearomatization mechanism.^{178,179} During the hydrogenation reaction, [RuH(CO)(P4)] reversibly converts to [RuH(CO)(P5)] (P5: a CO₂⁻ derivative of P3, Chart 2) in which the CO₂⁻ moiety of the P5 ligand coordinates to the Ru

center.¹⁷⁸ The non-innocent nature of the pincer ligands is crucial in the activation of CO₂, and is responsible for the widespread utility of pincer complexes in the activation of small molecules such as H₂ and CO₂ through metal-ligand cooperation.¹⁸⁰⁻¹⁸² With optimized catalytic conditions, the [RuH(CO)(P6)] complex provided a TON up to 23,000 and a TOF of up to 2200 h⁻¹ at 200 °C over a period of 48 h under 4 MPa H₂/CO₂ (3/1) in diglyme in the presence of K₂CO₃.¹³³

In addition, the PCP pincer complexes, IrH₂(P7) (P7 = 2,6-C₆H₃-(CH₂P^tBu₂)₂, Chart 2) and IrH₂(P8) (P8 = 2,6-C₆H₃-(OP^tBu₂)₂, Chart 2) were reported to facilitate CO₂ insertion to afford κ^2 -formate complexes.¹⁸³ IrH₂(P8) was effective for the selective electrocatalytic reduction of CO₂ to formate in H₂O/CH₃CN. Noteworthy is that the addition of water played an important role in lowering the reduction potential during electrocatalysis and minimizing the production of H₂ from the background reduction of water. Subsequently, Meyer and Brookhart modified the catalyst by tethering a quaternary amine functional group to the ligand aiming to improve its solubility in aqueous media.¹⁸⁴ The IrH(P9)(MeCN) complex (Chart 2) produced a 93% Faradaic yield in the electrocatalytical reduction of CO₂ to formate with high selectivity. They demonstrated that a moderate hydricity of the catalyst was necessary in the CO₂ reduction catalysis in order to limit formation of H₂ while retaining the ability to reduce CO₂. Based on work by Meyer and Brookhart^{183,184} and Nozaki's earlier work,¹²⁴ Hazari et al. proposed different catalytic pathways for CO₂ insertion into five-coordinate iridium(III) dihydrides and four-coordinate iridium(I) monohydrides based on DFT calculations.¹⁸⁵ In the case of five-coordinate dihydrides, both *O*-bound κ^1 - and *O,O*-bound κ^2 -formate CO₂ insertion intermediates were predicted to be potentially important. In the case of four-coordinate Ir(I) monohydrides, the proposed mechanism for CO₂ insertion involved a single four-centered transition state in which the Ir–H bond is broken and simultaneously the carbon–hydride and iridium–oxygen bonds are

formed. They also predicted the activity of five-coordinate Ir(III) dihydride complexes with a variety of PCP and POCOP ligands that can facilitate CO₂ insertion.

Pidko et al. developed a highly stable temperature-switchable Ru-based system for the reversible hydrogenation of CO₂ that exhibits unprecedented rates for H₂ loading and release under mild conditions.¹³² Using DMF as a solvent, DBU as a base at 120 °C and 4 MPa H₂/CO₂ (3/1), the Ru PNP-pincer complex RuH(Cl)(CO)(P3) provided a TOF as high as 1,100,000 h⁻¹,¹³² which is superior to the TOF achieved by the Nozaki Ir(H)₃(P1) catalyst. The mechanism of CO₂ hydrogenation to formate using the Ru-PNP pincer complex in the presence of DBU was subsequently investigated by DFT calculations.^{131,186} Combining experimental and computational studies, they speculated that bis-hydrido Ru complex [Ru(H)₂(CO)(P3)] is the active species, while the ligand-assisted CO₂ adduct is an inactive state. Catalytic cycles involving metal-ligand cooperation contributed little to the catalysis due to the unstable intermediates and high free energy barriers. Two catalytic routes which do not involve metal-ligand cooperation were predicted to be predominant (Scheme 5).¹⁸⁶ The preferred route can be controlled by H₂ pressure, which is verified by kinetic experiments. By changing the molar ratio of H₂/CO₂ from 3/1 to 37/3, the apparent activation energy significantly decreased from 57 to 20 kJ mol⁻¹. This finding is contrary to the widely reported critical role of the ligand in facilitating the catalytic process. Although the PNP-type pincer ligands are undoubtedly versatile, their practical role deserves further exploration.



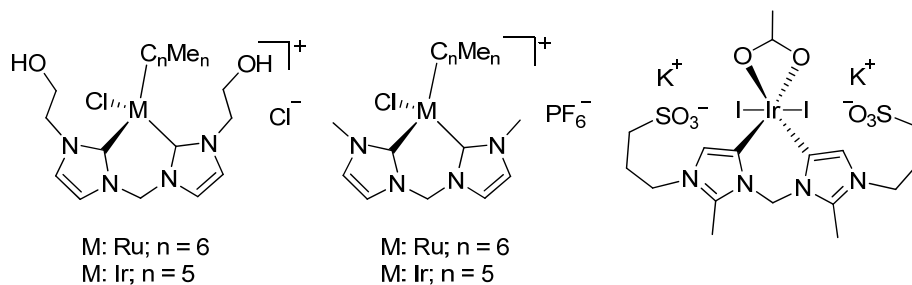
Scheme 5. Possible catalytic cycle for CO₂ hydrogenation to formate by complex [RuH(Cl)(CO)(P3)] based on Refs. 132,186.

2.3 Catalysts with *N*-heterocyclic carbene ligands

Peris et al. performed extensive studies of water-soluble Ru and Ir complexes using bis-NHC (*N*-heterocyclic carbenes) as electron-donating ligands.^{148,187,188} The high TON of 190,000 was achieved with complex IrI₂(AcO)(bis-NHC) (right in Chart 3), at 200 °C under 6 MPa H₂/CO₂ (1/1) for 75 h. Chelating-NHC ligands could impart a high thermal stability to the metal complexes and lead to high catalytic activity of the complex owing to their electron donor character. Incorporating sulfonate or hydroxy substituents into the carbon side chains improves the water solubility of the complexes, and their catalytic performance for the hydrogenation of CO₂ to HCO₂K was considerably improved. The Peris lab was the first to propose transfer hydrogenation using isopropanol as the hydrogen source for CO₂ hydrogenation to overcome inconveniences of using pressurized H₂. In aq. 0.5 M KOH/isopropanol (9/1) turnovers

approaching 1000 after 16 h at 200 °C were achieved. The lower activity compared to reactions with H₂ are likely associated with difficulty in generating the metal hydride from isopropanol.

Chart 3. Peris's NHC complexes for CO₂ hydrogenation in water.



2.4 Half-sandwich catalysts with/without proton-responsive ligands

2.4.1. Electronic effects. In contrast to the widely used phosphine complexes, molecular complexes with *N,N*- or *N,C*-chelated ligands have been less studied in the context of CO₂ hydrogenation.^{139,189-192} When Himeda and his group observed CO₂/H₂ generation in the transfer hydrogenation of ketones with the half-sandwich complex [Cp**Rh*(bpy)Cl]Cl in aqueous solutions of formic acid, they realized that the *Rh* complex could catalyze CO₂ hydrogenation in water.¹⁹³ The research of Jessop and Sakaki et al. had indicated that the strong electron-donating ability of the ligand leads to high activity of such a complex in CO₂ hydrogenation.^{194,195} Inspired by their studies, Himeda's group designed and synthesized a series of half-sandwich complexes [(C_nMe_n)M(4,4'-R₂-bpy)Cl]⁺ (n = 5, 6; M = Ir, Rh, Ru; R = OH, OMe, Me, H) by introducing different electron-donating groups to the bpy ligand of the prototype catalyst [(C_nMe_n)M(bpy)Cl]Cl.^{140,193,196,141} In the presence of water, the chloro ligand in these complexes readily hydrolyzes to form the corresponding aqua complexes.

The hydroxy-substituted bpy ligands are deprotonated upon increasing the solution pH beyond pH 5 to 6.¹⁹⁶ Such α-diimine ligands bearing pyridinol units are among those known as

“proton-responsive ligands” (Chart 4).¹⁷⁴ This property makes them pH-switchable and enables modification of the polarity and electron-donating ability of the ligand, thus tuning the catalytic activity and water-solubility of the complexes. The electron donating ability of the substituents is characterized by Hammett constants (σ_p^+): the more negative the σ_p^+ values, the stronger their ability to donate electrons.¹⁹⁷ Among these catalysts, complexes bearing OH substituents are of particular interest. Deprotonation of the OH group ($\sigma_p^+ = -0.92$) generates a much stronger oxyanion electron donor ($\sigma_p^+ = -2.30$) because of the effect of its “keto” resonance structure (Scheme 6). Catalyst recovery using the pH-dependent solubility of $[\text{Cp}^*\text{Ir}(\text{DHPT})(\text{OH}_2)]\text{Cl}$ (DHPT = 4,7-dihydroxy-1,10-phenanthroline) will be discussed below.

The Hammett plots show a good correlation between the initial TOFs and the σ_p^+ values of the substituents for the Ir, Rh, and Ru complexes (Figure 3). The electronic effects of the substituents on the rhodium and ruthenium complexes were moderate compared to those on the iridium complex (Figure 3). The initial TOF of 5100 h^{-1} of $[\text{Cp}^*\text{Ir}(\text{4DHBP})\text{Cl}]\text{Cl}$ (4DHBP = 4,4'-dihydroxy-2,2'-bipyridine, Chart 4) is over 1000 times higher than that of the unsubstituted analog $[\text{Cp}^*\text{Ir}(\text{bpy})\text{Cl}]\text{Cl}$ (4.7 h^{-1}) under the same conditions ($80 \text{ }^\circ\text{C}$, 1 MPa , $\text{CO}_2/\text{H}_2 = 1$). Apparently, the significant improvement in catalytic activity of the 4DHBP catalyst can be attributed to the strong electron-donating ability of the oxyanion. The high TOF of $42,000 \text{ h}^{-1}$ and TON of 190,000 using $[\text{Cp}^*\text{Ir}(\text{4DHBP})\text{Cl}]\text{Cl}$ was obtained at $120 \text{ }^\circ\text{C}$ and 6 MPa . This catalyst even converts CO_2 to formate at ambient temperature ($25 \text{ }^\circ\text{C}$) and pressure (0.1 MPa) in 1 M NaHCO_3 aqueous solution with the TOF of 7 h^{-1} . The high catalytic activity of $[\text{Cp}^*\text{Ir}(\text{4DHBP})\text{Cl}]\text{Cl}$ represents a breakthrough in CO_2 hydrogenation in aqueous solutions. Fukuzumi's group also found a proton-responsive catalyst $[\text{Cp}^*\text{Ir}(\text{N1})(\text{OH}_2)]^+$ that efficiently produces formate in 2.0 M KHCO_3 aqueous solution (pH 8.8) with the TOF of 6.8 h^{-1} and TON

of 100 (20 h) at 30 °C and ambient pressure of H₂ (0.1 MPa).¹⁴⁵ The active catalyst is the deprotonated complex [Cp*Ir(N1-H⁺)(OH₂)] because the p*K*_a values of the carboxylic acid group and the aqua ligand are 4.0 and 9.5, respectively. The catalytic activity increases to 22.1 h⁻¹ at 60 °C. While most catalysts required some pressure of CO₂ in basic aqueous solution, this complex can hydrogenate HCO₃⁻.

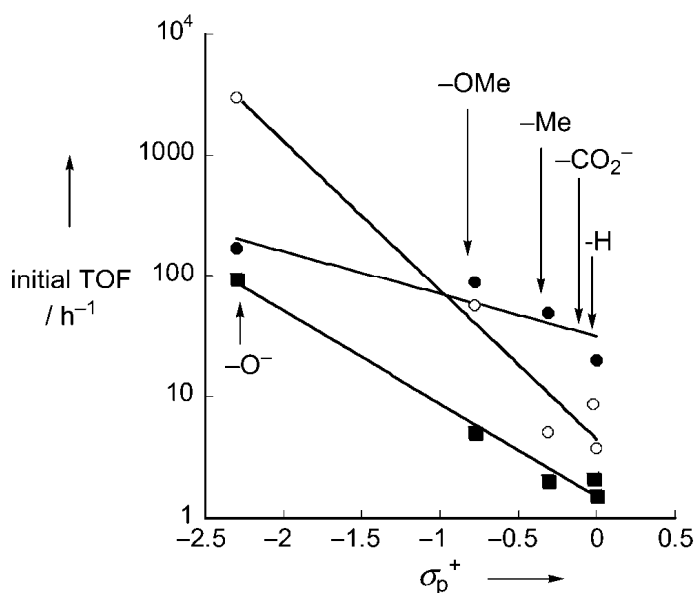
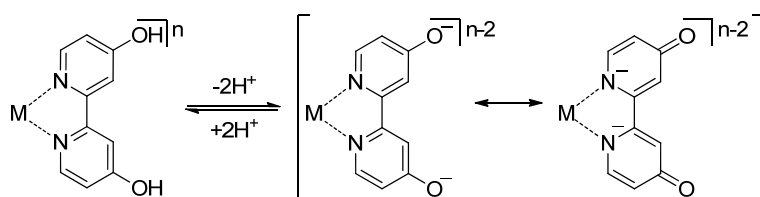
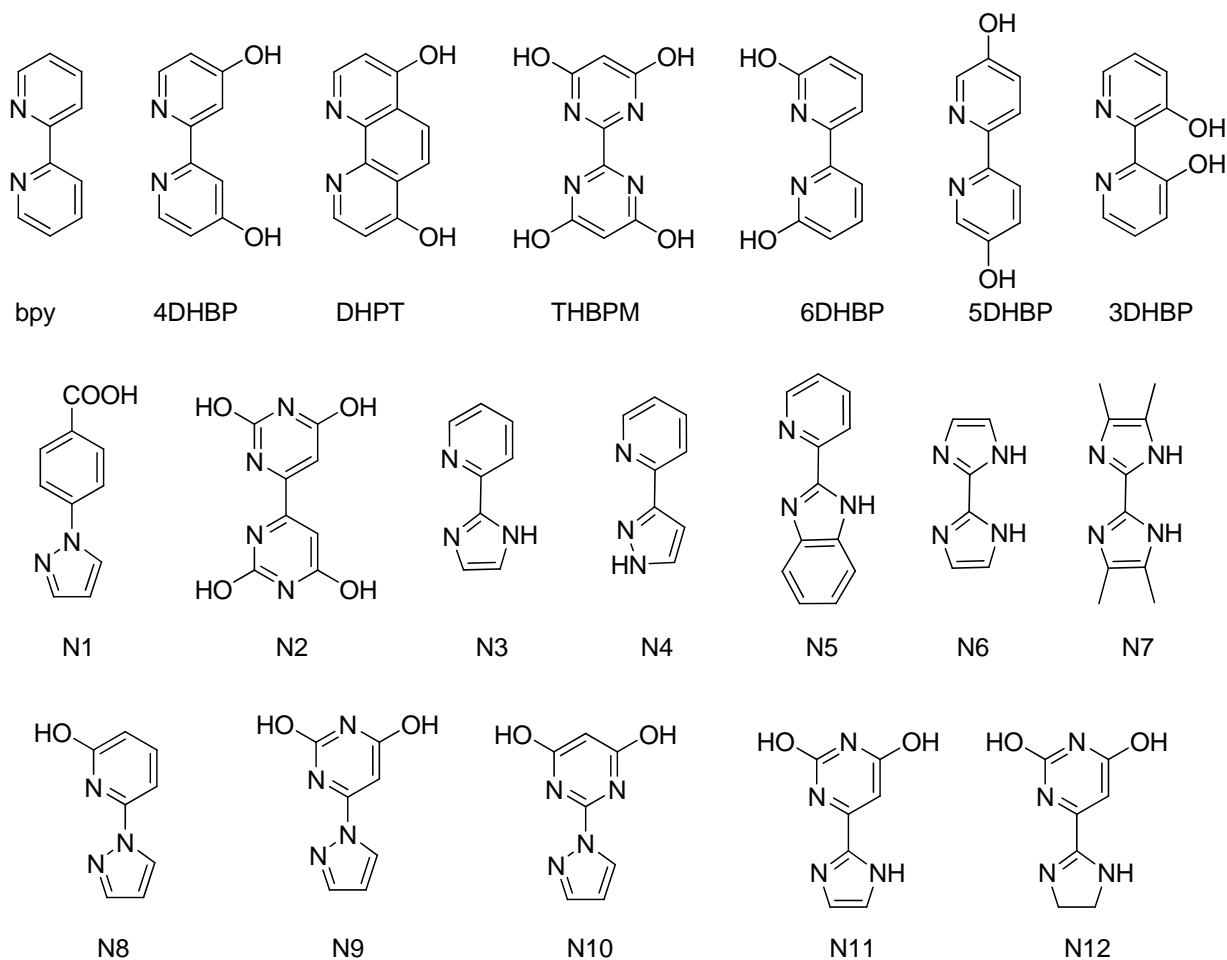


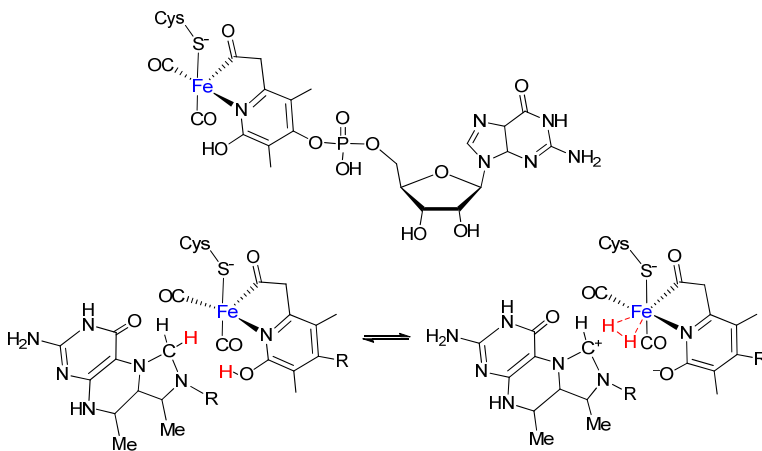
Figure 3. Correlation between initial TOFs and σ_p^+ values of substituents (R) for CO₂ hydrogenation catalyzed by [(C_nMe_n)M(4,4'-R₂-bpy)Cl]Cl. M = Ir, n = 5 (open circles); M = Rh, n = 5 (closed circles); M = Ru, n = 6; R = OH, OMe, Me, H (closed squares). The reactions were carried out in an aqueous 1 M KOH solution at 80 °C under 1 MPa (CO₂:H₂ = 1:1) for 20 h. Reprinted with permission from Ref. 141. Copyright (2011) WILEY-VCH Verlag GmbH & Co, KGaA, Weinheim.

Chart 4. Proton-responsive ligands used for CO₂ hydrogenation and/or dehydrogenation of formic acid.



Scheme 6. Acid-base equilibrium between hydroxy form and oxyanion form, and resonance structures of oxyanion form.

2.4.2. Second-coordination-sphere effects. A hydroxy group near the metal center may act as an important functional group, which can facilitate hydrogen dissociation and production as found in [Fe-Fe]-hydrogenase model complexes.^{170,177,198} In the reduction of CO₂ to methane by methanogens, the Fe-guanylpuridinol cofactor found in [Fe]-hydrogenase catalyzes a crucial intermediary step: the reversible reduction of methenyltetrahydromethanopterin (methenyl-H4MPT⁺) by H₂ to methylenetetrahydromethanopterin (methylene-H4MPT) and H⁺ (i.e., from a proton from puridinol and a hydride from C14 of methylene-H4MPT to the vacant coordination site of Fe, see Scheme 7).¹⁹⁹⁻²⁰¹ A computational study revealed that the pendent hydroxy group plays an important role in the activation of H₂ by forming a hydrogen bond.²⁰²



Scheme 7. Structure of the Fe-guanylpuridinol cofactor of [Fe]-hydrogenase and a proposed catalytic mechanism of H₂ heterolysis based on Ref. 201.

To understand and exploit the role of the hydroxy functional group in [Fe]-hydrogenase, chemists have expended great effort on the design and synthesis of complexes containing hydroxypyridine moieties and their derivatives for use in hydrogenation and dehydrogenation reactions.¹⁴⁶ Fujita and Yamaguchi et al. reported the dehydrogenation of alcohols and other

chemicals using Cp*Ir complexes with hydroxypyridine, 6-hydroxy-2-phenylpyridine, and 6-hydroxy-2,2'-bipyridine.²⁰³⁻²⁰⁶ Kelson and Phengsy reported the transfer hydrogenation of ketones to isopropanol using $[\text{Ru}(\text{tpy})(\text{OH}_2)]^{2+}$ (tpy = 2,2':6',2''-terpyridine) with two axial monodentate κN coordinated 2-pyridinato ligands.²⁰⁷ A collaboration between the Himeda and Fujita groups has developed a series of iridium complexes, $[\text{Cp}^*\text{Ir}(\text{nDHBP})(\text{OH}_2)]^{2+}$ (nDHBP = n,n'-dihydroxy-2,2'-bipyridine, n = 3, 4, 5, 6), $[(\text{Cp}^*\text{IrCl})_2(\text{THBPM})]^{2+}$ (THBPM = 4,4',6,6'-tetrahydroxy-2,2'-bipyrimidine), and $[\text{Cp}^*\text{Ir}(\text{Nn})(\text{OH}_2)]^{2+}$ (n = 2 - 12, Chart 4) as catalysts for carrying out CO₂ hydrogenation and formic acid dehydrogenation under mild conditions in environmentally benign and economically desirable water solvent.^{140,142-144,146,208-211}

Under various pH conditions, these complexes showed high activity and efficiency in aqueous catalysis such as hydrogenation or transfer hydrogenation of alkenes and ketones, CO₂ hydrogenation, and the dehydrogenation of formic acid.¹⁴⁴ Using formic acid or H₂, facile formation of the active iridium hydride occurs. Under basic conditions, the hydride reduces CO₂ to formate, while under acidic conditions it reacts with H⁺ to release H₂. Here we will summarize how the proton-responsive complexes catalyze these reactions efficiently under different pH conditions. Such unique properties as pH-dependent activity and selectivity, tuneable water solubility, recyclability, and pendent-base effects are discussed in detail.

The bio-inspired complexes $[\text{Cp}^*\text{Ir}(\text{6DHBP})(\text{OH}_2)]^{2+}$, $[\text{Cp}^*\text{Ir}(\text{N2})(\text{OH}_2)]^{2+}$ (N2 = 2,2',6,6'-tetrahydroxy-4,4'-bipyrimidine) and $[(\text{Cp}^*\text{IrCl})_2(\text{THBPM})]^{2+}$ bearing pendent OH groups exhibit significantly improved catalytic activity in CO₂ hydrogenation. To understand the factors responsible for the improved activity, the catalytic activity of $[\text{Cp}^*\text{Ir}(\text{6DHBP})(\text{OH}_2)]^{2+}$ and its analogues $[\text{Cp}^*\text{Ir}(6,6'\text{-R}_2\text{-bpy})(\text{OH}_2)]\text{SO}_4$ (R = OMe, Me, H) were further investigated. First, the electronic effect of the substituents at the 6,6'-positions was studied in the same manner as with

$[\text{Cp}^*\text{Ir}(4,4'\text{-R}_2\text{-bpy})(\text{OH}_2)]\text{SO}_4$ ($\text{R} = \text{OH}, \text{OMe}, \text{Me}, \text{H}$).¹⁴³ As shown in the Hammett plots (Figure 4), and similar to the 4,4'-substituted analogues, stronger electron-donating substituents lead to higher reaction rates. It is noteworthy that $[\text{Cp}^*\text{Ir}(6\text{DHBP})(\text{OH}_2)]^{2+}$ (TOF: 8050 h^{-1}) showed much higher activity than $[\text{Cp}^*\text{Ir}(4\text{DHBP})(\text{OH}_2)]^{2+}$ (TOF: 5100 h^{-1}) under the same conditions. Since the electron-donating ability of the hydroxy group at the *para* and *ortho* positions should be almost the same, Himeda et al. proposed that the additional rate enhancement arises from the proximity of the hydroxy groups in 6DHBP to the metal center and a possible cooperative effect in the activation of the substrate.

2.4.3. Mechanistic investigations. Experimental and computational studies on the reaction mechanism have been published for CO_2 hydrogenation using $[\text{Cp}^*\text{Ir}(6\text{DHBP})(\text{OH}_2)]^{2+}$ and $[\text{Cp}^*\text{Ir}(4\text{DHBP})(\text{OH}_2)]^{2+}$.^{143,144,146} NMR experiments suggested that, in the presence of H_2 , $[\text{Cp}^*\text{Ir}(6\text{DHBP})(\text{OH}_2)]^{2+}$ is able to form the Ir–H species much more easily than $[\text{Cp}^*\text{Ir}(4\text{DHBP})(\text{OH}_2)]^{2+}$ can. For instance, 95% of $[\text{Cp}^*\text{Ir}(6\text{DHBP})(\text{OH}_2)]^{2+}$ converted to the Ir–H complex after 0.5 h under 0.2 MPa H_2 , while only 90% of $[\text{Cp}^*\text{Ir}(4\text{DHBP})(\text{OH}_2)]^{2+}$ transformed to the corresponding Ir–H complex after 40 h under 0.5 MPa H_2 . Preliminary DFT calculations on the $[\text{Cp}^*\text{Ir}(6\text{DHBP})(\text{OH}_2)]^{2+}$ complex under basic conditions (pH 8.3)¹⁴³ suggested that the heterolysis of dihydrogen is the rate-determining step, not CO_2 insertion as Ogo and Fukuzumi had reported.²¹² Moreover, the calculations indicate that the adjacent oxyanions, from deprotonated hydroxy groups under basic conditions, act as pendent bases and assist the heterolysis of H_2 (Scheme 8, A-D). The calculations also suggested that CO_2 insertion into the Ir–H bond is stabilized by a weak hydrogen bond between the hydrido ligand and deprotonated pendent base (Scheme 8, E).¹⁴³

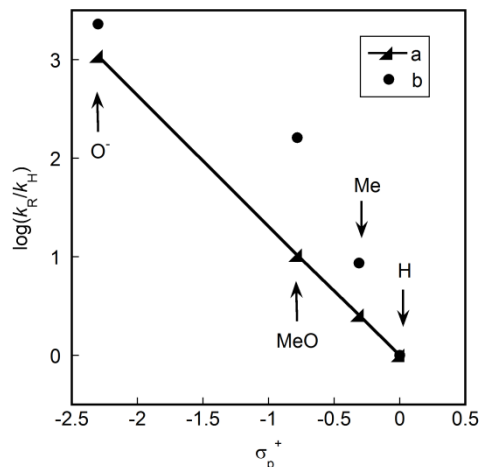
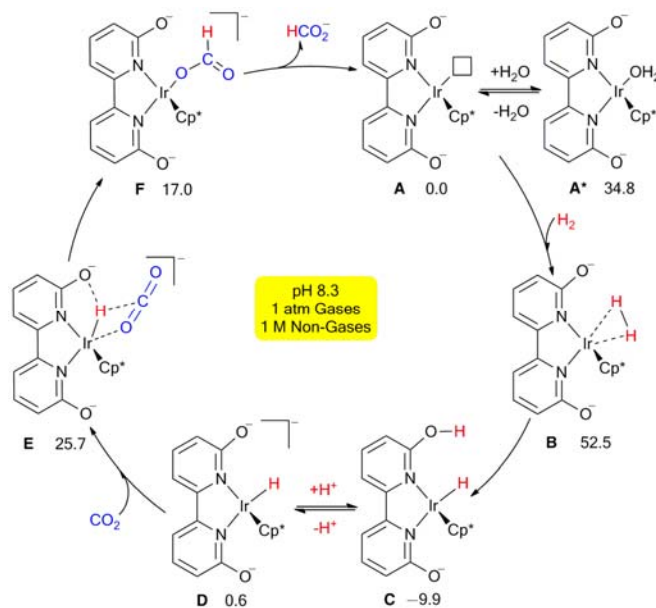


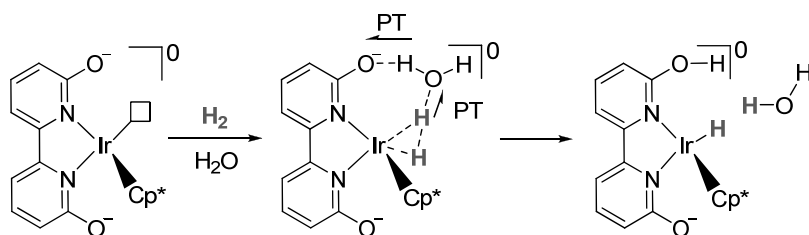
Figure 4. Correlation between initial TOFs and σ_p^+ values of substituents (R) for the CO_2 hydrogenation catalyzed by (a) $[\text{Cp}^*\text{Ir}(4,4'\text{-R}_2\text{-bpy})(\text{OH}_2)]\text{SO}_4$ (R = OH, OMe, Me, H; triangles) and (b) $[\text{Cp}^*\text{Ir}(6,6'\text{-R}_2\text{-bpy})(\text{OH}_2)]\text{SO}_4$ (R = OH, OMe, Me, H; circles). Reaction conditions: 1 MPa of H_2/CO_2 (1/1), 80 °C, (a) 0.02–0.2 mM catalyst in 1 M KOH; and (b) 0.01–0.2 mM catalyst in 1 M NaHCO_3 . Reproduced from Ref. 143 with permission from The Royal Society of Chemistry.



Scheme 8. Proposed mechanism for the CO_2 hydrogenation by $[\text{Cp}^*\text{Ir}(6\text{DHBP})(\text{OH}_2)]^{2+}$. Computed free energies at pH 8.3 are indicated in units of kJ mol^{-1} relative to 1 M A in aqueous

solution and 1 atm H₂ and CO₂ gases. The calculated change in free energy around the cycle is -42.0 kJ mol⁻¹. Reproduced from Ref. 143 with permission from The Royal Society of Chemistry.

Furthermore, clear evidence was found for the involvement of a water molecule in the rate-limiting heterolysis of H₂, and the enhancement of proton transfer through the formation of a water bridge in CO₂ hydrogenation catalyzed by [Cp*Ir(6DHBP)(OH₂)]²⁺ and [Cp*Ir(N₂)(OH₂)]²⁺ bearing a pendent base.¹⁴⁶ A deuterium kinetic isotope effect study was carried out using D₂/KDCO₃/D₂O instead of H₂/KHCO₃/H₂O. For [Cp*Ir(4DHBP)(OH₂)]²⁺ bearing no pendent OH, D₂ led to an apparent decrease in reaction rate both in KHCO₃/H₂O (KIE: 1.19) and KDCO₃/D₂O (KIE: 1.20) solution. D₂O led to no substantial rate decrease for the case of H₂/KDCO₃ (KIE: 0.98). This suggests that D₂ is involved in the rate-determining step (RDS) for [Cp*Ir(4DHBP)(OH₂)]²⁺. In contrast, for [Cp*Ir(6DHBP)(OH₂)]²⁺ and [Cp*Ir(N₂)(OH₂)]²⁺ bearing pendent OH groups, D₂O resulted in a larger rate decrease than with D₂, indicating that D₂O is involved in the RDS for [Cp*Ir(6DHBP)(OH₂)]²⁺ and [Cp*Ir(N₂)(OH₂)]²⁺. Therefore, it was concluded that water is involved in the rate-limiting heterolysis of dihydrogen for [Cp*Ir(6DHBP)(OH₂)]²⁺ and [Cp*Ir(N₂)(OH₂)]²⁺ but not for [Cp*Ir(4DHBP)(OH₂)]²⁺. It was proposed that a water molecule forms a hydrogen bond with the pendent base, and the heterolysis of an H₂ approaching the metal center is assisted by a proton relay (Scheme 9).



Scheme 9. Proposed mechanism for H_2 heterolysis assisted by the pendant base and a water molecule through a proton relay. The arrows labeled by PT indicate the movement of protons via a proton relay. Reprinted with permission from Ref. 146. Copyright (2013) American Chemical Society.

The participation of H_2O in the transition state was further demonstrated by DFT calculations. Using the deprotonated $[\text{Cp}^*\text{Ir}(\text{6DHBP}-2\text{H}^+)]$ (the left structure in Scheme 9) as a prototype, Himeda et al. identified two different transition states for the rate-determining H_2 heterolysis step to produce $[\text{Cp}^*\text{Ir}(\text{H})(\text{6DHBP}-\text{H}^+)]$.¹⁴⁶ The calculated transition state with a water molecule is 14.2 kJ mol^{-1} lower than that without H_2O . This is the first clear evidence obtained from both experimental and theoretical investigations for the involvement of a water molecule in the H_2 heterolysis that is the RDS of CO_2 hydrogenation for complexes bearing pendant OH groups. The acceleration of proton transfer by forming a water bridge is similar to a proton channel in proteins.

More recently, in a DFT study by Suna et al. comparing the CO_2 reduction activity of the $[\text{Cp}^*\text{Ir}(\text{4DHBP}-2\text{H}^+)]$ and $[\text{Cp}^*\text{Ir}(\text{6DHBP}-2\text{H}^+)]$ complexes,¹⁴⁴ the calculated activation free energies indicated that for both complexes the H_2 heterolysis to form the iridium hydride intermediate was the rate-determining step, but the presence of the basic oxyanion groups adjacent to the metal center in $[\text{Cp}^*\text{Ir}(\text{6DHBP}-2\text{H}^+)]$ facilitates the H_2 heterolysis and leads to a substantial lowering of the activation free energy consistent with faster observed rates for

formate generation. Barriers were also found for the CO₂ insertion into the Ir–H bond step for both complexes (with the 6DHBP complex being somewhat lower). This result was later contradicted by DFT calculations by Hou et al.,²¹³ who reported finding another pathway with a much lower activation free energy for the 6DHBP complex corresponding to “ligand assisted hydride transfer” for formic acid formation. This result is questionable because geometry optimizations and vibrational frequency calculations were carried out in the absence of a continuum solvent model. The absence of stabilization of the charge separation in the true transition state imparted by such a solvent model is likely to have led to a transition state geometry close to the structure of the formate adduct that would not be a transition state in the presence of a solvation model.

2.4.4. pH-dependent solubility and catalyst recovery. The ability to design novel homogeneous catalysts possessing pH-tuneable catalytic activity and reaction-controlled water solubility provides a new strategy for efficient catalyst recycling.^{214,215} The acid-base equilibrium of a proton-responsive complex not only changes the electronic properties but also affects its polarity and thus its water solubility. Catalyst recycling was achieved using [Cp*Ir(DHPT)(Cl)]⁺ (DHPT = 4,7-dihydroxy-1,10-phenanthroline, Chart 4) because it has tuneable water solubility by controlling the solution pH.²⁰⁹ Himeda et al. examined the Ir concentrations in a formate solution of various catalysts with IPC-MS at different solution pH.¹⁴⁰ [Cp*Ir(4DHBP)(Cl)]⁺ showed pH-dependent solubility which decreased initially from pH 2 with increasing solution pH and then increased above pH 7. However, considerable water solubility (~1 ppm) was observed even at the lowest point of the curve (around pH 7, Figure 5). Thus [Cp*Ir(4DHBP)(OH₂)]²⁺ is not suitable for efficient catalyst recycling by precipitation from an aqueous formate solution by

adjusting the solution pH. To further decrease the water solubility, the bpy ligand was replaced with phen (1,10-phenanthroline). $[\text{Cp}^*\text{Ir}(\text{DHPT})(\text{Cl})]^+$ exhibited negligible solubility in a weakly acidic formate solution with pH between 4 and 7, and was precipitated as protonated and deprotonated forms. The lowest Ir concentration at pH 5 was found to be ca. 100 ppb (Figure 5). The poor water solubility of $[\text{Cp}^*\text{Ir}(\text{DHPT})(\text{Cl})]^+$ makes it recyclable. When KOH added as a base in the reaction solution was gradually consumed by the progress of the CO_2 hydrogenation, the solution pH decreased correspondingly. As a consequence, the deprotonated DHPT catalyst changed to its protonated form and spontaneously precipitated owing to its decreased water solubility at the lower pH. Eventually, a heterogeneous system was formed and the reaction terminated automatically (Figure 6). The precipitated catalyst could be recovered by simple filtration for reuse, and the iridium complex remaining in the filtrate was less than 2% of the catalyst loading (0.11 ppm). A recovery efficiency of more than 91% (by mass) was achieved after three cycles. The recovered catalyst was found to retain a high catalytic activity through the three cycles.¹⁴⁰ These results suggested that advantages of both homogeneous and heterogeneous catalysts can be combined using a proton-responsive complex with tunable solubility. Moreover, $[\text{Cp}^*\text{Ir}(\text{DHPT})(\text{Cl})]^+$ showed activity similar to $[\text{Cp}^*\text{Ir}(\text{4DHBP})(\text{Cl})]^+$ and can catalyze the CO_2 hydrogenation at atmospheric pressure.

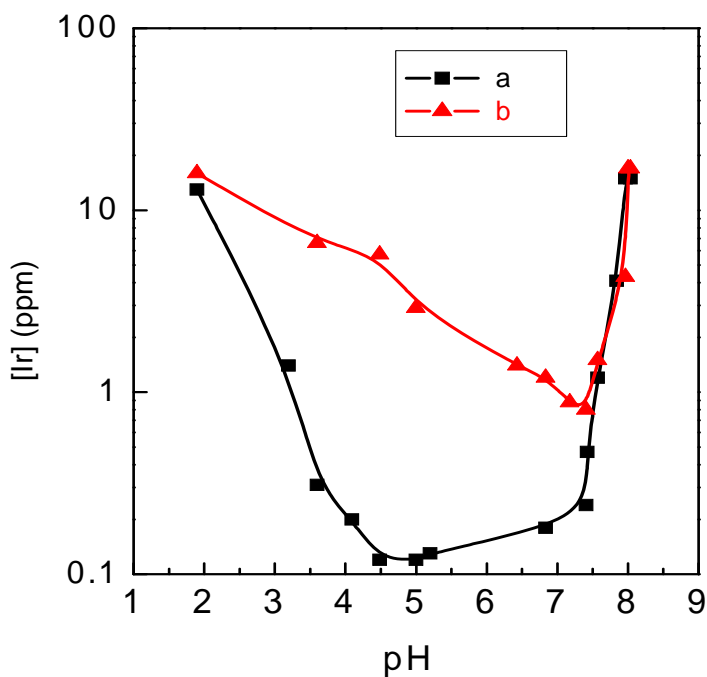


Figure 5. The pH-dependent solubility of (a) $[\text{Cp}^*\text{Ir}(\text{DHPT})(\text{Cl})]^+$ and (b) $[\text{Cp}^*\text{Ir}(4\text{DHBP})(\text{Cl})]^+$ in a 1 M aqueous formate solution. Redrawn from Ref. 140. Copyright (2007) American Chemical Society.

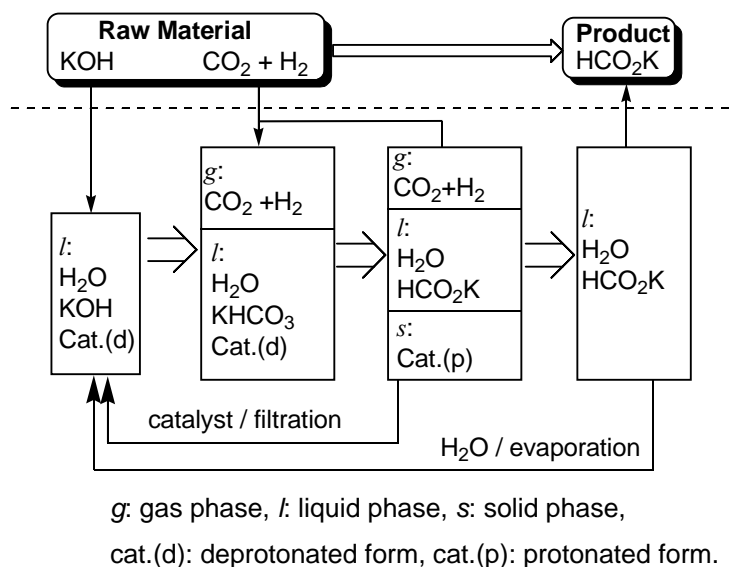


Figure 6. Recycling system for the conversion of CO₂/H₂ into HCO₂K using [Cp*Ir(DHPT)(Cl)]⁺ in aqueous KOH solution. Ref. 140. Copyright (2007) American Chemical Society.

3. Formic Acid Dehydrogenation with Various Metal Complexes

The dehydrogenation of FA (eq. 10), which is a low-volatility and non-toxic organic acid, as a companion reaction to CO₂ hydrogenation is an indispensable step in a hydrogen storage system using formic acid as the hydrogen storage material.^{216,217} Many heterogeneous catalysts for decomposition of formic acid have been reported.^{218,219} However, these systems usually require high temperature, which causes CO contamination by FA dehydration (eq. 11). For practical utilization, the CO content is generally required to be less than 10 ppm because it is a well-known poison to the catalyst in the proton exchange membrane (PEM) fuel cells. On the other hand, the homogeneous catalysis of the dehydrogenation of FA has been less studied, although FA has been widely used as a hydrogen donor in transfer hydrogenation in the field of organic synthesis.²²⁰⁻²²² Renewed interest in FA as an H₂ carrier has been stimulated by the discovery of highly active homogeneous catalysts for its selective dehydrogenation under mild conditions.^{103,104,142,223-226} In this context, several aspects of catalyst design deserve to be highlighted including the use of phosphine ligands, pincer ligands, proton-responsive ligands, and non-precious metals as described below and in Table 2.

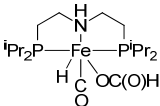
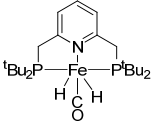
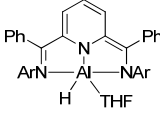
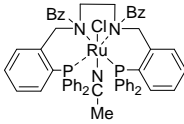
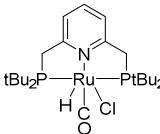
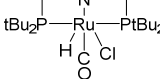
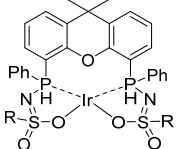


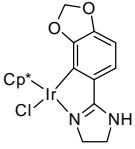
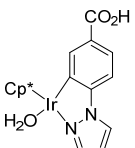
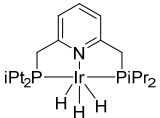
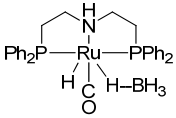
$$\Delta G^\circ = -32.8 \text{ kJ mol}^{-1}$$



$$\Delta G^\circ = -12.4 \text{ kJ mol}^{-1}$$

Table 2. Dehydrogenation of formic acid.^a

Catalyst	Solvent	additive	T / °C	Time	TON	Initial TOF / h ⁻¹	CO ^c / Ref. ppm
IrH ₃ (PPh ₃) ₃	AcOH		118		>11,000	8900	n.d. 227
[RuCl ₂ (PPh ₃) ₃]	DMF	Et ₃ N	40	2 h	890	2700	n.d. 228
RuCl ₃ /tppts	H ₂ O	HCO ₂ Na	120			670	n.d. 229,230
[Ru(OH ₂) ₆](tos) ₂ / tppts	H ₂ O	HCO ₂ Na	120	90 h	>40,000	460	n.d. 229,230
RuCl ₂ (DMSO) ₄	–	Et ₃ N	120	> 2.5 h	25,000	18,000	200 231,232
Fe(BF ₄) ₂ /PP ₃	PC		80	19 h	92,400	9425	< 20 233
	dioxane	LiBF ₄	80	9.5 h	984,000	197,000	< 0.5% 234
	dioxane	Et ₃ N	40	10 d	100,000		650 235
	THF	Et ₃ N	65	1 h	2200	5200	n.d. 236
[RuCl ₂ (C ₆ H ₆) ₂]/ dppe		HexNMe ₂	25	264 h	260,000	900	n.d. 237
		DMOA	25	45 d	1,000,000	1000	< 2 238
RuCl ₃ /PPh ₃	H ₂ O/ toluene	SDS	100			100	n.d. 239
	toluene	DBU	100	70 m	1330	1100	< 10 ppm 128
	DMF	Et ₃ N	90	2 h	326,500	257,000	n.d. 132
	DMF	Et ₃ N	90	5 h	1,060,000	250,000	n.d. 132
	dioxane		85	<10 m	> 250	3300	(< 10 240 ppm)

Ru(acac) ₃ /triphos		DMOA	80	7 h	10,000	1500	n.d.	241
		Et ₃ N	25	2 h	490	1960	n.d.	242
[Cp*Ir(OH ₂)(bpm)Ru (bpy) ₂](SO ₄)	H ₂ O	HCO ₂ Na	25	20 m	140	430	n.d.	243
	H ₂ O	HCO ₂ K	25	10 m		1880	n.d.	145
[Cp*Ir(4DHBP)Cl] ⁺	H ₂ O		60 60	4 h	5000	2400 760	n.d. n.d.	244 244
[Cp*Ir(6DHBP)(H ₂ O)] ²⁺	H ₂ O	HCO ₂ Na	60	4.5 h	5300	5440	n.d.	211
[Cp*Ir(N2)(OH ₂)] ²⁺	H ₂ O	HCO ₂ Na	60	6 h	6340	12,200	n.d.	211
[(Cp*IrCl) ₂ (THBPM)] ²⁺	H ₂ O	HCO ₂ Na	90	7 h	165,000	228,000	n.d.	142
[Cp*Ir(N7)(OH ₂)] ²⁺	H ₂ O		80	0.5 h	10,000	34,000	n.d.	210
[Cp*Ir(N9)(OH ₂)] ²⁺	H ₂ O		60	580 h	2,050,000		n.d.	192
	H ₂ O	HCO ₂ Na	60	1.5 h	8700	18000	n.d.	192
[Cp*Ir(N12)(OH ₂)] ²⁺	H ₂ O	HCO ₂ Na	60	0.5 h	7850	32,500	n.d.	192
	H ₂ O	HCO ₂ Na	100	0.5 h	68,000	322,000	n.d.	192
	^t BuOH	Et ₃ N	80	4 h	5000	120,000 ^b	n.d. (100)	125
	dioxane / H ₂ O	HCO ₂ Na	69	4.5 h	1000	286	n.d.	245

^a Insignificant digits are rounded. PP₃ = P(CH₂CH₂PPh₂)₃, PC = propylene carbonate, DMOA = dimethyloctylamine, dppe = 1,2-bis(diphenylphosphino)ethane, tos = *p*-toluene sulfonate, SDS = sodium dodecyl sulfate, triphos = 1,1,1-tris-(diphenylphosphinomethyl)ethane, NP3 = tetradentate tris[2-(diphenylphosphino)ethyl]amine. ^b This TOF is for the first 1 minute. For 4 h, the TOF was 1200 h⁻¹. ^c n.d.: not detected (or not reported).

3.1. Catalysts with phosphine ligands

Pioneering work on FA dehydrogenation using homogenous catalysts was reported by Coffey in 1967.²²⁷ Platinum-metal-based catalysts, e.g., Pt, Ru, and Ir, with phosphine ligands were used in acetic acid at 118 °C. Other catalysts were subsequently reported, but suffered from poor activity and low durability.^{193,246-251} In 2008, Beller²²⁸ and Laurenczy²²⁹ independently reported outstanding examples of catalysts that could be used under mild reaction conditions and evolved H₂ and CO₂ exclusively.

3.1.1. Organic solvent systems. Beller et al. reported the dehydrogenation of a formic acid/Et₃N azeotropic mixture using ruthenium-based catalysts with triphenylphosphine-type ligands. The high initial TOF of 2700 h⁻¹ (initial 20 min) and a TON of 890 (2 h) at 40 °C were obtained with the commercially available ruthenium complex [RuCl₂(PPh₃)₃].²²⁸ The generated hydrogen after removing traces of volatile amines by charcoal was used to drive a H₂/O₂ PEM fuel cell, which provided a maximum electric power of approximately 47 mW at a potential of 374 mV for 29 h. Then the effects of different phosphine ligands, amines, and ruthenium complexes on catalytic activity and durability were investigated.²⁵² The combination of [RuCl₂(C₆H₆)]₂ and a bidentate phosphine ligand, dppe, improved the catalytic performance. The continuous long-term stability of this system, [RuCl₂(C₆H₆)]₂/dppe, was then investigated under both atmospheric and pressurized conditions.^{237,238} Since the presence of an amine is beneficial for hydrogen production, loss of the amine by volatilization led to a decrease in reaction rate. Use of a less volatile amine, DMOA (dimethyloctylamine), resulted in the highest TON of 1,000,000 and a TOF of 1000 h⁻¹ for 1080 h at 25 °C. During the course of the reaction, CO concentration did not exceed 2 ppm. Several examples based on this catalytic system using ruthenium catalysts and an organic amine were reported. Wills reported dehydrogenation of formic acid/amine mixture with

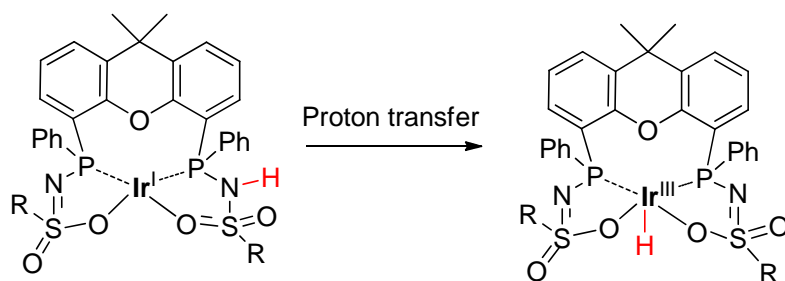
[RuCl₂(DMSO)₄]. Although CO (190–440 ppm) was detected by GC, the high TOF of 18,000 h⁻¹ was observed at 120 °C.²³² They also reported long-term operation under continuous flow conditions. Gas production rates as high as 1.5 L min⁻¹ and total gas production of 462 L were obtained during 6 h.²³¹ Plietker et al. investigated recyclability and long-term stability using a PNNP-Ru complex (Chart 1) in toluene/DBU.¹²⁸ Under pressure-free conditions the DBU formate salt decomposed at 100 °C in the presence of 0.075 mol% of the complex within 70 min. CO impurities were not detectable in the gas mixture down to 10 ppm. Up to five charging-discharging cycles were performed in combination with CO₂ hydrogenation. The concern over the long-term reactions of all the FA/amine systems is the volatility of the amine, which causes contamination of gaseous products and a decrease of reaction rate.

Gonsalvi et al.²⁴¹ adopted *in-situ* complexes using Ru(acac)₃ (acac = acetylacetonate) and facially capping ligands, such as 1,1,1-tris-(diphenylphosphinomethyl)ethane (triphos, Chart 1) and tetradentate tris[2-(diphenylphosphino)ethyl]amine (NP₃, Chart 1), to catalyze the dehydrogenation of formic acid. With 0.01 mol% of the complexes [Ru(κ³-triphos)(MeCN)₃](OTf)₂ or [Ru(κ⁴-NP₃)Cl₂], a TON of 10,000 was obtained after 6 h. Three labile solvent ligands make three coordination sites available for substrate coordination and activation. Moreover, the catalyst (0.1 mol%) could provide a total TON of 8000 after 14 h of continuous reaction at 80 °C with recycling up to eight runs in the presence of OctNMe₂. They also utilized DFT calculations to explore the nature, stability, and activation pathways of the intermediates of this system.²⁵³ For the [Ru(κ³-triphos)(MeCN)₃](OTf)₂ complex, a ligand-centered outer-sphere mechanism incorporating the release of H₂ and CO₂ from the formate ligands without the need of a Ru-hydrido species was illustrated. In contrast, the [Ru(κ⁴-NP₃)Cl₂] complex followed a metal-centered, inner-sphere pathway. Beller and co-workers utilized a

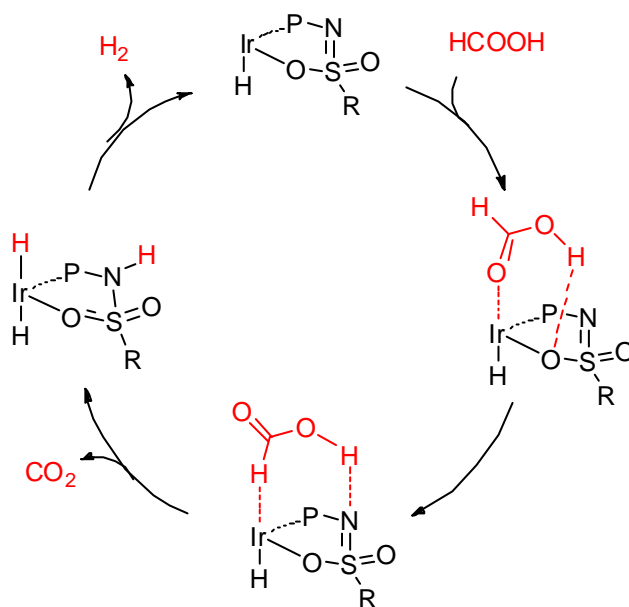
[RuCl₂(benzene)]₂ pre-catalyst and a dppe ligand to catalyze the dehydrogenation of FA.^{237,238,254}

Both temperature and pressure influenced the equilibrium of the reversible reaction, but the influence of temperature was more pronounced.²⁵⁴

Reek et al.^{240,255} reported base-free FA dehydrogenation using iridium complexes with a phosphine-functionalized sulfonamide (bisMETAMORPhos), the anionic form of which can function as an internal base.²⁴⁰ The system produced CO-free H₂ with the TOF of 3270 h⁻¹ in dioxane at 85 °C. The initial Ir(I) complex underwent a slow proton transfer from the neutral ligand arm to the metal, resulting in the formation of the active Ir(III)–H complex (Scheme 10). The bifunctional ligand allowed the direct hydride transfer from FA to the Ir center rather than the common β-hydride elimination. It also facilitated the release of hydrogen (Scheme 11).



Scheme 10. Formation of active species for complex Ir(bisMETAMORPhos) via internal proton transfer, Ref. 240.



Scheme 11. Proposed mechanism for FA dehydrogenation. Redrawn with a part of the bisMETAMORPhos ligand based on Ref. 255.

Enthaler et al. synthesized a novel kind of ruthenium solid catalyst with polyformamidine (PF) as the dual ligand/basic supports in the dehydrogenation of FA in DMF without basic additives.²⁵⁶ The catalyst, denoted $Ru\&PPh_3@PF$, showed higher activity (TON: 325 for 3h) than the unsupported $[RuCl_2(p\text{-cymene})]_2$ (TON: 37) under the same conditions. This is attributed to the dual effect of polyformamidine which functions as both a ligand and a base. However the catalytic activity decreased considerably in recycling experiments owing to leaching of the ruthenium.

3.1.2. Aqueous solvent systems. Another outstanding example of FA dehydrogenation reported by Laurency et al. is an aqueous system of HCO_2H/HCO_2Na using a ruthenium catalyst with a water-soluble phosphine ligand, e.g., $tppts$.^{229,230} The TOF of 460 h^{-1} was observed at $120\text{ }^\circ\text{C}$ without the use of an organic amine, but instead a small amount of the inorganic base HCO_2Na

was used for the activation of the catalyst. Constant hydrogen generation with total TON > 40,000 was achieved by continuous addition of formic acid. Interestingly, gas generation in a closed vessel led to pressurization up to 750 bar. This suggests that the reaction was not inhibited by system pressure. No CO was detected by FTIR analysis (detection limit of 3 ppm). The reaction mechanism was subsequently investigated.^{257,258} Interesting aspects of the mechanism include coordination of formate to Ru followed by β -hydride elimination to a stable CO₂ complex [Ru(H)(H₂O)(η^2 -CO₂)(tppts)₃]. After a series of ligand substitutions, a proposed protonation of the hydride by coordinated formic acid forms a dihydrogen complex which expels H₂ and re-enters the catalytic cycle. Laurency and co-workers also investigated other water-soluble phosphine ligands.^{259,260} A series of ruthenium complexes containing different oligocationic, ammoniomethyl-substituted triarylphosphines was used to catalyze the dehydrogenation of formic acid in aqueous media. A correlation between the catalytic performance and the hydrophilic, electronic, and steric properties of the phosphines was established. Catalyzed by a ruthenium complex with tppta (Chart 1) as the ligand, the dehydrogenation of formic acid proceeded with a TOF of 1950 h⁻¹ with well-defined tppta/Ru ratios of 2:1 and 3:1 at 120 °C. Furthermore, the system of tppta/Ru (2:1) could retain high activity for more than 30 runs by the addition of pure HCO₂H at 90 °C and gave a total TON over 10,000 after 10 h. Gonsalvi and Laurency et al. studied a series of monodentate aryl sulfonated phosphines and selected tetrasulfonated diphosphines with Ru(III) and Ru(II) metal precursors for aqueous-phase formic acid dehydrogenation.²⁶⁰ They found that a higher basicity and hence a stronger σ -donation of the ligands promoted HCO₂H dehydrogenation, while the Ru/ligand ratio did not significantly affect the catalytic performance. The catalytic system of aryl diphosphines (DPPBTS, DPPPTS, DPPETS, Chart 1) exhibited high stability. The MBTS (Chart

1) system showed good recycling capacity and could be used for up to 11 consecutive recharges. Olah investigated the dehydrogenation of FA using ruthenium carbonyl complexes with phosphine ligands in a toluene/water biphasic system.^{239,261} The use of surfactants (e.g., sodium dodecyl sulfate or alkylammonium salts) to form emulsions provided a medium in which the active catalyst could be formed in-situ from water soluble RuCl_3 and formate and water insoluble PPh_3 . While the surfactant was not required for catalysis, approximately 7-fold enhancement in activity was observed in its presence. Characterization studies by NMR and IR spectroscopy and X-ray crystallography revealed $[\text{Ru}(\text{PPh}_3)_2(\text{CO})_2(\text{HCO}_2)]$, $[\text{Ru}(\text{PPh}_3)_3(\text{CO})_2]$, and binuclear $[\text{Ru}_2(\text{PPh}_3)_2(\text{CO})_4(\mu\text{-HCO}_2)_2]$ as products of the emulsion synthesis. In all mechanistic investigations, caution is needed when presuming stable isolated species are active catalysts or intermediates. In this case the authors tested authentic samples of each isolated complex for formic acid dehydrogenation and found very low activity (< 2% of the best reaction) suggesting minimal contribution to the overall catalysis. Joó et al. found that addition of sodium formate can improve the reaction rate of the hydrogenation of itaconic acid with $\text{Na}_2[\text{Ir}(\text{bmim})(\eta^4\text{-cod})(\text{tppts})]$ in water.²⁶² Moreover, CO_2 was detected in the gas phase. This result indicated that the stable NHC-Ir complex is capable of decomposing formate in aqueous solution.

3.2. Catalysts with pincer-type ligands

Milstein's pincer complexes are extraordinary catalysts for FA dehydrogenation as well as CO_2 hydrogenation owing to the functional PNP ligands. The combination of pincer ligands with non-precious metals is discussed in the following section. Milstein et al. reported a very rare rhenium-based PNP pincer complex $[\text{Re}(\text{CO})_2(\text{P4})]$ (Chart 2)²⁶³ that showed similar behavior to the Ru congeners they previously reported.¹⁷⁸ The dearomatized $[\text{Re}(\text{CO})_2(\text{P4})]$ could generate aromatized $[\text{ReH}(\text{CO})_2(\text{P3})]$ and $[\text{Re}(\text{CO})_2(\text{P5})]$ via a [1,3]-addition with H_2 and CO_2 ,

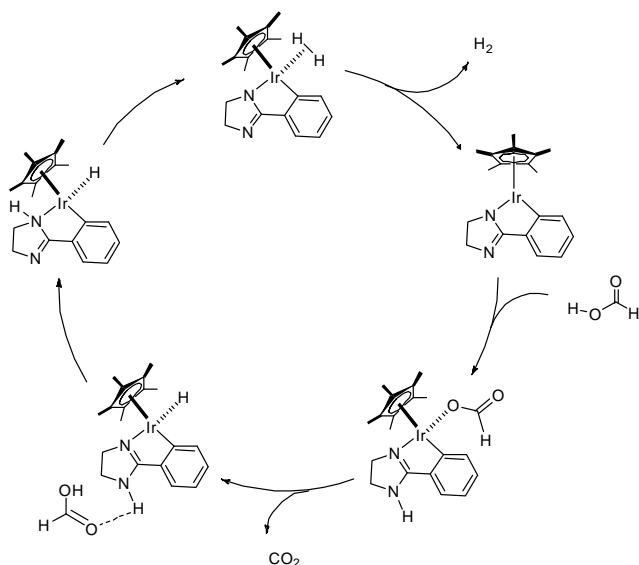
respectively, to the Re and the exo-cyclic methine carbon through metal-ligand cooperation. A formate complex $[\text{Re}(\text{CO})_2(\text{P3})(\text{OCHO})]$ was obtained by the reaction of the $[\text{Re}(\text{CO})_2(\text{P4})]$ with formic acid. The formate complex $[\text{Re}(\text{CO})_2(\text{P3})(\text{OCHO})]$ could liberate CO_2 at high temperature and generate the hydride complex $[\text{ReH}(\text{CO})_2(\text{P3})]$, which reformed the formate complex by reaction with formic acid. When dehydrogenation of FA (11.7 mmol) was carried out using $[\text{Re}(\text{CO})_2(\text{P3})(\text{OCHO})]$ (0.03 mol%) in dioxane at 120 °C in the absence of base, CO_2 and H_2 were evolved without CO generation. Elevating the temperature to 180 °C shortened the reaction time from 48 to 1 h. The FA dehydrogenation and transformation between these complexes requiring much higher temperature than the Ru analogues suggests that the Re binds the substrates much more strongly. The highly efficient PNP-Ir catalyst for CO_2 hydrogenation reported by Nozaki et al. also dehydrogenated formic acid in aqueous media.¹²⁵ However, the activity declined in the presence of water, unlike the case of CO_2 hydrogenation. The high TOF of 120,000 h^{-1} over the initial 1 min was obtained in *t*BuOH in the presence of Et_3N . Pidko et al. reported the PNP-pincer complex $[\text{RuH}(\text{Cl})(\text{CO})(\text{P3})]$ is highly active for CO_2 hydrogenation as well as the FA dehydrogenation in DMF/ Et_3N . A high TOF of 257,000 h^{-1} and TON of 1,063,000 (for 5 h) were achieved with continuous addition of FA at 90 °C in separate experiments.^{131,132,186} The loss of volatile Et_3N at 90 °C is a major problem for this system. When non-nucleophilic DBU is used, the TOF decreased apparently to 93,100 h^{-1} .

3.3. Catalysts with bidentate *C,N*-/*N,N*-ligands

In 2008, Fukuzumi et al. reported FA dehydrogenation in aqueous solutions with half-sandwich complexes with bidentate 2,2'-bipyridine derivatives.²⁶⁴ With the addition of HCO_2Na , the system gave a TON of 30 in 2 h at pH 3.8. The water-soluble heterodinuclear iridium-ruthenium complex $[\text{Cp}^*\text{Ir}(\text{OH}_2)(\text{bpm})\text{Ru}(\text{bpy})_2](\text{SO}_4)_2$ (bpm: 2,2'-bipyrimidine), which gave an

initial TOF of 426 h^{-1} for 20 min at room temperature in $\text{HCO}_2\text{H}/\text{HCO}_2\text{Na}$ at pH 3.8, was reported by Fukuzumi and co-workers.²⁴³ More recently, they demonstrated the dehydrogenation of formic acid using a *C,N*-cyclometallated organo iridium complex bearing a proton-responsive carboxylic acid.¹⁴⁵ A maximum TOF of 1880 h^{-1} was obtained at pH 2.8 and $25 \text{ }^\circ\text{C}$.

Xiao reported that *C,N*-cyclometallated iridium complexes based on 2-aryl imidazoline ligands were highly efficient catalysts for FA dehydrogenation in Et_3N .²⁴² The initial TOF of $147,000 \text{ h}^{-1}$ was obtained at $40 \text{ }^\circ\text{C}$ for 10 sec without CO formation. The suggested rate-limiting step was hydride protonation, which involves participation of both formic acid and the distal NH functional group in the imidazoline moiety (Scheme 12). As proof, methylation of the NH functionality deactivated the imidazoline-based catalysts. Himeda et al. reported half-sandwich complexes $[\text{Cp}^*\text{IrL}(\text{OH}_2)]^{2+}$ ($\text{L} = \text{N}3 - \text{N}7$) for FA dehydrogenation in aqueous solutions.²¹⁰ The tetramethyl substituted biimidazole complex was the most effective and produced the high TOF of $34,000 \text{ h}^{-1}$ at $80 \text{ }^\circ\text{C}$ in 1 M FA solution. Ward and co-workers synthesized and evaluated a series of known half-sandwich complexes.²⁶⁵ They found that $[\text{Cp}^*\text{Ir}(\text{pz})(\text{OH}_2)]^+$ ($\text{pz} = 1$ -phenylpyrazole) showed comparable activity to the most effective $[\text{Cp}^*\text{Ir}(\text{pzCO}_2\text{H})(\text{OH}_2)]^+$ and $[\text{Cp}^*\text{Ir}(\text{N}7)(\text{OH}_2)]^{2+}$ complexes. The proton-responsive *N,N*-chelated complexes developed by Himeda and co-workers are among the most effective catalysts for FA dehydrogenation owing to several unique properties. The studies of these proton-responsive complexes are described in the following section.



Scheme 12. Proposed catalytic cycle for the FA dehydrogenation. Reproduced from Ref. 242 with permission from The Royal Society of Chemistry.

3.4 Half-sandwich catalysts with/without proton-responsive ligands

3.4.1. Electronic effects. Recently, significant progress in formic acid dehydrogenation with half-sandwich complexes bearing a proton-responsive N,N - or C,N -chelating ligand has been achieved.^{145,244} The electronic effect of the substituents in iridium complexes has been investigated in the context of formic acid dehydrogenation in acidic solutions.^{141,244} Note that the hydroxy-substituted complexes exist in their protonated forms in acidic solution. The TOF of $[\text{Cp}^*\text{Ir}(\text{4DHBP})(\text{OH}_2)]^{2+}$ with hydroxy groups ($\sigma_p^+ = -0.91$) at the 4- and 4'-positions was about 90 times higher than that of the unsubstituted analogue, $[\text{Cp}^*\text{Ir}(\text{bpy})(\text{OH}_2)]\text{SO}_4$ (Figure 7). Hammett plots indicated that the initial TOF values correlate well with the Hammett constants of the substituents on the ligands. The tendency is similar to that for CO_2 hydrogenation, indicating that an electron-donating ligand can improve the activity of the complex for both CO_2 hydrogenation and FA dehydrogenation.

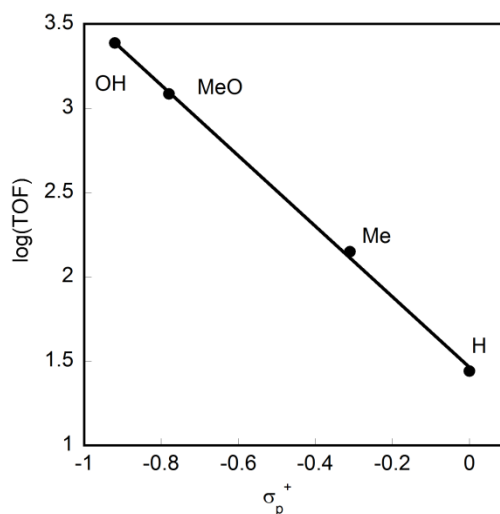


Figure 7. Hammett plot of the initial TOF vs. σ_p^+ value of the substituent (R) for a series of complexes: $[\text{Cp}^*\text{Ir}(4,4'\text{-R}_2\text{-bpy})(\text{OH}_2)]\text{SO}_4$ (R = OH, OMe, Me, H). The reaction was carried out in the presence of catalysts (0.5–2.0 mM) at 60 °C in 10 mL of 1 M HCO_2H . Redrawn based on Ref. 244.

Recently, Himeda's group has incorporated electron-rich azole ligands (N3 - N7, Chart 4) into the design of new catalysts, $[\text{Cp}^*\text{Ir}(\text{Nn})(\text{OH}_2)]^{2+}$ (n = 3 - 7).²¹⁰ Complex $[\text{Cp}^*\text{Ir}(\text{N7})(\text{OH}_2)]^{2+}$ (N7 = tetramethyl biimidazole) showed excellent activity (TOF: 34,000 h^{-1} at 80 °C) that is higher than the TOF value of any other mononuclear complex yet reported for formic acid dehydrogenation. Although the electron-donating ability of the azole ligand is sufficient for activation of the catalyst in formic acid dehydrogenation, these complexes are not so effective in catalyzing CO_2 hydrogenation under basic conditions.²¹⁰ By comparing azole complexes with OH-substituted complexes, it is apparent that OH-substituted complexes offer more advantages through their tunable activity and their capability to efficiently catalyze the reactions in both directions in the interconversion of CO_2/H_2 and formic acid under different pH conditions.

3.4.2. Pendent-base effect changing RDS of formic acid dehydrogenation. The proton-responsive complexes also allowed tunable activity in formic acid dehydrogenation. Interestingly, the pH dependence of the reaction rate was markedly different for different complexes. $[\text{Cp}^*\text{Ir}(\text{6DHBP})(\text{OH}_2)]^{2+}$, $[\text{Cp}^*\text{Ir}(\text{N}_2)(\text{OH}_2)]^{2+}$, and $[(\text{Cp}^*\text{IrCl})_2(\text{THBPM})]^{2+}$ bearing OH groups at the *ortho* position exhibited bell-shaped rate vs. pH profiles (Figure 8).²¹¹ The initial TOF peaks around pH 4.0, close to the $\text{p}K_a$ values of the complex (i.e., ligand OH groups) and formic acid. Himeda et al. proposed that these results are due to the combined effect of the deprotonation of the OH groups on the ligands (i.e., electronic effect) and the ionization of formic acid with increasing solution pH. The deprotonation of the OH generates the much stronger electron-donating $-\text{O}^-$ (phenoxide) at relatively higher pH, and thereby improves the activity of the complex. On the other hand, an increase in formate concentration also contributes to the improvement of the reaction rate via affecting the catalytic process (Step I, Scheme 13). In contrast, complexes bearing no pendent OH groups, such as complex $[\text{Cp}^*\text{Ir}(\text{4DHBP})(\text{OH}_2)]^{2+}$, $[\text{Cp}^*\text{Ir}(4,4'-(\text{MeO})_2\text{-bpy})(\text{OH}_2)]^{2+}$, and $[\text{Cp}^*\text{Ir}(6,6'-(\text{MeO})_2\text{-bpy})(\text{OH}_2)]^{2+}$, showed a strikingly different pH dependence from that of complexes $[\text{Cp}^*\text{Ir}(\text{6DHBP})(\text{OH}_2)]^{2+}$, $[\text{Cp}^*\text{Ir}(\text{N}_2)(\text{OH}_2)]^{2+}$, and $[(\text{Cp}^*\text{IrCl})_2(\text{THBPM})]^{2+}$ (Figure 8). The initial TOF of these complexes merely decreased with increasing solution pH. This tendency suggests that the proton concentration in the reaction solution exhibited a much more important effect on the reaction rate (via Step III, Scheme 13) for $[\text{Cp}^*\text{Ir}(\text{4DHBP})(\text{OH}_2)]^{2+}$. These results indicate that the different pH dependence between $[\text{Cp}^*\text{Ir}(\text{4DHBP})(\text{OH}_2)]^{2+}$ and complexes with the *ortho* OH $[\text{Cp}^*\text{Ir}(\text{6DHBP})(\text{OH}_2)]^{2+}$ and $[\text{Cp}^*\text{Ir}(\text{N}_2)(\text{OH}_2)]^{2+}$ may be associated with their different catalytic mechanisms.

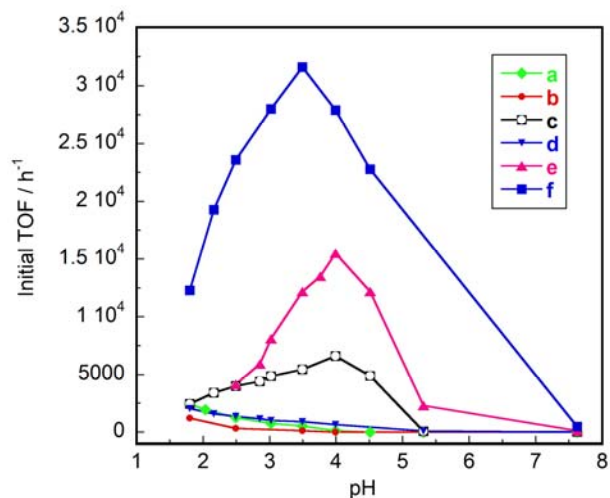


Figure 8. The pH dependence of the formic acid dehydrogenation rate using a) $[\text{Cp}^*\text{Ir}(\text{4DHBP})(\text{OH}_2)]^{2+}$; b) $[\text{Cp}^*\text{Ir}(\text{4,4'-(MeO)}_2\text{-bpy})(\text{OH}_2)]^{2+}$; c) $[\text{Cp}^*\text{Ir}(\text{6DHBP})(\text{OH}_2)]^{2+}$; d) $[\text{Cp}^*\text{Ir}(\text{6,6'-(MeO)}_2\text{-bpy})(\text{OH}_2)]^{2+}$; e) $[\text{Cp}^*\text{Ir}(\text{N}_2)(\text{OH}_2)]^{2+}$; and f) $[(\text{Cp}^*\text{IrCl})_2(\text{THBPM})]^{2+}$ in 10 mL $\text{HCO}_2\text{H}/\text{HCO}_2\text{Na}$ solution (1 M) at 60 °C. The solution pH is adjusted by changing the ratio of HCO_2H and HCO_2Na while keeping their total concentration constant (1 M). Reprinted with permission from Ref. 211. Copyright (2014) WILEY-VCH Verlag GmbH & Co, KGaA, Weinheim with slight modifications.

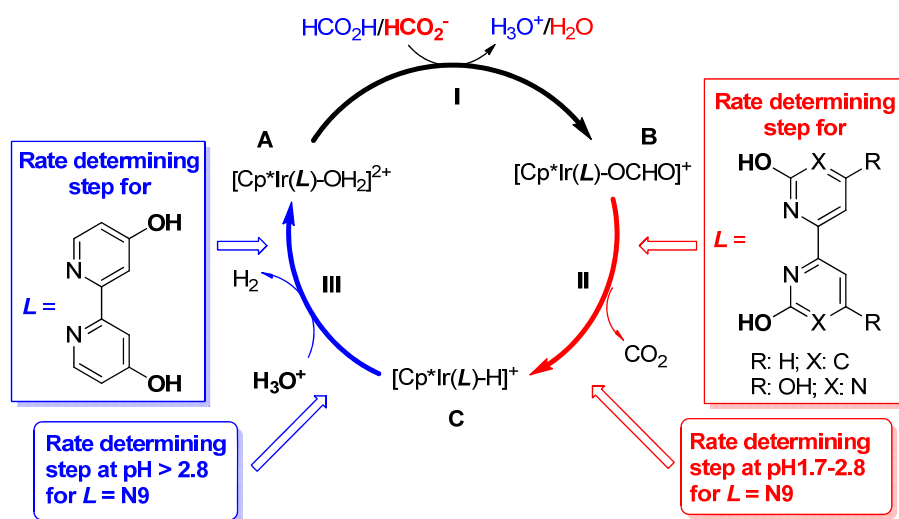
Formic acid dehydrogenation generally proceeds through three steps (Scheme 13): formation of a formate complex **B** (Step I), release of CO_2 via β -hydride elimination to generate the Ir hydride complex **C** (Step II), and production of H_2 from the reaction of Ir–H and a proton (Step III). To understand the different pH dependences, Himeda et al. carried out a mechanistic study with KIE experiments using complexes $[\text{Cp}^*\text{Ir}(\text{4DHBP})(\text{OH}_2)]^{2+}$, $[\text{Cp}^*\text{Ir}(\text{6DHBP})(\text{OH}_2)]^{2+}$, and $[\text{Cp}^*\text{Ir}(\text{N}_2)(\text{OH}_2)]^{2+}$. When the substrates or solvents were replaced with deuterated reagents, the reaction rate decreased considerably. For $[\text{Cp}^*\text{Ir}(\text{6DHBP})(\text{OH}_2)]^{2+}$ and $[\text{Cp}^*\text{Ir}(\text{N}_2)(\text{OH}_2)]^{2+}$, the KIE values are about 2 when DCO_2D replaces HCO_2H , while the KIE values are about 1 when D_2O replaces H_2O . These results suggest that the deuterated formate substrate influences the

reaction rate to a greater extent than the deuterated solvent does, indicating that deuterated formate is involved in the rate limiting step. Accordingly, it was proposed that, for $[\text{Cp}^*\text{Ir}(\text{6DHBP})(\text{OH}_2)]^{2+}$ and $[\text{Cp}^*\text{Ir}(\text{N2})(\text{OH}_2)]^{2+}$, the generation of Ir–H from the formate complex (Step II, Scheme 13) should be rate-determining. This is consistent with the previously reported DFT calculations.¹⁴³ Therefore, increasing the solution pH from 2 to 4 could increase the reaction rate (Figure 8, c and e) because it could facilitate the formation of the formate intermediate (**B**) and enhance the rate, consistent with the report of Fukuzumi.²⁴³ The increased reaction rate may be partially due to the deprotonation of the OH groups on the ligand, and consequent increased electron-donating ability with increasing solution pH as discussed above.

In contrast, the KIE experiments with $[\text{Cp}^*\text{Ir}(\text{4DHBP})(\text{OH}_2)]^{2+}$ and proton non-responsive complex $[\text{Cp}^*\text{Ir}(\text{6,6'-(MeO)}_2\text{-bpy})(\text{OH}_2)]\text{SO}_4$ using D_2O in place of H_2O led to higher KIE values (2.1) than when using DCO_2D instead of HCO_2H (1.4).²⁶⁶ Therefore, D_2O or D^+ is most likely involved in the rate determining step. The reaction of Ir–H (**C**) with a proton to release dihydrogen (Step III, Scheme 13) is proposed to be rate-limiting for $[\text{Cp}^*\text{Ir}(\text{4DHBP})(\text{OH}_2)]^{2+}$ and its MeO analogue. Therefore, a higher proton concentration (low pH) will lead to higher reaction rates. The reaction rate will merely decrease with increasing pH of the reaction solution, consistent with the pH dependence that was observed (Figure 8).

As mentioned above in the context of CO_2 hydrogenation, the pendent $-\text{O}^-$ facilitates the heterolysis of H_2 by forming a proton relay incorporating a H_2O molecule.^{143,146} Thus in the reverse reaction, under acidic conditions, a water molecule and a hydroxy group at the *ortho* position can also form a proton relay and assist the reaction of Ir–H with a proton. The proton relay stabilizes the Ir– H_2 transition state, lowering the free-energy barrier for generating H_2 (Step III, Scheme 13). Consequently, the β -hydride elimination of the formate complex (Step II)

becomes the rate limiting step for the complexes bearing OH groups at *ortho* positions. In contrast, proton non-responsive complexes and complex $[\text{Cp}^*\text{Ir}(\text{4DHBP})(\text{OH}_2)]^{2+}$ bearing no pendant bases have a relatively higher free-energy barrier for generating H_2 from the Ir–H and a proton (Step III), which remains rate limiting. Therefore, the different position of OH groups in complexes $[\text{Cp}^*\text{Ir}(\text{4DHBP})(\text{OH}_2)]^{2+}$ and $[\text{Cp}^*\text{Ir}(\text{6DHBP})(\text{OH}_2)]^{2+}$ results in the RDS changing and consequently to a different pH dependence.



Scheme 13. Proposed mechanism and rate determining step changes influenced respectively by solution pH and complexes with and without OH in *ortho* positions in formic acid dehydrogenation. Redrawn based on Refs. 192,211.

3.4.3. Solution pH changing RDS of formic acid dehydrogenation. The above-mentioned KIE studies were limited to the regime in which the reaction rates were increasing (see Figure 8). The KIE results can explain the rate increase with increasing solution pH, but cannot explain the reaction rate decrease with further increase of solution pH. The high catalytic activity of these

complexes at low pH and high pH above and below the peak motivated further studies of the KIE values at pH values on both sides of the peak of the bell-shaped activity curve. Accordingly, a KIE study was performed with complex $[\text{Cp}^*\text{Ir}(\text{N9})(\text{OH}_2)]^{2+}$, for which activity peaked at pH 2.8 as shown in the pH vs. rate profile (Figure 9).¹⁹² The KIE experiments were carried out in 1 M formic acid solution (pH 1.7) and 1 M $\text{HCO}_2\text{H}/\text{HCO}_2\text{Na}$ (1/1) solution (pH 3.5). The results suggest that at pH 1.7 DCO_2D (KIE: 2.04) is more influential than D_2O (KIE: 1.46) on the reaction rate. Therefore, the β -hydride elimination step (Scheme 13, Step II), which involves Ir–D bond formation when DCO_2D is used, was designated as the rate-determining step. This result was consistent with the results for complex $[\text{Cp}^*\text{Ir}(\text{6DHBP})(\text{OH}_2)]^{2+}$. When a KIE study was carried out at pH 3.5 using $\text{HCO}_2\text{H}/\text{HCO}_2\text{Na}$ in the ratio of 1/1, the results were surprising. The KIE value (2.70) using D_2O is higher than that (1.48) using $\text{DCO}_2\text{D}/\text{DCO}_2\text{Na}$, suggesting that H_2O or H_3O^+ is involved in the rate determining step. Therefore, as shown in Scheme 13, the RDS should be the H_2 bond formation (Step III) when $\text{pH} > 2.8$. DFT calculations also supported the KIE results. The calculated KIE values follow the same trends as the experiments shown. More importantly, the calculated free energies of activation for the β -hydride elimination and H_2 generation steps showed a clear reversal in magnitude upon changing the solution pH from 1.7 to 3.5. The experimentally observed dependence of KIEs on pH, taken together with the calculated KIEs, supported the notion of a change in rate determining step from β -hydride elimination to H_2 generation with increasing pH.

Based on the previous results that complexes with five-membered azole ligands are effective for FA dehydrogenation owing to their high electron donating abilities, Himeda's group recently designed a series of new catalysts by combining azole and pyridine or pyrimidine moieties bearing pendent OH groups (N9 - N12, Chart 4).¹⁹² The pH-dependent initial TOFs of these

catalysts for FA dehydrogenation reaction (Figure 9) resemble those of $[\text{Cp}^*\text{Ir}(\text{6DHBP})(\text{OH}_2)]^{2+}$ and $[\text{Cp}^*\text{Ir}(\text{N2})(\text{OH}_2)]^{2+}$ (Figure 8). Moreover, these complexes showed extraordinary stability and activity for FA dehydrogenation in water. The highest TOF of $332,000 \text{ h}^{-1}$ was achieved in 4 M $\text{HCO}_2\text{H}/\text{HCO}_2\text{Na}$ (7/3) with complex $[\text{Cp}^*\text{Ir}(\text{N12})(\text{OH}_2)]^{2+}$. Using $[\text{Cp}^*\text{Ir}(\text{N9})(\text{OH}_2)]^{2+}$ in 8 MPa at $100 \text{ }^\circ\text{C}$, a TON $> 400,000$ and TOF of $173,000 \text{ h}^{-1}$ were obtained in 4 h. The TOF was increased to $269,000 \text{ h}^{-1}$ in 4 M $\text{HCO}_2\text{H}/\text{HCO}_2\text{Na}$ (98/2). An unprecedented TON of more than 2,050,000 was achieved in a 6 M FA solution with addition of FA (50 wt%) after 167 h at $60 \text{ }^\circ\text{C}$ over 580 h. This catalyst currently represents the most durable and highest performing FA dehydrogenation catalyst in water.

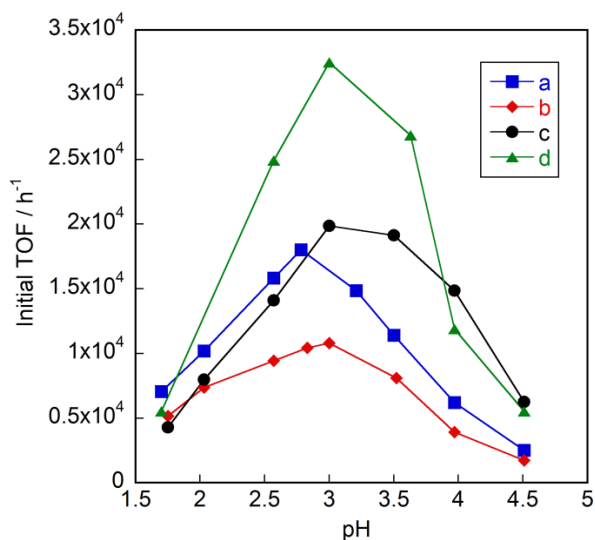
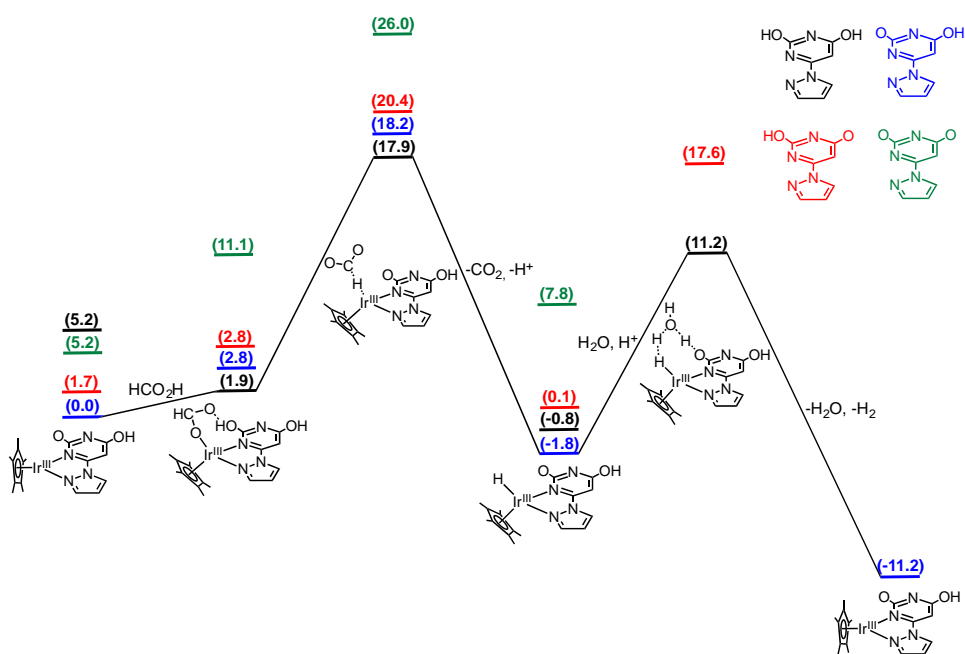


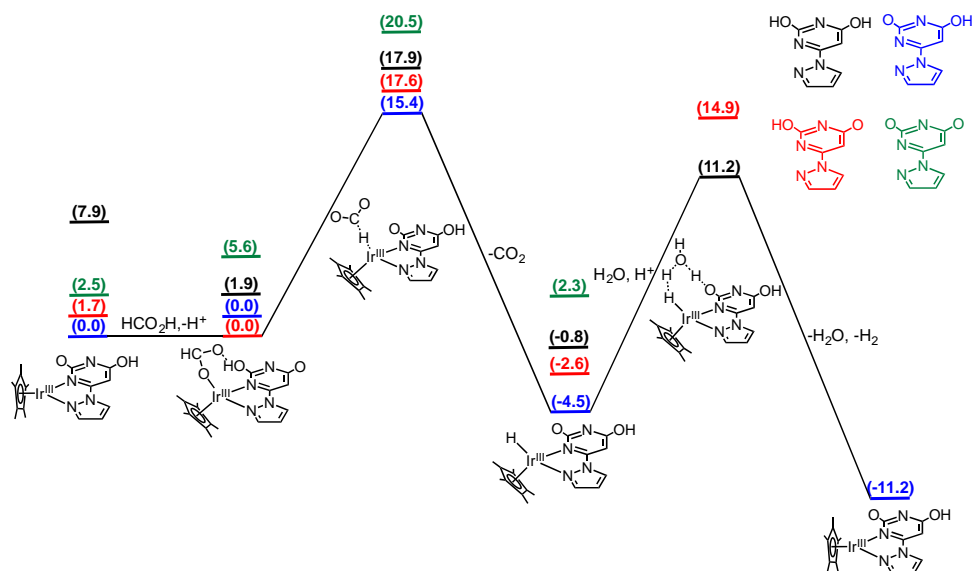
Figure 9. pH dependence of FA dehydrogenation using $100 \mu\text{M}$ complex (a) $[\text{Cp}^*\text{Ir}(\text{N9})(\text{OH}_2)]^{2+}$, (b) $[\text{Cp}^*\text{Ir}(\text{N10})(\text{OH}_2)]^{2+}$, (c) $[\text{Cp}^*\text{Ir}(\text{N11})(\text{OH}_2)]^{2+}$, (d) $[\text{Cp}^*\text{Ir}(\text{N12})(\text{OH}_2)]^{2+}$ in 1 M $\text{HCO}_2\text{H}/\text{HCO}_2\text{Na}$ (10 mL) solution at $60 \text{ }^\circ\text{C}$. Ref. 192.

Another aspect of the role of pH on the control of catalytic hydrogenation/dehydrogenation reactions has recently been explored theoretically by Wang et al.¹⁹² In addition to the effect of

pH on the thermochemistry of reaction steps that consume or release a proton, the concept of speciation at each step of the reaction mechanism was examined. In particular, at a given pH (e.g., the pH of the relevant experiment) catalyst species in different protonation states may co-exist in solution, especially when the solution pH is near the average pK_a of the protonated hydroxy-substituted ligand. It was assumed that fast equilibration among protonation sites with comparable pK_a values could occur on the longer timescale of catalytic steps with large free-energy barriers such as the β -hydride elimination/ CO_2 insertion and H_2 formation/ H_2 heterolysis steps in the catalytic mechanism. With that assumption, the relevant protonation species at a given step is simply the one with the lowest free energy. This is illustrated in Schemes 14 and 15 for the case of FA dehydrogenation by $[\text{Cp}^*\text{Ir}(\text{N}9)(\text{OH}_2)]^{2+}$.



Scheme 14. Proposed mechanism for HCO_2H dehydrogenation by $[\text{Cp}^*\text{Ir}(\text{N}9)(\text{OH}_2)]^{2+}$ at pH 1.7 and 333.15 K. The relative free energies are reported in units of kcal mol^{-1} . Ref. 192.



Scheme 15. Proposed mechanism for HCO₂H dehydrogenation by [Cp*Ir(N9)(OH)₂]²⁺ at pH 3.5 and 333.15 K. The relative free energies are reported in units of kcal mol⁻¹. Ref. 192.

In the energetic analysis of the proposed FA decomposition catalytic cycle, the free energies associated with the most stable species for each reaction intermediate as shown in Schemes 14 and 15 connected by a solid black line were used. The color code for the protonation state of the various entries at each step is shown by the color of the structures in the upper right corner of each figure. The calculated free energies of activation, ΔG^\ddagger , at pH 1.7 for the β -hydride elimination and H₂ generation steps were 16.0 and 13.0 kcal mol⁻¹, respectively, indicating that the former is the rate-determining step (Scheme 14). On the other hand, at pH 3.5 the ΔG^\ddagger s were 15.4 kcal mol⁻¹ for β -hydride elimination and 15.7 kcal mol⁻¹ for H₂ generation, indicating that the latter was becoming the rate-determining step as the pH was increased (Scheme 15). These calculated data indicate that β -hydride elimination is the rate-determining step at low pH, but the free-energy cost for H₂ generation increases with increasing pH. The catalyst exhibits the highest rate at moderate pH when the ΔG^\ddagger s of the two steps are about the same, consistent with the experimental observation of the bell shaped pH vs. rate profile (Figure 9) and, as suggested by

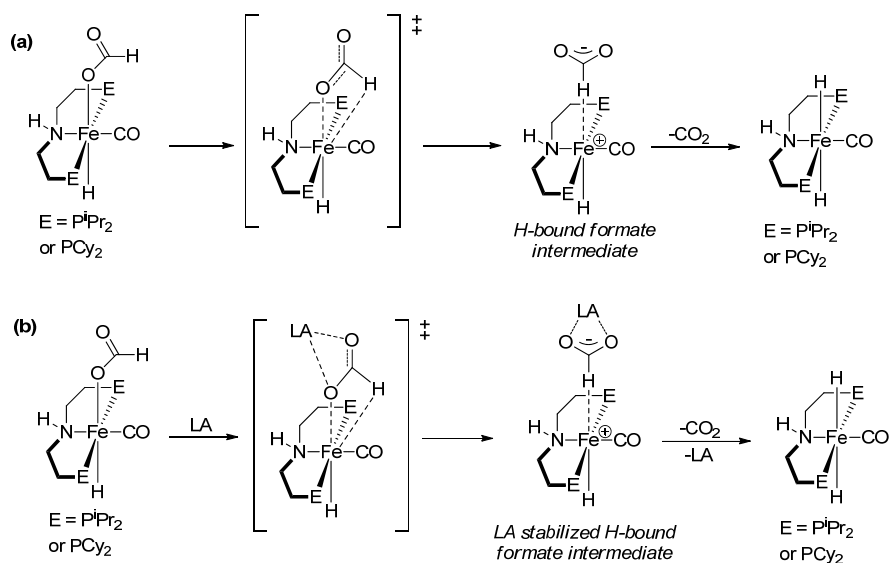
the KIE experiments, the H₂ generation step becoming rate-determining with a further increase in pH.

3.5. Non-precious metals

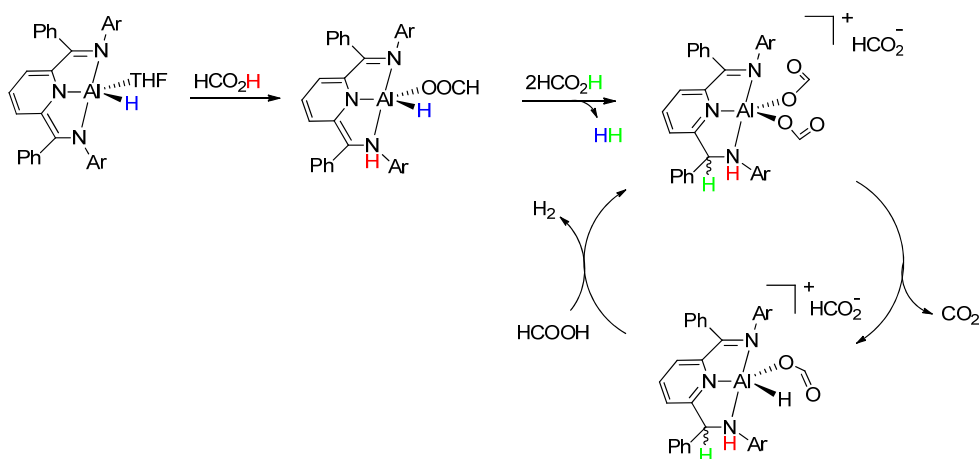
Most catalysts used for the transformation of CO₂ contain precious metals such as Ir, Rh, Ru, etc. In order to decrease the catalyst cost, a number of catalysts with earth-abundant metals have been developed. In 2009, Wills reported results of screening tests using CoCl₂, FeCl₃, FeCl₂, and NiCl₂ in FA/Et₃N at 120 °C.²³² Later Beller investigated various non-precious metal-base complexes under photolytic conditions.²⁶⁷ The use of an *in-situ* catalyst from [Fe₃(CO)₁₂] with triphenylphosphine and 2,2':6'2''-terpyridine in FA/Et₃N (5:1) yielded the TON of 1266 after 51 h.²⁶⁸ Unfortunately, the catalyst systems showed low activity and poor selectivity. The activity and stability of the iron-based catalyst was improved significantly by using a tetradentate phosphine ligand (PP₃: P(CH₂CH₂PPh₂)₃). The very high TOF of 9425 h⁻¹ and TON of 92,417 at 80 °C were observed in propylene carbonate without further additives.²³³ Subsequently, they reported the results of a detailed investigation of the effect of various ligands, metal salts, solvent, and additives (e.g., chloride, fluoride, formate).²⁶⁹ The addition of water resulted in a decrease in catalytic activity. The iron η²-formate [Fe(η²-O₂CH)(PP₃)] was identified as the key active species for the catalysis by DFT and spectroscopic investigations (IR, Raman, UV-vis, XAS); however, this active species was deactivated in the presence of chloride ions. Subsequently, Yang and Ahlquist et al. reported the mechanism of the FA dehydrogenation catalyzed by [FeH(PP₃)]⁺ through DFT calculations. Yang et al.²⁷⁰ showed that the β-hydride elimination process is the rate-limiting step, and the neutral pathway beginning with direct hydrogen transfer from HCO₂⁻ to Fe is less beneficial than the β-hydride elimination pathway, while Ahlquist et al.²⁷¹ considered that the neutral pathway is the appropriate one. They also proposed that only

one site is used despite there being two possible active sites on the catalyst, as one of the hydrides is not involved in the reaction.

Milstein et al.^{235,263} applied iron-based PNP pincer complexes [*t*-Bu-PNP)Fe(H)₂(CO)] (*t*-Bu-PNP = 2,6-bis(di-*tert*-butylphosphinomethyl)pyridine) as catalysts for the dehydrogenation of FA. The reaction in dioxane in the presence of 50 mol% Et₃N at 40 °C led to a total TON of 100,000 in 10 days. The poor activity in water is likely to be due to low solubility of the catalyst. Hazari's and Schneider's groups²³⁴ reported Lewis acid assisted FA dehydrogenation catalyzed by iron-based PNP pincer complexes Fe(^RPN^HP) (^RPN^HP = HN{CH₂CH₂(PR₂)}₂; R = *i*Pr or Cy, see Scheme 16a) in dioxane without the need for an external base. The presence of Lewis acid (LA) co-catalysts provided the high TOF of 196,700 h⁻¹ and TON of 1,000,000 in 9.5 h in dioxane at 80 °C. Unfortunately, CO (less than 0.5%) was detected in the produced gas mixture. Scheme 16b shows the LA assisted decarboxylation of a key iron formate intermediate.²³⁴ Berben et al. reported that aluminum pincer complexes with the phenyl-substituted bis(imino)pyridine (^{Ph}I₂P) ligands showed the high initial TOF of 5200 h⁻¹ in Et₃N/THF at 65 °C without CO production.²³⁶ They characterized each of the elementary steps in the catalytic cycle. The complex (^{Ph}I₂P²⁻)Al(THF)H reacted with 3 eq. of HCO₂H to afford the doubly protonated species as a resting state. They proposed that β-hydride elimination from the doubly protonated form affords an Al-H intermediate, which smoothly releases H₂ upon protonation (Scheme 17).²³⁶



Scheme 16. Proposed pathways for decarboxylation in absence and presence of a Lewis acid (LA). Ref. 234. Copyright 2014 American Chemical Society.



Scheme 17. Proposed mechanism for FA dehydrogenation by $(\text{PhI}_2\text{P}^{2-})\text{Al}(\text{THF})\text{H}$ based on Ref. 236.

4. Interconversion of CO₂ and Formic acid

Although the concept using CO₂ for hydrogen storage was proposed about thirty years ago,²¹⁶ an efficient hydrogen storage cycle using CO₂ has remained an elusive challenge. Through the

significant progress in CO₂ hydrogenation and FA dehydrogenation, the interconversion between CO₂/H₂ and formic acid/formate appears to be the most promising strategy. However, catalysts capable of promoting both reactions are quite limited. Moreover, *efficient* catalysts for both reactions have scarcely been reported.

4.1. Background

In 1994, Leitner and coworkers²⁵¹ reported the first reversible hydrogen storage process using a FA/Et₃N/acetone system with the *in-situ* catalyst [Rh(cod)(μ-Cl)₂]/dppb (dppb = 1,2-bis(diphenylphosphino)butane). The CO₂ hydrogenation exhibited a TOF of 54 h⁻¹ under 40 atm H₂/CO₂ (1/1) and the FA dehydrogenation gave a TOF of 30 h⁻¹ at room temperature. The rate was low; only one and a half cycles were achieved after 90 h. Puddephatt and coworkers used a dinuclear Ru complex [Ru₂(μ-CO)(CO)₄(μ-dppm)₂] for CO₂ hydrogenation in the presence of Et₃N and obtained a TON of 2160 after 21 h under 1020 psi of H₂/CO₂ (1/1) in acetone at room temperature.²⁴⁷ For the dehydrogenation of FA, the reaction rate is about 70 h⁻¹ at 20 °C.²⁷² Although the dinuclear complex could catalyze both reactions, no consecutive reversible reaction was examined. The Nozaki group has reported one of the most efficient CO₂ hydrogenation to formate systems using a PNP-Ir pincer complex in H₂O/THF with KOH as a base. However, this catalyst is not effective for the reverse reaction using the same solvents and additives.¹²⁵ When employing the organic base triethanolamine (TEOA), the catalyst could promote both reactions in water, albeit with a significant decrease in the catalytic performance. For instance, when TEOA was used instead of KOH, the maximum TOF decreased from 73,000 to 14,000 h⁻¹ for CO₂ hydrogenation. For FA dehydrogenation, the reaction could proceed when NaOH was replaced with TEOA, although the TOF was only 1000 h⁻¹.

4.2. Reversible H₂ storage controlled by temperature or pressure

Using [RuCl₂(C₆H₆)₂]₂ and dppm, Beller and co-workers studied the hydrogenation of bicarbonates and carbonates in H₂O/THF and dehydrogenation of formate in H₂O/DMF.²⁷³ The hydrogenation of bicarbonate alone with 80 bar H₂ at 70 °C gave a TON of 1108 after 2 h. The TON was improved to 1731 with the addition of 30 bar CO₂ and a decrease in H₂ pressure to 50 bar. Upon using sodium carbonate instead of sodium bicarbonate under 80 bar H₂/CO₂ (5/3), the TON decreased to 1038. Furthermore, when LiOH, NaOH or KOH was used as a base additive, LiOH gave the best TON. These results suggested that, in addition to the catalyst, a base additive should be carefully selected in order to achieve high performance. The dehydrogenation of formate using the same catalyst was performed at 60 °C in DMF/H₂O (20/5 mL) by varying the cations including Li⁺, Na⁺, K⁺, Mg²⁺ and Ca²⁺. Lithium formate gave the highest TOF of 2923 h⁻¹, while the released gas contained 33.7% CO₂ which was higher than the case of HCO₂Na (8.3%). Therefore HCO₂Na was selected as a substrate despite the TOF being slightly lower (2592 h⁻¹). Two sets of consecutive hydrogenation/dehydrogenation sequences were demonstrated. In sequence I, the dehydrogenation of sodium formate in DMF/H₂O (v/v 4/1) produced more than 90% conversion, while the following hydrogenation of sodium bicarbonate with 80 bar H₂ in THF/H₂O (v/v 1/2) gave back sodium formate with 80% yield. In sequence II, the first hydrogenation of bicarbonate afforded formate with 95% yield, and the following dehydrogenation reverted back to sodium bicarbonate and H₂ with 80% yield. Since the dehydrogenation/hydrogenation reactions used different organic solvents and water, it was necessary to remove solvents before the next step.

To couple these two half-cycles easily, Joó et al. used water soluble $[\text{RuCl}_2(\text{tppms})_2]_2$ to perform the hydrogenation of bicarbonate and dehydrogenation of formate in pure aqueous solution without organic co-solvents.²⁷⁴ For the dehydrogenation of sodium formate, the complex gave a TON of 120 at 80 °C in 1 h corresponding to a 47% yield. The combination of the two half-cycles was demonstrated in an NMR scale reaction using $[\text{RuCl}_2(\text{tppms})_2]_2/\text{tppms}$ in aqueous $\text{NaH}^{13}\text{CO}_3$. The hydrogenation gave $\text{H}^{13}\text{CO}_2\text{Na}$ with a yield of 90% at 83 °C and 100 bar in 200 min. Subsequently, the dehydrogenation was initiated by releasing the pressure and heating to 83 °C. As expected, 40–50% of the formate was converted back to H_2/CO_2 , which suggests that half the H_2 storage capacity of this system can be utilized. The hydrogenation/dehydrogenation cycle was repeated three times in 2.5 days.

Fachinetti first reported the hydrogenation of CO_2 in the presence of Et_3N to give a $\text{HCO}_2\text{H}/\text{Et}_3\text{N}$ adduct using a $[\text{RuCl}_2(\text{PMe}_3)_4]$ complex without solvents.²⁷⁵ A $\text{HCO}_2\text{H}/\text{Et}_3\text{N}$ adduct with acid/amine ratio of 1.78 was obtained within hours at 40 °C under 120 bar H_2/CO_2 (1/1). Since the catalyst can also promote the dehydrogenation under the reaction conditions, the reaction reached equilibrium at a certain temperature and pressure. Catalyst deactivation by treatment with KCN was required to avoid the reverse decomposition reaction during distillation of the product. Later, Beller and Laurency et al. investigated the formic acid/amine adducts as hydrogen storage media.²⁷⁶ From an economic viewpoint, the solvent-free reaction is preferred; however, a polar solvent such as DMF is required for high yield. Using the *in-situ* catalyst $[\text{RuCl}_2(\text{C}_6\text{H}_6)_2]/\text{dppe}$, dehydrogenation of FA in the presence of *N,N*-dimethylhexylamine afforded a TOF of $47,970 \text{ h}^{-1}$ at 80 °C.²⁷⁶ With constant addition of FA, the highest TON of 800,000 was achieved. For CO_2 hydrogenation, Et_3N was superior among several other organic bases tested. They achieved the high FA/ Et_3N ratio of 2.31 (TON = 3190) in DMF using the

well-defined complex $[\text{RuH}_2(\text{dppm})_2]$ instead of the *in-situ* catalyst. Building upon these results, a reversible H_2 storage system was developed by $[\text{RuH}_2(\text{dppm})_2]$ -catalyzed interconversion between CO_2/H_2 and $\text{FA}/\text{Et}_3\text{N}$. The initial cycle was carried out with 2 mL Et_3N and 20 mL DMF in an autoclave under 60 bar H_2/CO_2 (1/1) for 16 h at room temperature. Then the dehydrogenation started simply by releasing the pressure and stirring. However, replacement of the amine after each run was required owing to the loss of Et_3N in the turbulent H_2/CO_2 gas evolution process. Slight deactivation was observed after 7 cycles.

Plietker et al. reported a rechargeable hydrogen battery using H_2/CO_2 and $\text{HCO}_2\text{H}/\text{DBU}$ catalyzed by a $[\text{Ru}(\text{PNNP})(\text{CH}_3\text{CN})(\text{Cl})]$ complex (Chart 1).¹²⁸ The autoclave was filled with DBU and catalyst and then charged with 20 g dry ice and 70 bar H_2 at room temperature. When heated to 100 °C, the pressure reached 140 bar. After 2.5 h, the pressure had dropped to 100 bar and the reaction was over. Cooling the autoclave to room temperature prevented the dehydrogenation of the product, while elevated temperature is required to trigger the H_2 release. This system is much easier to control than previous ones, and five charging-discharging cycles were achieved.

Enthaler et al. reported the synthesis, characterization and application of nickel complexes modified by a PCP pincer ligand.²⁷⁷ This work enabled the first hydrogen storage and release cycle performed by a well-defined nickel catalyst $[\text{Ni}(\text{P7})\text{H}]$. The formate complex $[\text{Ni}(\text{P7})(\text{OCHO})]$ is an important intermediate in the catalytic cycle of interconversion of CO_2/FA . For dehydrogenation of $\text{FA}/n\text{OctNMe}_2$ (11/10), complex $[\text{Ni}(\text{P7})\text{H}]$ achieves a TON of 626 at 80 °C after 3 h with propylene carbonate as solvent. The amine additives and solvents greatly impact the activity. No reaction was observed without amines, and substituting other solvents for propylene carbonate diminished productivity of the catalyst by 30-50%. The reverse

reaction, hydrogenation of CO₂, was ineffective in the presence of *n*OctNMe₂, but hydrogenation of sodium bicarbonate in MeOH was accomplished with a TON of 3000 after 20 h at 150 °C under 55 bar H₂.

Pidko reported a highly efficient system using a pincer PNP-Ru complex for reversible hydrogen storage.¹³² Based on the high activity of complex [RuH(Cl)(CO)(P3)] for both reactions as summarized above, they performed cyclic operation with 1.42 μmol [RuH(Cl)(CO)(P3)] in DMF/DBU (30/5 mL) at 65 and 90 °C, respectively, for the loading and releasing processes. The DBU was superior to Et₃N, both for its high FA loading capacity and low loss in the hydrogen release process. With alternating high- (40 bar) and low-pressure (5 bar) loading procedures in less than 3 h and hydrogen liberation in less than 1 h, 10 storage-release cycles were achieved without catalyst deactivation over a week.

Very recently, Olah and co-workers reported an amine-free reversible hydrogen storage system using commercially available Ru pincer complexes (See Table 2).²⁴⁵ The PNP-Ru complex can catalyze the hydrogenation of CO₂ or bicarbonate to formate in a mixture of water and organic solvent such as THF, DMF, and 1,4-dioxane at 70-85 °C under 40-80 bar of H₂ or H₂ and/ CO₂. The dehydrogenation of sodium formate with the same catalyst (20 μmol) at 69 °C afforded an initial TOF of 286 and a TON of 1000 after 4.5 h with complete transformation of formate. Consecutive charge and discharge processes were performed with the PNP-Ru complex for six cycles without loss in activity and a total TON of 11,500 was obtained. It is worth noting that more than a 90 % yield was achieved in both directions.

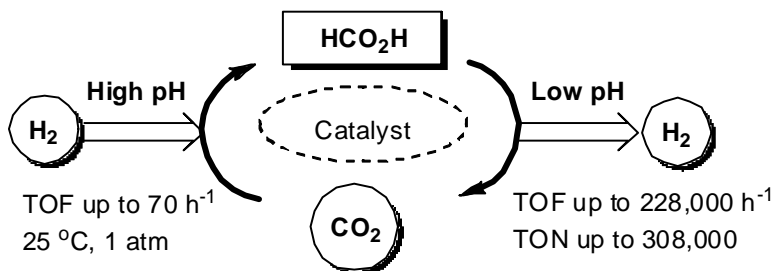
4.3. Reversible H₂ storage controlled by pH

Some water soluble proton responsive complexes have been developed for the catalytic interconversion of H₂/CO₂ and FA/formate in water. The activity showed apparent pH

dependence, therefore, the reaction direction could be controlled by adjusting the solution pH. Fukuzumi et al. reported a *C,N*-cyclometalated water-soluble iridium complex, $[\text{Cp}^*\text{Ir}(\text{N1})(\text{OH}_2)]^+$, for interconversion between H_2/CO_2 and FA at ambient temperature and pressure in water by controlling pH.¹⁴⁵ A K_2CO_3 (0.1 M) solution containing the Ir complex was bubbled with H_2/CO_2 (1/1) under atmospheric pressure at pH 7.5 and 30 °C. A TOF of 6.8 h^{-1} was obtained, and the TON reached 100 after 15 h. The dehydrogenation gave a maximum TOF of 1880 h^{-1} at pH 2.8 and 25 °C. No consecutive hydrogenation/dehydrogenation was demonstrated.

The roles of electron donor and pendent base have been demonstrated to be important for the activation of a functional complex containing a proton responsive ligand. To fulfill the dual activation of the complex, Himeda et al. designed and synthesized tetrahydroxy-substituted mononuclear $[\text{Cp}^*\text{Ir}(\text{N2})(\text{OH}_2)]^{2+}$ and dinuclear $[(\text{Cp}^*\text{IrCl})_2(\text{THBPM})]^{2+}$.^{142,146} The activity of these complexes is significantly improved over that of their dihydroxy analogues. For CO_2 hydrogenation, the catalytic activity of $[\text{Cp}^*\text{Ir}(\text{N2})(\text{OH}_2)]^{2+}$ and $[(\text{Cp}^*\text{IrCl})_2(\text{THBPM})]^{2+}$ is similar and more than double that of $[\text{Cp}^*\text{Ir}(\text{6DHBP})(\text{OH}_2)]^{2+}$.¹⁴⁶ Especially noteworthy is the unprecedented activity of $[(\text{Cp}^*\text{IrCl})_2(\text{THBPM})]^{2+}$ toward both CO_2 hydrogenation (TOF: 70 h^{-1} , 25 °C, 1 atm H_2/CO_2) and formic acid dehydrogenation (TOF: $228,000 \text{ h}^{-1}$, 90 °C, Scheme 18). This complex has been demonstrated to be the most effective catalyst for CO_2 hydrogenation and formic acid dehydrogenation in an aqueous medium. Using this complex, reversible hydrogen storage in aqueous media near ambient conditions was achieved. In the reaction solution, the catalyst can be reused at least twice by simply adjusting the pH by addition of acid and base in each cycle. The extraordinary activity of $[(\text{Cp}^*\text{IrCl})_2(\text{THBPM})]^{2+}$ is attributed to the synergistic effect between the ligand's roles as electron-donor and pendent base ($-\text{OH}$). Comparison of the

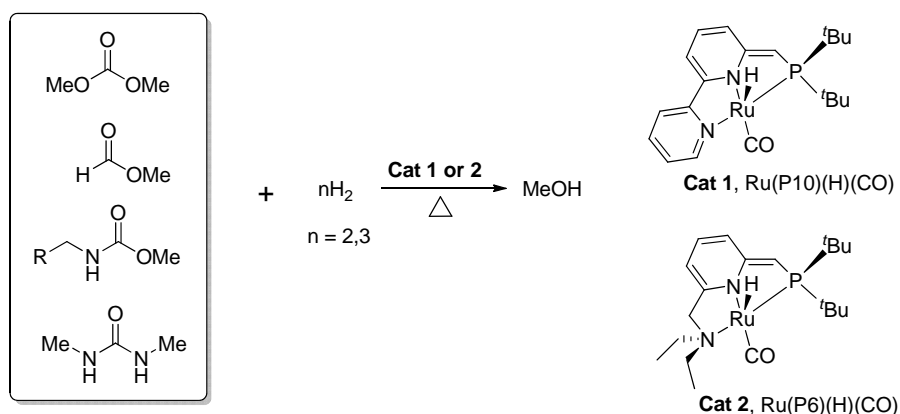
performance of $[\text{Cp}^*\text{Ir}(\text{N}_2)(\text{OH}_2)]^{2+}$ and $[(\text{Cp}^*\text{IrCl})_2(\text{THBPM})]^{2+}$ over that of $[\text{Cp}^*\text{Ir}(\text{6DHBP})(\text{OH}_2)]^{2+}$ indicates that while a dinuclear metal center effect is apparent, it is of secondary importance to the enhanced electronic effect.



Scheme 18. High turnover formate-based hydrogen storage system for carbon neutral energy applications at near ambient temperature and pressure using complex $[(\text{Cp}^*\text{IrCl})_2(\text{THBPM})]^{2+}$. Ref. 142,146.

5. Recent developments in CO_2 hydrogenation to methanol

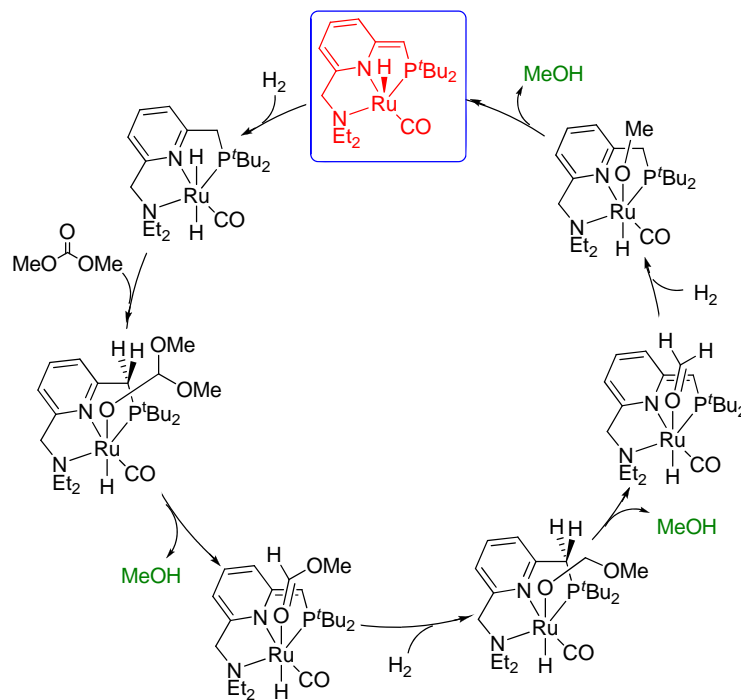
5.1. Hydrogenation of formate, carbonate, carbamate, and urea derivatives to MeOH



Scheme 19. MeOH generation from catalytic hydrogenation of alkyl formate, carbonate, carbamate, and urea derivatives. Based on Ref. 278.

Conversion of CO₂ to salicylic acid, alkyl carbonates and urea derivatives is one of the widely used methods for CO₂ fixation.^{3,5} However, highly toxic phosgene, is still used for synthesis of isocyanates, polycarbonates and polyurethanes, and the replacement of phosgene by CO₂ is highly desirable. These conversions are thermodynamically downhill reactions. Furthermore, transformations of CO₂ and H₂ to fuels such as MeOH^{279,280} are also downhill reactions, but are difficult to carry out.^{281,282} Reports with homogeneous catalysts are scarce in the literature. Milstein and co-workers employed urea derivatives, organic carbonates, carbamates and formates as substrates for the synthesis of methanol catalyzed by dearomatized PNN-Ru(II) pincer complexes [Ru(P6)(H)(CO)] and [Ru(P10)(H)(CO)] under mild conditions (Scheme 19).²⁷⁸ This study provided an effective route for the indirect hydrogenation of CO₂ to methanol. For the substrate dimethyl carbonate, the high TON of 4400 was obtained with [Ru(P10)(H)(CO)], Cat **1**, under 50 atm H₂ at 110 °C for 14 h. Under the same conditions, a TON of 4700 for MeOH was achieved for the methyl formate substrate. Interestingly, hydrogenation of carbamate derivatives with Cat **1** gave the corresponding amines and MeOH. The carbonyl group was reduced to give MeOH, unlike the common hydrogenolysis with Pd/C that releases CO₂. The transformation to methanol even proceeded well in the absence of solvent without any waste or byproduct, representing the definitions of “green” and “atom economy” reactions. The excellent catalytic capability for substrates with different structures suggests that PNN ligands (P6 and P10, Chart 2) could incorporate a range of compounds. Their remarkable catalytic properties suggest that they are capable of breaking C-N and C-O bonds along with the simultaneous reduction of a carbonyl group. In addition, Milstein et al. proposed a hydrogenation mechanism for the dimethyl carbonate substrate based on the process of ligand aromatization-dearomatization as shown in Scheme 20.²⁷⁸ Their mechanism suggests that the protonation and

deprotonation of the benzylic arm is important for hydrogen transfer and the reduction of the carbonate and formaldehyde intermediates to facilitate the generation of MeOH.²⁷⁸ Urea derivatives were also hydrogenated by Cat **1** to amines and MeOH.²⁸³ Hydrogenation of 1,3-dimethylurea under 1.36 MPa H₂ at 110 °C with 2 mol% Cat **1** produced 93 % yield of MeOH after 72 h. Various alkyl and aryl urea derivatives were also tested, and moderate to good yields were obtained. Surprisingly, even the tetra-substituted ureas could also be reduced to generate MeOH in moderate yields. A stepwise hydrogenation is suggested because a trace of formamides could be observed. The cleavage of a C-N bond releases a formamide intermediate which is then rapidly hydrogenated to give MeOH and an amine.

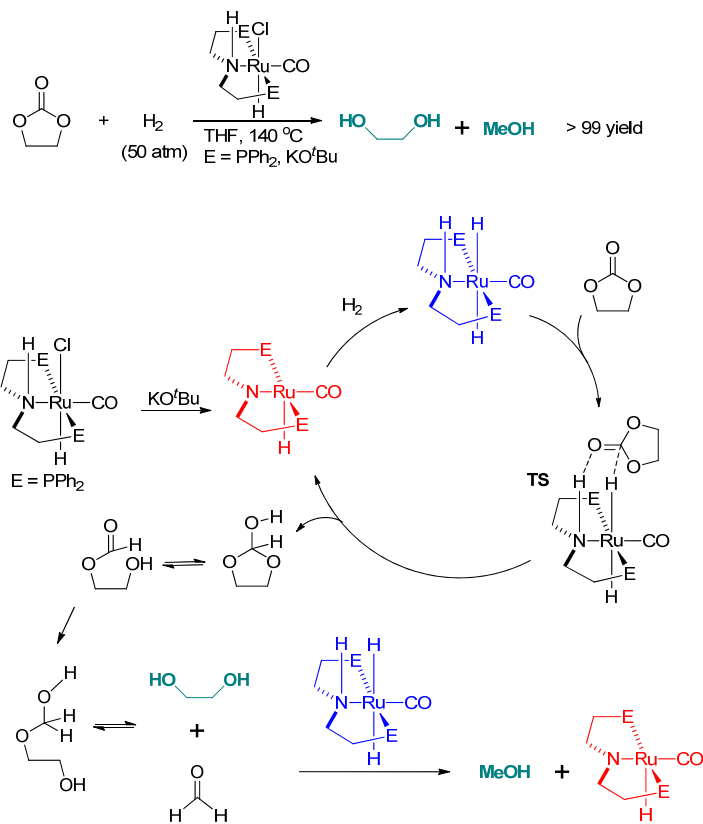


Scheme 20. Proposed mechanism for MeOH production from catalytic hydrogenation of alkyl formate and carbonate by Ru(P₆)(H)(CO). Based on Ref. 278.

Later, Yang investigated the mechanism of dimethyl carbonate hydrogenation to MeOH with complex Cat **2** (see Scheme 19) using density functional theory.²⁸⁴ Three cascade catalytic cycles involving the splitting of three H₂ and the generation of three MeOH molecules by the hydrogenation of dimethyl carbonate, methyl formate, and formaldehyde were proposed. Similar proton transfer steps were proposed for each hydrogenation reaction. The rate-determining step of the overall reaction was found in the hydrogenation of methyl formate step that involved a transition state from which cleavage of the C–O bond in MeOCH₂O[−] was accompanied by transfer of a methylene proton from the benzylic arm to the leaving MeO[−] group. The overall free energy barrier of 28.1 kcal mol^{−1} is in good agreement with the observed TOF of 24 h^{−1}. Based on this calculation, Yang proposed an iron pincer complex, [*trans*-(PNN)Fe(H)₂(CO)], as an alternative catalyst in which the free energy barrier of the rate-determining step is lowered by 3.4 kcal mol^{−1}.

Dimethyl carbonate is rather difficult to synthesize from CO₂, which limits its potential application in the indirect method for MeOH production from CO₂. On the other hand, ethylene carbonate is readily obtainable from CO₂ insertion into ethylene oxide, which is thermodynamically favorable. Ding et al. reported the hydrogenation of ethylene carbonate with a pincer Ru(II) complex bearing a N-H functional group.²⁸⁵ [Ru(P₂)(H)(Cl)(CO)] (see Scheme 21) catalyzed the hydrogenation of various cyclic carbonates, even the polycarbonates, into MeOH and the corresponding diols at 50 atm H₂ and 140 °C. The observation that the N-Me substituted complex showed no activity for this reaction, implicates the N-H group as a critical component. It is supposed that the N-H forms a hydrogen bond with the carbonyl substrate and assists the proton transfer to generate 1,3-dioxolan-2-ol as the initial reduction intermediate. The

reduction also goes through multistep reductions involving intermediates of 2-hydroxyethylformate, 2-(hydroxymethoxy)ethanol, and formaldehyde.



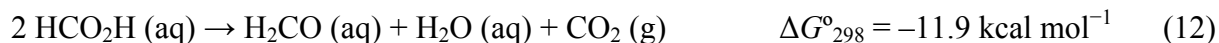
Scheme 21. MeOH production from catalytic hydrogenation of ethylene carbonate and proposed mechanism. Redrawn based on the results in Ref. 285.

5.2. Catalytic disproportionation of formic acid to MeOH

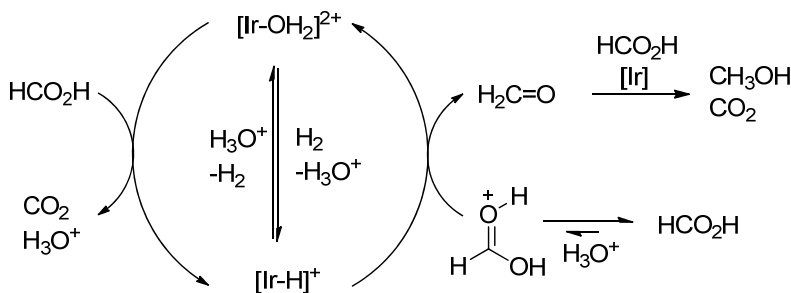
Generation of methanol directly from CO₂ requires direct electro-reduction or high pressure H₂, but the selectivity and yield are limited. On the other hand, formic acid is relatively easy to access from CO₂ as mentioned above. In 2013, Miller and Goldberg et al. reported disproportionation of formic acid to methanol using [Cp*Ir(bpy)(OH₂)](OTf)₂ as a catalyst.²⁸⁶

The decomposition of FA usually releases H₂ and CO₂ by dehydrogenation or produces CO and H₂O by dehydration. Their study demonstrated for the first time that FA could be converted

to MeOH, water and CO₂ with the Ir complex in aqueous solution at 80 °C. They estimated the thermodynamics of FA disproportionation using electrochemical standard potentials and found that both pathways shown in eq. 12 (disproportionation of FA to formaldehyde) and eq. 13 (direct formation of MeOH) are possible.²⁸⁶



Furthermore, their investigations using D₂O and DCO₂D showed that the existing C–H (or C–D) bond of formic acid is preserved during the reduction, indicating that the formaldehyde is an intermediate as shown in Scheme 22. Under optimized conditions of low catalyst loading (12.5 mM), low temperature (60 °C), low solution pH (0.4), and high FA concentration (12 M), they obtained the highest MeOH selectivity of 12 % corresponding to a TON of 70. Although the highest TON for methanol production was merely 200 after 120 h, this study provided a promising approach to MeOH generation directly from FA.



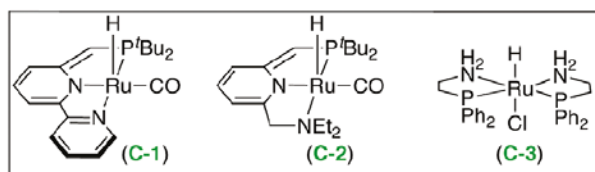
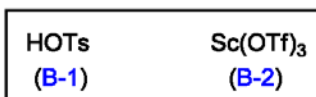
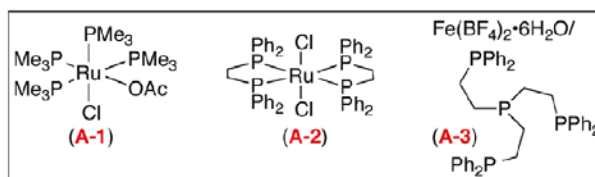
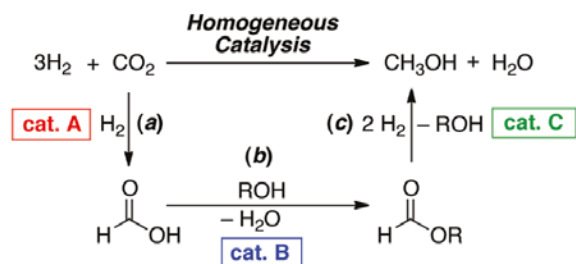
Scheme 22. Proposed mechanism of FA disproportionation to methanol with $[\text{Cp}^*\text{Ir}(\text{bpy})(\text{OH}_2)]^{2+}$ in water, based on Ref. 286.

Soon after that, Cantat et al. reported significantly improved yields of FA disproportionation to MeOH using ruthenium catalysts.²⁸⁷ Using the precursor [Ru(cod)(methylallyl)₂], an additional triphos (CH₃C(CH₂PPh₂)₃) ligand, and MSA (methanesulfonic acid), they achieved the highest selectivity for FA disproportionation to MeOH in a THF solution at 150 °C. Consistent with the report of Miller et al.,²⁸⁶ high FA concentration and low pH were favorable for the FA disproportionation, while high pressure and temperature (150 °C) were required by the Ru complex. Their mechanistic study included treatment of the isolated intermediate (and active catalyst), [Ru(triphos)(κ¹-HCO₂)(κ²-HCO₂)] with 2 equivalents formic acid after which CH₃OH, H₂, and CO₂ were detected. This experiment showed that MeOH is formed by transfer hydrogenation of formic acid but not from hydrogenation of CO₂. A theoretical analysis suggested hydride migration from Ru-H to a formyl ligand forming a coordinated acetal which dissociates, dehydrates to formaldehyde and is reduced to methanol. Although the Ru complex is less reactive for FA dehydrogenation than the Ir complex, it showed high selectivity for methanol production. These two studies suggest that complexes that are inactive for FA dehydrogenation are more likely to be effective for FA disproportionation. This observation might help in finding more efficient catalysts for this promising transformation.

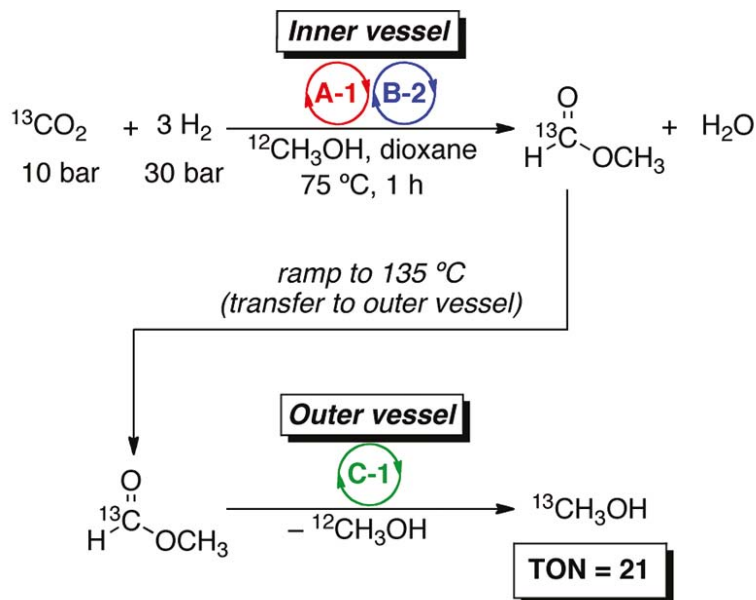
5.3. Cascade catalysis of CO₂ to MeOH

Noting the difficulty of one-step synthesis of MeOH from CO₂, Sanford et al. approached this challenge using a multiple-step method.²⁸⁸ This strategy involves several catalysts to promote a three step cascade catalysis sequence of: (a) FA generation from CO₂ and H₂; (b) transformation of FA to a formate ester; and (c) MeOH production by hydrogenation of the ester (Scheme 23). Actually, a series of different catalysts have been used in a single vessel to promote

various steps of CO₂ reduction.²⁸⁹ The distinct advantage of this approach is that the rate and selectivity of each step are tunable simply by changing the catalyst. Conversely, this is also a disadvantage because of the potential incompatibility of three kinds of catalysts. The catalyst bearing the highest activity cannot be used directly for the whole catalytic reaction because the compatibility has to be verified by elaborate screening experiments. Under optimized conditions, CO₂ hydrogenation/esterification occurred with 40 turnovers, while separately the hydrogenation of the ester yielded methanol quantitatively at 135 °C. In the one-pot reaction using three catalysts, only the low TON of 2.5 for MeOH was obtained. A vapor transfer method in which catalysts **A** and **B** in an inner vessel were separated from catalyst **C** in an outer vessel was used to avoid the deactivation of catalyst **C** by Sc(OTf)₃ (Scheme 24). The deactivation was thus prevented, while the generated methyl formate was transferred into the outer vessel simply by elevating the reaction temperature to 135 °C. The hydrogenation of the ester proceeded smoothly in the outer vessel and an improved overall TON of 21 for MeOH was achieved.



Scheme 23. Hydrogenation of CO₂ to MeOH with a strategy of cascade catalysis and catalysts used. Ref. 288. Copyright 2011 American Chemical Society.

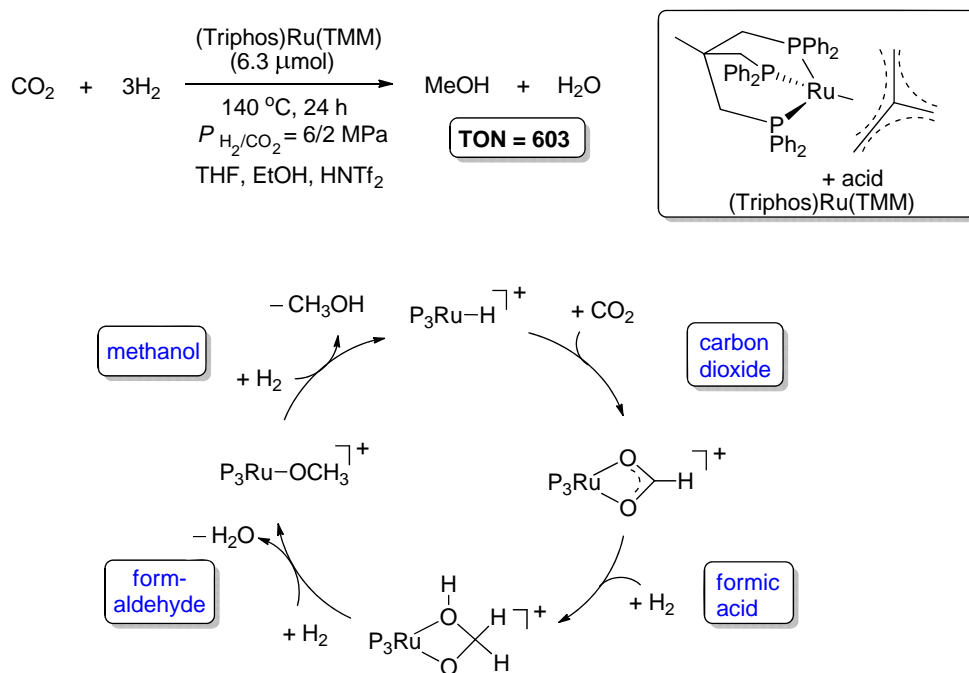


Scheme 24. A simple method to avoid incompatibility of applied catalysts for cascade catalytic CO₂ hydrogenation. Ref. 288. Copyright 2011 American Chemical Society.

5.4. Direct hydrogenation of CO₂ to MeOH

At present, most of the catalytic hydrogenation of CO₂ to MeOH requires the addition of an alcohol or amine to transform CO₂ to an alkyl formate, carbonate or urea first. Leitner and co-workers demonstrated via comprehensive mechanistic studies that a Ru triphos complex, [Ru(triphos)(TMM)] (TMM = trimethylenemethane), can catalyze the direct hydrogenation of CO₂ to MeOH as shown in Scheme 25.²⁹⁰ The Ru complex with one equivalent of bis(trifluoromethane)sulfonimide (HNTf₂) gave a TON of 603 for MeOH under CO₂/H₂ (20/60 bar at room temperature) after recharging the H₂/CO₂ three times at 140 °C. The initial TOF of 70 h⁻¹ indicates that the catalytic activity is comparable to the most effective heterogeneous system. Their experiments revealed that the resting state is a formate complex, [Ru(triphos)(η²-O₂CH)(solvent)]⁺, while other complexes isolated from the reaction mixture ([Ru(triphos)(H)(CO)₂]⁺, [Ru₂(μ-H)₂(triphos)₂] and [Ru(triphos)(H)(CO)(Cl)]) are inactive

catalysts and are therefore deactivation pathways. A theoretical mechanism predicted hydride migration from Ru to the formic acid ligand in $[\text{Ru}(\text{triphos})(\text{H})(\text{H}_2)(\text{HCO}_2\text{H})]^+$ as a crucial step in formation of a Ru hydroxymethanolate species with a $15.5 \text{ kcal mol}^{-1}$ energy barrier.



Scheme 25. MeOH production from direct catalytic hydrogenation of CO_2 and proposed mechanism based on Ref. 290.

6. Summary and Future Outlook

In this review, we have described CO_2 hydrogenation as an alternative method for so-called artificial photosynthesis to produce fuels, such as formate/formic acid and methanol, with good selectivity and high efficiency. Recent progress in CO_2 hydrogenation using homogeneous catalysts has been remarkable and, combined with formic acid dehydrogenation without producing detectable CO , contributes greatly to the realization of a hydrogen economy.

For CO_2 hydrogenation, an inexpensive and green source of H_2 is needed in contrast to the industrial reforming of natural gas. While H_2 could be produced by electrolysis of water in the

presence of a catalyst using solar generated-electricity, obtaining high pressure H_2 for storage and transportation requires additional energy input and engineering considerations. Thus, the storage of H_2 in formic acid as a transportable liquid is attractive provided the technology for clean conversion of CO_2/H_2 and formic acid under mild conditions is developed. For this purpose, scientists have been applying various strategies including utilization of solvents, additives, and the design of sophisticated catalysts. With basic amine additives, solvent-free systems can be achieved, although in most cases an organic solvent such as DMSO or DMF is required. The formate/amine system generally exhibits higher catalytic performance than an aqueous system with the one drawback of losing volatile amines during the hydrogen release process. A few aqueous systems with Cp^*Ir catalysts in high formic acid concentrations (4 M to almost pure FA) show promising results. Such a system is ecofriendly and easier to operate. Therefore, development of efficient and water-soluble catalysts for aqueous FA systems is highly desirable. Water soluble phosphine ligands and PNP-type pincer complexes have been applied in aqueous systems with considerable success, although the latter require a small amount of organic co-solvent. As for additives, the addition of bases can greatly promote the reaction, but it also results in a product separation problem. To obtain formic acid for the regeneration of H_2 or use in fuel cells, additional acid must be added to neutralize the formate. Application of ionic liquids to facilitate the evaporation of formic acid is a promising solution to this problem. Moreover, the separation of formic acid is not necessary because the direct use of the formate-containing system for hydrogen regeneration has also been achieved. As an alternative to the use of a base in CO_2 hydrogenation, a Lewis acid is a useful additive for H_2 release from formic acid. To reduce the cost, catalysis with earth-abundant metals such as Fe or Co is highly desirable, and considerable progress has been achieved. However, the high stability of certain hydride species

sometimes requires large (e.g., stoichiometric) amounts of expensive additives such as Verkade's base to produce a vacant coordination site for catalytic hydrogenation reactions. It is still questionable whether the real cost is reduced considering the relatively lower activity and durability of such catalysts compared to the currently widely used platinum-group catalysts. Development of catalysts with non-noble metals is an important subject for further research; nevertheless exploration of highly active and durable platinum-group catalysts is still worth pursuing.

The most important aspect of future research is the design of efficient and durable catalysts for CO₂ transforming systems. Innovative ligands with functional groups that contribute to improved activity through metal-ligand cooperation have shown promise. These non-innocent ligands include electro-responsive ligands capable of gaining or losing one or more electrons, ligands having a hydrogen bonding function, proton-responsive ligands capable of gaining or losing one or more protons and photo-responsive ligands capable of undergoing a useful change in properties upon irradiation. Theoretical calculations are frequently used to predict and explain these non-innocent ligand effects because the specific contributions of the ligand are often difficult to resolve experimentally. Pincer complexes efficiently activate small molecules such as H₂ and CO₂ via unique de-aromatization reactions and/or hydrogen-bonding interactions. Catalysts designed to mimic enzymes such as hydrogenases are also very successful. The bio-inspired proton-responsive complexes bearing hydroxy groups at *ortho* positions to the coordinating N atoms in aromatic *N*-heterocyclic ligands exhibited extraordinary activity for the catalytic transformation of H₂/CO₂ in aqueous solution under mild conditions. While electronic effects of the substituents are important, the pendent bases in the second coordination sphere of such ligands greatly improve the catalytic activity through the smooth movement of protons.

Kinetic isotope effects and computational studies provide clear evidence for the involvement of a water molecule in the rate-determining heterolysis of H₂ in CO₂ hydrogenation that accelerates proton transfer through the formation of a water bridge. Solution pH alters the rate determining step for H₂ generation from formic acid with these bio-inspired complexes. These unique properties, similar to those of enzymes, demonstrated the remarkable success of learning from nature. We believe innovative explorations to improve metal catalysts via the rational design of ligands (i.e., electronic and geometric effects, proton-responsive properties, pendant bases in the second-coordination sphere, etc.) to promote reactions under mild conditions, and to optimize the use of water as a solvent are essential for creating carbon-neutral energy sources and for avoiding catastrophic global warming.

Although homogeneously catalyzed hydrogenation of CO₂ to MeOH is rather difficult to achieve, significant progress has been made through indirect hydrogenation of formate, carbonate, or urea, disproportionation of formic acid, multiple-step synthesis and, most recently, direct CO₂ hydrogenation by a Ru triphos complex. Development of efficient non-noble metal catalysts and metal-free organo-catalysts such as frustrated Lewis pairs will be important directions. Great attention is devoted to the transformation of CO₂ to fuels, and the likelihood of significant successes in the near future is quite high.

Biographical Information

Wan-Hui Wang was born in 1982 in Shandong, China. He received his B.S. and M.S. from University of Jinan and his Ph.D. from Saitama University under the guidance of Professor T. Hirose. In 2011, he began his postdoctoral research with Y. Himeda at National Institute of

Advanced Industrial Science and Technology (AIST). In 2014, he joined the School of Petroleum and Chemical Engineering at Dalian University of Technology as an associate professor. His research interests lie in chemical energy storage and utilization of carbon dioxide.

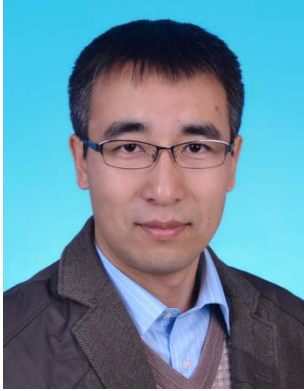
Yuichiro Himeda is a Senior Researcher at National Institute of Advanced Industrial Science and Technology (AIST). He received his Ph.D. in Organic Chemistry from Osaka University (1994). After a postdoctoral stay with Prof. Andrew D. Hamilton at the University of Pittsburgh (1995), he worked on the development of homogeneous catalysis for CO₂ reduction at AIST. His research interests include development of homogeneous catalysts based on new concepts, activation of small molecule, and CO₂ utilization for energy storage.

James T. Muckerman, Senior Chemist at Brookhaven National Laboratory (BNL), received his B.A. degree from Carlton College in 1965, and his Ph.D. degree in theoretical physical chemistry from the University of Wisconsin in 1969. He joined the scientific staff in the Chemistry Department at BNL immediately thereafter, and has carried out theoretical/computation research there ever since. In 2004 he changed his field of research from gas-phase molecular dynamics to artificial photosynthesis, and is now engaged in mechanistic research on water oxidation, hydrogen production, CO₂ reduction and CO₂ hydrogenation catalysis.

Gerald F. Manbeck received his B.S. degree from Bucknell University in 2006 and his Ph.D. from the University of Rochester in 2011 where he studied luminescent transition metal complexes relevant to OLED devices under the supervision of Prof. Richard Eisenberg. From 2011-2013 he pursued research in supramolecular photocatalysts for hydrogen production as a postdoctoral associate with Prof. Karen Brewer at Virginia Tech. In 2013, he moved to BNL as a

research associate in the Artificial Photosynthesis group to study electro- and photo-chemical reduction of carbon dioxide.

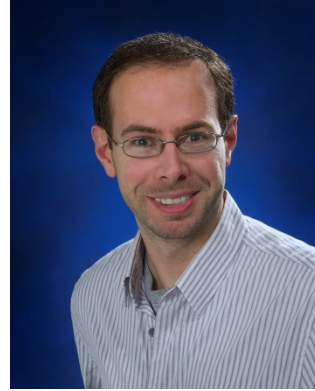
Etsuko Fujita received a B.S. in Chemistry from Ochanomizu University, Tokyo and a Ph.D. in Chemistry from the Georgia Institute of Technology. She joined in the Chemistry Department at BNL in 1986 after working in another department there, and currently is a Senior Chemist and leads the Artificial Photosynthesis group. Her research interests span solar fuels generation including water splitting and CO₂ utilization, mechanistic inorganic chemistry, and thermodynamics/kinetics of small molecule binding/activation.



Wang



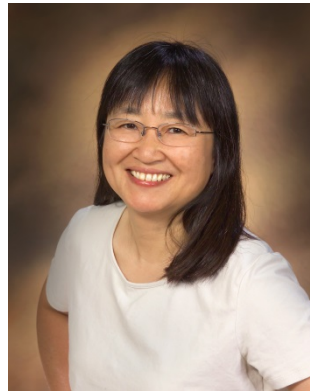
Himeda



Manbeck



Muckerman



Fujita

Acknowledgement

W.-H. W. thanks the financial support from Dalian University of Technology (Xinghai Scholars Program; the Fundamental Research Funds for the Central Universities, Grant No. DUT14RC(3)082) and National Natural Science Foundation of China (Grant No. 21402019). Y. H. thanks the Japan Science and Technology Agency (JST), CREST for financial support. The work at BNL was carried out under contract DE-SC00112704 with the U.S. Department of Energy, Office of Science, Office of Basic Energy Sciences.

Author Contributions

The manuscript was written through contributions of all authors. All authors have given approval to the final version of the manuscript.

References

- (1) Arakawa, H.; Aresta, M.; Armor, J. N.; Barteau, M. A.; Beckman, E. J.; Bell, A. T.; Bercaw, J. E.; Creutz, C.; Dinjus, E.; Dixon, D. A.; Domen, K.; DuBois, D. L.; Eckert, J.; Fujita, E.; Gibson, D. H.; Goddard, W. A.; Goodman, D. W.; Keller, J.; Kubas, G. J.; Kung, H. H.; Lyons, J. E.; Manzer, L. E.; Marks, T. J.; Morokuma, K.; Nicholas, K. M.; Periana, R.; Que, L.; Rostrup-Nielson, J.; Sachtler, W. M. H.; Schmidt, L. D.; Sen, A.; Somorjai, G. A.; Stair, P. C.; Stults, B. R.; Tumas, W. Catalysis research of relevance to carbon management: Progress, challenges, and opportunities. *Chem. Rev.* **2001**, *101*, 953-996.
- (2) Lewis, N. S.; Nocera, D. G. Powering the Planet: Chemical Challenges in Solar Energy Utilization. *Proc. Natl. Acad. Sci. U.S.A.* **2006**, *103*, 15729-15735.
- (3) Aresta, M.; Dibenedetto, A. Utilisation of CO₂ as a chemical feedstock: opportunities and challenges. *Dalton Trans.* **2007**, 2975-2992.
- (4) Appel, A. M.; Bercaw, J. E.; Bocarsly, A. B.; Dobbek, H.; DuBois, D. L.; Dupuis, M.; Ferry, J. G.; Fujita, E.; Hille, R.; Kenis, P. J. A.; Kerfeld, C. A.; Morris, R. H.; Peden, C. H. F.; Portis, A. R.; Ragsdale, S. W.; Rauchfuss, T. B.; Reek, J. N. H.; Seefeldt, L. C.; Thauer, R. K.; Waldrop, G. L. Frontiers, Opportunities, and Challenges in Biochemical and Chemical Catalysis of CO₂ Fixation. *Chem. Rev.* **2013**, *113*, 6621-6658.
- (5) Aresta, M.; Dibenedetto, A.; Angelini, A. Catalysis for the valorization of exhaust carbon: from CO₂ to chemicals, materials, and fuels. technological use of CO₂. *Chem. Rev.* **2014**, *114*, 1709-1742.
- (6) Harriman, A. Prospects for conversion of solar energy into chemical fuels: the concept of a solar fuels industry. *Phil. Trans. R. Soc. A* **2013**, 371.
- (7) Darensbourg, D. J. Making plastics from carbon dioxide: Salen metal complexes as catalysts for the production of polycarbonates from epoxides and CO₂. *Chem. Rev.* **2007**, *107*, 2388-2410.
- (8) Olah, G. A.; Prakash, G. K. S.; Goepfert, A. Anthropogenic Chemical Carbon Cycle for a Sustainable Future. *J. Am. Chem. Soc.* **2011**, *133*, 12881-12898.
- (9) Peters, M.; Koehler, B.; Kuckshinrichs, W.; Leitner, W.; Markewitz, P.; Mueller, T. E. Chemical Technologies for Exploiting and Recycling Carbon Dioxide into the Value Chain. *ChemSusChem* **2011**, *4*, 1216-1240.
- (10) Markewitz, P.; Kuckshinrichs, W.; Leitner, W.; Linssen, J.; Zapp, P.; Bongartz, R.; Schreiber, A.; Mueller, T. E. Worldwide innovations in the development of carbon capture technologies and the utilization of CO₂. *Energy Environ. Sci.* **2012**, *5*, 7281-7305.
- (11) Kondratenko, E. V.; Mul, G.; Baltrusaitis, J.; Larrazabal, G. O.; Perez-Ramirez, J. Status and perspectives of CO₂ conversion into fuels and chemicals by catalytic, photocatalytic

- and electrocatalytic processes. *Energy Environ. Sci.* **2013**, *6*, 3112-3135.
- (12) Ganesh, I. Conversion of carbon dioxide into methanol - a potential liquid fuel: Fundamental challenges and opportunities (a review). *Renew. Sust. Energ. Rev.* **2014**, *31*, 221-257.
 - (13) Schwarz, H. A.; Dodson, R. W. Reduction potential of CO₂- and alcohol radicals. *J. Phys. Chem.* **1989**, *93*, 409-414.
 - (14) Benson, E. E.; Kubiak, C. P.; Sathrum, A. J.; Smieja, J. M. Electrocatalytic and homogeneous approaches to conversion of CO₂ to liquid fuels. *Chem. Soc. Rev.* **2009**, *38*, 89-99.
 - (15) Hori, Y. Electrochemical CO₂ Reduction on Metal Electrodes. In *Modern Aspects of Electrochemistry*; Vayenas, C., Ed.; Springer: New York, 2008, pp 89-189.
 - (16) Morris, A. J.; Meyer, G. J.; Fujita, E. Molecular Approaches to the Photocatalytic Reduction of Carbon Dioxide for Solar Fuels. *Acc. Chem. Res.* **2009**, *42*, 1983-1994.
 - (17) Rakowski DuBois, M.; DuBois, D. L. Development of Molecular Electrocatalysts for CO₂ Reduction and H₂ Production/Oxidation. *Acc. Chem. Res.* **2009**, *42*, 1974-1982.
 - (18) Doherty, M. D.; Grills, D. C.; Muckerman, J. T.; Polyansky, D. E.; Fujita, E. Toward more efficient photochemical CO₂ reduction: Use of scCO₂ or photogenerated hydrides. *Coord. Chem. Rev.* **2010**, *254*, 2472-2482.
 - (19) Takeda, H.; Ishitani, O. Development of efficient photocatalytic systems for CO₂ reduction using mononuclear and multinuclear metal complexes based on mechanistic studies. *Coord. Chem. Rev.* **2010**, *254*, 346-354.
 - (20) Takeda, H.; Koike, K.; Morimoto, T.; Inumaru, H.; Ishitani, O. Photochemistry and Photocatalysis of Rhenium(I) Diimine Complexes. In *Advances in Inorganic Chemistry, Vol 63: Inorganic Photochemistry*, 2011, pp 137-186.
 - (21) Schneider, J.; Jia, H. F.; Muckerman, J. T.; Fujita, E. Thermodynamics and kinetics of CO₂, CO, and H⁺ binding to the metal centre of CO₂ reduction catalysts. *Chem. Soc. Rev.* **2012**, *41*, 2036-2051.
 - (22) Tamaki, Y.; Morimoto, T.; Koike, K.; Ishitani, O. Photocatalytic CO₂ reduction with high turnover frequency and selectivity of formic acid formation using Ru(II) multinuclear complexes. *Proc. Nat. Acad. Sci. U.S.A.* **2012**, *109*, 15673-15678.
 - (23) Izumi, Y. Recent advances in the photocatalytic conversion of carbon dioxide to fuels with water and/or hydrogen using solar energy and beyond. *Coord. Chem. Rev.* **2013**, *257*, 171-186.
 - (24) Navalon, S.; Dhakshinamoorthy, A.; Alvaro, M.; Garcia, H. Photocatalytic CO₂ Reduction using Non-Titanium Metal Oxides and Sulfides. *ChemSusChem* **2013**, *6*, 562-577.
 - (25) Costentin, C.; Robert, M.; Saveant, J. M. Catalysis of the electrochemical reduction of carbon dioxide. *Chem. Soc. Rev.* **2013**, *42*, 2423-2436.
 - (26) Clark, M. L.; Grice, K. A.; Moore, C. E.; Rheingold, A. L.; Kubiak, C. P. Electrocatalytic CO₂ reduction by M(bpy-R)(CO)₄ (M = Mo, W; R = H, tBu) complexes. Electrochemical, spectroscopic, and computational studies and comparison with group 7 catalysts. *Chem. Sci.* **2014**, *5*, 1894-1900.
 - (27) Protti, S.; Albin, A.; Serpone, N. Photocatalytic generation of solar fuels from the reduction of H₂O and CO₂: a look at the patent literature. *Phys. Chem. Chem. Phys.* **2014**, *16*, 19790-19827.
 - (28) Lu, X.; Leung, D. Y. C.; Wang, H.; Leung, M. K. H.; Xuan, J. Electrochemical Reduction

- of Carbon Dioxide to Formic Acid. *ChemElectroChem* **2014**, *1*, 836-849.
- (29) Manbeck, G. F.; Fujita, E. A Review of Iron and Cobalt Porphyrins, Phthalocyanines, and Related Complexes for Electrochemical and Photochemical Reduction of Carbon Dioxide. *J. Porphyrins Phthalocyanines* **2015**, *19*, 45-64.
- (30) Das, S.; Daud, W. M. A. W. Photocatalytic CO₂ transformation into fuel: A review on advances in photocatalyst and photoreactor. *Renew. Sust. Energ. Rev.* **2014**, *39*, 765-805.
- (31) Oh, Y.; Hu, X. Organic molecules as mediators and catalysts for photocatalytic and electrocatalytic CO₂ reduction. *Chem. Soc. Rev.* **2013**, *42*, 2253-2261.
- (32) Yang, C. C.; Yu, Y. H.; van der Linden, B.; Wu, J. C. S.; Mul, G. Artificial Photosynthesis over Crystalline TiO₂-Based Catalysts: Fact or Fiction? *J. Am. Chem. Soc.* **2010**, *132*, 8398-8406.
- (33) Kraeutler, B.; Bard, A. J. Heterogeneous photocatalytic synthesis of methane from acetic acid - new Kolbe reaction pathway. *J. Am. Chem. Soc.* **1978**, *100*, 2239-2240.
- (34) Wilson, J. N.; Idriss, H. Effect of surface reconstruction of TiO₂(001) single crystal on the photoreaction of acetic acid. *J. Catal.* **2003**, *214*, 46-52.
- (35) Yui, T.; Kan, A.; Saitoh, C.; Koike, K.; Ibusuki, T.; Ishitani, O. Photochemical Reduction of CO₂ Using TiO₂: Effects of Organic Adsorbates on TiO₂ and Deposition of Pd onto TiO₂. *ACS Appl. Mater. Interfaces* **2011**, *3*, 2594-2600.
- (36) Mochizuki, K.; Manaka, S.; Takeda, I.; Kondo, T. Synthesis and structure of [6,6'-bi(5,7-dimethyl-1,4,8,11-tetraazacyclotetradecane)]dinickel(II) triflate and its catalytic activity for photochemical CO₂ reduction. *Inorg. Chem.* **1996**, *35*, 5132-5136.
- (37) Lehn, J.-M.; Ziessel, R. Photochemical reduction of carbon dioxide to formate catalyzed by 2,2'-bipyridine- or 1,10-phenanthroline-ruthenium(II) complexes. *J. Organometal. Chem.* **1990**, *382*, 157-173.
- (38) Pellegrin, Y.; Odobel, F. Molecular devices featuring sequential photoinduced charge separations for the storage of multiple redox equivalents. *Coord. Chem. Rev.* **2011**, *255*, 2578-2593.
- (39) Ogata, T.; Yanagida, S.; Brunschwig, B. S.; Fujita, E. Mechanistic and Kinetic Studies of Cobalt Macrocycles in a Photochemical CO₂ Reduction System: Evidence of Co-CO₂ Adducts as intermediates. *J. Am. Chem. Soc.* **1995**, *117*, 6708-6716.
- (40) Fujita, E.; Furenlid, L. R.; Renner, M. W. Direct XANES evidence for charge transfer in Co-CO₂ complexes. *J. Am. Chem. Soc.* **1997**, *119*, 4549-4550.
- (41) Hayashi, Y.; Kita, S.; Brunschwig, B. S.; Fujita, E. Involvement of a Binuclear Species with the Re-C(O)O-Re Moiety in CO₂ Reduction Catalyzed by Tricarbonyl Rhenium(I) Complexes with Diimine Ligands: Strikingly Slow Formation of the Re-Re and Re-C(O)O-Re Species from Re(dmb)(CO)₃S (dmb = 4,4'-dimethyl-2,2'-bipyridine, S = solvent). *J. Am. Chem. Soc.* **2003**, *125*, 11976-11987.
- (42) Tamaki, Y.; Koike, K.; Morimoto, T.; Ishitani, O. Substantial improvement in the efficiency and durability of a photocatalyst for carbon dioxide reduction using a benzoimidazole derivative as an electron donor. *J. Catal.* **2013**, *304*, 22-28.
- (43) Sato, S.; Arai, T.; Morikawa, T.; Uemura, K.; Suzuki, T. M.; Tanaka, H.; Kajino, T. Selective CO₂ Conversion to Formate Conjugated with H₂O Oxidation Utilizing Semiconductor/Complex Hybrid Photocatalysts. *J. Am. Chem. Soc.* **2011**, *133*, 15240-15243.
- (44) Arai, T.; Sato, S.; Uemura, K.; Morikawa, T.; Kajino, T.; Motohiro, T. Photoelectrochemical reduction of CO₂ in water under visible-light irradiation by a *p*-

- type InP photocathode modified with an electropolymerized ruthenium complex. *Chem. Commun.* **2010**, *46*, 6944-6946.
- (45) Yamanaka, K.-i.; Sato, S.; Iwaki, M.; Kajino, T.; Morikawa, T. Photoinduced Electron Transfer from Nitrogen-Doped Tantalum Oxide to Adsorbed Ruthenium Complex. *J. Phys. Chem. C* **2011**, *115*, 18348-18353.
- (46) Sekizawa, K.; Maeda, K.; Domen, K.; Koike, K.; Ishitani, O. Artificial Z-Scheme Constructed with a Supramolecular Metal Complex and Semiconductor for the Photocatalytic Reduction of CO₂. *J. Am. Chem. Soc.* **2013**, *135*, 4596-4599.
- (47) Li, C. W.; Kanan, M. W. CO₂ Reduction at Low Overpotential on Cu Electrodes Resulting from the Reduction of Thick Cu₂O Films. *J. Am. Chem. Soc.* **2012**, *134*, 7231-7234.
- (48) Chen, Y.; Li, C. W.; Kanan, M. W. Aqueous CO₂ Reduction at Very Low Overpotential on Oxide-Derived Au Nanoparticles. *J. Am. Chem. Soc.* **2012**, *134*, 19969-19972.
- (49) Ba, X.; Yan, L.-L.; Huang, S.; Yu, J.; Xia, X.-J.; Yu, Y. New Way for CO₂ Reduction under Visible Light by a Combination of a Cu Electrode and Semiconductor Thin Film: Cu₂O Conduction Type and Morphology Effect. *J. Phys. Chem. C* **2014**, *118*, 24467-24478.
- (50) Costentin, C.; Drouet, S.; Robert, M.; Saveant, J. M. A Local Proton Source Enhances CO₂ Electroreduction to CO by a Molecular Fe Catalyst *Science* **2012**, *338*, 90-94
- (51) Costentin, C.; Passard, G.; Robert, M.; Saveant, J. M. Pendant Acid-Base Groups in Molecular Catalysts: H-Bond Promoters or Proton Relays? Mechanisms of the Conversion of CO₂ to CO by Electrogenerated Iron(0)Porphyrins Bearing Prepositioned Phenol Functionalities. *J. Am. Chem. Soc.* **2014**, *136*, 11821-11829.
- (52) Rosen, B. A.; Salehi-Khojin, A.; Thorson, M. R.; Zhu, W.; Whipple, D. T.; Kenis, P. J. A.; Masel, R. I. Ionic Liquid-Mediated Selective Conversion of CO₂ to CO at Low Overpotentials. *Science* **2011**, *334*, 643-644.
- (53) DiMeglio, J. L.; Rosenthal, J. Selective Conversion of CO₂ to CO with High Efficiency Using an Inexpensive Bismuth-Based Electrocatalyst. *J. Am. Chem. Soc.* **2013**, *135*, 8798-8801.
- (54) Grills, D. C.; Matsubara, Y.; Kuwahara, Y.; Gollisz, S. R.; Kurtz, D. A.; Mello, B. A. Electrocatalytic CO₂ Reduction with a Homogeneous Catalyst in Ionic Liquid: High Catalytic Activity at Low Overpotential. *J. Phys. Chem. Lett.* **2014**, *5*, 2033-2038.
- (55) Sampson, M. D.; Froehlich, J. D.; Smieja, J. M.; Benson, E. E.; Sharp, I. D.; Kubiak, C. P. Direct observation of the reduction of carbon dioxide by rhenium bipyridine catalysts. *Energy Environ. Sci.* **2013**, *6*, 3748-3755.
- (56) Beley, M.; Collin, J.-P.; Ruppert, R.; Sauvage, J.-P. Nickel(II)-Cyclam: an Extremely Selective Electrocatalyst for Reduction of CO₂ in Water. *J. Chem. Soc., Chem. Commun.* **1984**, 1315-1316.
- (57) Beley, M.; Collin, J. P.; Ruppert, R.; Sauvage, J. P. Electrocatalytic Reduction of CO₂ by Ni cyclam²⁺ in water - Study of the Factors Affecting the Efficiency and the Selectivity of the Process *J. Am. Chem. Soc.* **1986**, *108*, 7461-7467.
- (58) Schneider, J.; Jia, H. F.; Kobiro, K.; Cabelli, D. E.; Muckerman, J. T.; Fujita, E. Nickel(II) macrocycles: highly efficient electrocatalysts for the selective reduction of CO₂ to CO. *Energy Environ. Sci.* **2012**, *5*, 9502-9510.
- (59) Barelli, L.; Bidini, G.; Gallorini, F.; Servili, S. Hydrogen production through sorption-enhanced steam methane reforming and membrane technology: A review. *Energy* **2008**,

- 33, 554-570.
- (60) Fihri, A.; Artero, V.; Razavet, M.; Baffert, C.; Leibl, W.; Fontecave, M. Cobaloxime-based photocatalytic devices for hydrogen production. *Angew. Chem. Int. Ed.* **2008**, *47*, 564-567.
- (61) Gloaguen, F.; Rauchfuss, T. B. Small molecule mimics of hydrogenases: Hydrides and redox. *Chem. Soc. Rev.* **2009**, *38*, 100-108.
- (62) Bigi, J. P.; Hanna, T. E.; Harman, W. H.; Chang, A.; Chang, C. J. Electrocatalytic reduction of protons to hydrogen by a water-compatible cobalt polypyridyl platform. *Chem. Commun.* **2010**, *46*, 958-960.
- (63) Losse, S.; Vos, J. G.; Rau, S. Catalytic hydrogen production at cobalt centres. *Coord. Chem. Rev.* **2010**, *254*, 2492-2504.
- (64) Artero, V.; Chavarot-Kerlidou, M.; Fontecave, M. Splitting Water with Cobalt. *Angew. Chem. Int. Ed.* **2011**, *50*, 7238-7266.
- (65) Kilgore, U. J.; Roberts, J. A. S.; Pool, D. H.; Appel, A. M.; Stewart, M. P.; DuBois, M. R.; Dougherty, W. G.; Kassel, W. S.; Bullock, R. M.; DuBois, D. L. $[\text{Ni}(\text{P}^{\text{Ph}_2}\text{N}^{\text{C}_6\text{H}_4\text{X}_2})_2]^{2+}$ Complexes as Electrocatalysts for H_2 Production: Effect of Substituents, Acids, and Water on Catalytic Rates. *J. Am. Chem. Soc.* **2011**, *133*, 5861-5872.
- (66) Du, P.; Eisenberg, R. Catalysts made of earth-abundant elements (Co, Ni, Fe) for water splitting: Recent progress and future challenges. *Energy Environ. Sci.* **2012**, *5*, 6012-6021.
- (67) McCrory, C. C. L.; Uyeda, C.; Peters, J. C. Electrocatalytic Hydrogen Evolution in Acidic Water with Molecular Cobalt Tetraazamacrocycles. *J. Am. Chem. Soc.* **2012**, *134*, 3164-3170.
- (68) Smestad, G. P.; Steinfeld, A. Review: Photochemical and Thermochemical Production of Solar Fuels from H_2O and CO_2 Using Metal Oxide Catalysts. *Ind. Eng. Chem. Res.* **2012**, *51*, 11828-11840.
- (69) Tran, P. D.; Barber, J. Proton reduction to hydrogen in biological and chemical systems. *Phys. Chem. Chem. Phys.* **2012**, *14*, 13772-13784.
- (70) Wang, M.; Chen, L.; Sun, L. C. Recent progress in electrochemical hydrogen production with earth-abundant metal complexes as catalysts. *Energy Environ. Sci.* **2012**, *5*, 6763-6778.
- (71) Chen, W. F.; Iyer, S.; Sasaki, K.; Wang, C. H.; Zhu, Y. M.; Muckerman, J. T.; Fujita, E. Biomass-derived electrocatalytic composites for hydrogen evolution. *Energy Environ. Sci.* **2013**, *6*, 1818-1826.
- (72) Chen, W. F.; Muckerman, J. T.; Fujita, E. Recent developments in transition metal carbides and nitrides as hydrogen evolution electrocatalysts. *Chemical Communications* **2013**, *49*, 8896-8909.
- (73) Eckenhoff, W. T.; McNamara, W. R.; Du, P. W.; Eisenberg, R. Cobalt complexes as artificial hydrogenases for the reductive side of water splitting. *Biochim. Biophys. Acta Bioenerg.* **2013**, *1827*, 958-973.
- (74) King, A. E.; Surendranath, Y.; Piro, N. A.; Bigi, J. P.; Long, J. R.; Chang, C. J. A mechanistic study of proton reduction catalyzed by a pentapyridine cobalt complex: evidence for involvement of an anation-based pathway. *Chem. Sci.* **2013**, *4*, 1578-1587.
- (75) Thoi, V. S.; Sun, Y. J.; Long, J. R.; Chang, C. J. Complexes of earth-abundant metals for catalytic electrochemical hydrogen generation under aqueous conditions. *Chem. Soc. Rev.* **2013**, *42*, 2388-2400.
- (76) Wiedner, E. S.; Appel, A. M.; DuBois, D. L.; Bullock, R. M. Thermochemical and

- Mechanistic Studies of Electrocatalytic Hydrogen Production by Cobalt Complexes Containing Pendant Amines. *Inorg. Chem.* **2013**, *52*, 14391-14403.
- (77) Zhang, P.; Wang, M.; Gloaguen, F.; Chen, L.; Quentel, F.; Sun, L. Electrocatalytic hydrogen evolution from neutral water by molecular cobalt tripyridine-diamine complexes. *Chem. Commun.* **2013**, *49*, 9455-9457.
- (78) Chen, W. F.; Schneider, J. M.; Sasaki, K.; Wang, C. H.; Schneider, J.; Iyer, S.; Zhu, Y. M.; Muckerman, J. T.; Fujita, E. Tungsten Carbide-Nitride on Graphene Nanoplatelets as a Durable Hydrogen Evolution Electrocatalyst. *ChemSuschem* **2014**, *7*, 2414-2418.
- (79) Faber, M. S.; Jin, S. Earth-abundant inorganic electrocatalysts and their nanostructures for energy conversion applications. *Energy Environ. Sci.* **2014**, *7*, 3519-3542.
- (80) Huang, Z. P.; Chen, Z. Z.; Chen, Z. B.; Lv, C. C.; Humphrey, M. G.; Zhang, C. Cobalt phosphide nanorods as an efficient electrocatalyst for the hydrogen evolution reaction. *Nano Energy* **2014**, *9*, 373-382.
- (81) Laga, S. M.; Blakemore, J. D.; Henling, L. M.; Brunschwig, B. S.; Gray, H. B. Catalysis of Proton Reduction by a BO_4 -Bridged Dicobalt Glyoxime. *Inorg. Chem.* **2014**, *53*, 12668-12670.
- (82) McKone, J. R.; Marinescu, S. C.; Brunschwig, B. S.; Winkler, J. R.; Gray, H. B. Earth-abundant hydrogen evolution electrocatalysts. *Chem. Sci.* **2014**, *5*, 865-878.
- (83) Liu, Y. M.; Yu, H. T.; Quan, X.; Chen, S.; Zhao, H. M.; Zhang, Y. B. Efficient and durable hydrogen evolution electrocatalyst based on nonmetallic nitrogen doped hexagonal carbon. *Sci. Rep.* **2014**, *4*, 6843.
- (84) Pan, L. F.; Li, Y. H.; Yang, S.; Liu, P. F.; Yu, M. Q.; Yang, H. G. Molybdenum carbide stabilized on graphene with high electrocatalytic activity for hydrogen evolution reaction. *Chem. Commun.* **2014**, *50*, 13135-13137.
- (85) Wiedner, E. S.; Helm, M. L. Comparison of $[\text{Ni}(\text{PPh}_2\text{NPh}_2)_2(\text{CH}_3\text{CN})]^{2+}$ and $[\text{Pd}(\text{PPh}_2\text{NPh}_2)_2]^{2+}$ as Electrocatalysts for H_2 Production. *Organometallics* **2014**, *33*, 4617-4620.
- (86) Xiao, P.; Sk, M. A.; Thia, L.; Ge, X. M.; Lim, R. J.; Wang, J. Y.; Lim, K. H.; Wang, X. Molybdenum phosphide as an efficient electrocatalyst for the hydrogen evolution reaction. *Energy Environ. Sci.* **2014**, *7*, 2624-2629.
- (87) Clough, A. J.; Yoo, J. W.; Mecklenburg, M. H.; Marinescu, S. C. Two-Dimensional Metal-Organic Surfaces for Efficient Hydrogen Evolution from Water. *J. Am. Chem. Soc.* **2015**, *137*, 118-121.
- (88) Cui, W.; Liu, Q.; Xing, Z. C.; Asiri, A. M.; Alamry, K. A.; Sun, X. MoP nanosheets supported on biomass-derived carbon flake: One-step facile preparation and application as a novel high-active electrocatalyst toward hydrogen evolution reaction. *Appl. Catal. B* **2015**, *164*, 144-150.
- (89) Han, A.; Jin, S.; Chen, H. L.; Ji, H. X.; Sun, Z. J.; Du, P. W. A robust hydrogen evolution catalyst based on crystalline nickel phosphide nanoflakes on three-dimensional graphene/nickel foam: high performance for electrocatalytic hydrogen production from pH 0-14. *J. Mater. Chem. A* **2015**, *3*, 1941-1946.
- (90) Morozan, A.; Goellner, V.; Zitolo, A.; Fonda, E.; Donnadiou, B.; Jones, D.; Jaouen, F. Synergy between molybdenum nitride and gold leading to platinum-like activity for hydrogen evolution. *Phys. Chem. Chem. Phys.* **2015**, *17*, 4047-4053.
- (91) Chen, W.-F.; Muckerman, J. T.; Fujita, E. Recent developments in transition metal carbides and nitrides as hydrogen evolution electrocatalysts. *Chem. Commun.* **2013**, *49*,

- 8896-8909.
- (92) Jiang, H. L.; Singh, S. K.; Yan, J. M.; Zhang, X. B.; Xu, Q. Liquid-Phase Chemical Hydrogen Storage: Catalytic Hydrogen Generation under Ambient Conditions. *ChemSusChem* **2010**, *3*, 541-549.
 - (93) Yu, X.; Pickup, P. G. Recent advances in direct formic acid fuel cells (DFAFC). *J. Power Sources* **2008**, *182*, 124-132.
 - (94) Nielsen, M.; Alberico, E.; Baumann, W.; Drexler, H. J.; Junge, H.; Gladiali, S.; Beller, M. Low-temperature aqueous-phase methanol dehydrogenation to hydrogen and carbon dioxide. *Nature* **2013**, *495*, 85-89.
 - (95) Alberico, E.; Nielsen, M. Towards a methanol economy based on homogeneous catalysis: Methanol to H₂ and CO₂ to methanol. *Chem. Commun.* **2015**, *51*, 6714-6725.
 - (96) Alberico, E.; Sponholz, P.; Cordes, C.; Nielsen, M.; Drexler, H.-J.; Baumann, W.; Junge, H.; Beller, M. Selective Hydrogen Production from Methanol with a Defined Iron Pincer Catalyst under Mild Conditions. *Angew. Chem. Int. Ed.* **2013**, *52*, 14162-14166.
 - (97) Jessop, P. G.; Ikariya, T.; Noyori, R. Homogeneous Hydrogenation of Carbon-Dioxide. *Chem. Rev.* **1995**, *95*, 259-272.
 - (98) Bonilla, R. J.; James, B. R.; Jessop, P. G. Colloid-catalysed arene hydrogenation in aqueous/supercritical fluid biphasic media. *Chem. Commun.* **2000**, 941-942.
 - (99) Zeller, K. P.; Schuler, P.; Haiss, P. The hidden equilibrium in aqueous sodium carbonate solutions - Evidence for the formation of the dicarbonate anion. *Eur. J. Inorg. Chem.* **2005**, 168-172.
 - (100) Kovacs, G.; Schubert, G.; Joó, F.; Papai, I. Theoretical investigation of catalytic HCO₃⁻ hydrogenation in aqueous solutions. *Catal. Today* **2006**, *115*, 53-60.
 - (101) Jessop, P. G.; Joó, F.; Tai, C. C. Recent advances in the homogeneous hydrogenation of carbon dioxide. *Coord. Chem. Rev.* **2004**, *248*, 2425-2442.
 - (102) Himeda, Y. Conversion of CO₂ into formate by homogeneously catalyzed hydrogenation in water: Tuning catalytic activity and water solubility through the acid-base equilibrium of the ligand. *Eur. J. Inorg. Chem.* **2007**, 3927-3941.
 - (103) Loges, B.; Boddien, A.; Gartner, F.; Junge, H.; Beller, M. Catalytic Generation of Hydrogen from Formic acid and its Derivatives: Useful Hydrogen Storage Materials *Top. Catal.* **2010**, *53*, 902-914.
 - (104) Fukuzumi, S. Bioinspired energy conversion systems for hydrogen production and storage. *Eur. J. Inorg. Chem.* **2008**, 1351-1362.
 - (105) Li, Y.-N.; Ma, R.; He, L.-N.; Diao, Z.-F. Homogeneous hydrogenation of carbon dioxide to methanol. *Catal. Sci. Technol.* **2014**, *4*, 1498-1512.
 - (106) Li, Y.; Junge, K.; Beller, M. Improving the Efficiency of the Hydrogenation of Carbonates and Carbon Dioxide to Methanol. *ChemCatChem* **2013**, *5*, 1072-1074.
 - (107) Choudhury, J. New Strategies for CO₂-to-Methanol Conversion. *ChemCatChem* **2012**, *4*, 609-611.
 - (108) Wang, W.; Wang, S.; Ma, X.; Gong, J. Recent advances in catalytic hydrogenation of carbon dioxide. *Chem. Soc. Rev.* **2011**, *40*, 3703-3727.
 - (109) Leitner, W. Carbon Dioxide as a Raw Material: Synthesis of Formic Acid and its Derivatives from CO₂ *Angew. Chem. Int. Ed.* **1995**, *34*, 2207-2221.
 - (110) Leitner, W.; Dinjus, E.; Gassner, F. CO₂ Chemistry. In *Aqueous-Phase Organometallic Catalysis, Concepts and Applications*; Cornils, B., Herrmann, W. A., Eds.; Wiley-VCH: Weinheim, 1998, pp 486-498.

- (111) Jessop, P. G. Homogeneous hydrogenation of carbon dioxide. In *Handbook of Homogeneous Hydrogenation*; De Vries, J. G., Elsevier, C. J., Eds.; Wiley-VCH: Weinheim, 2007, pp 489-511.
- (112) Inoue, Y.; Izumida, H.; Sasaki, Y.; Hashimoto, H. Catalytic fixation of carbon dioxide to formic acid by transition-metal complexes under mild conditions. *Chem. Lett.* **1976**, 863-864.
- (113) Ezhova, N. N.; Kolesnichenko, N. V.; Bulygin, A. V.; Slivinskii, E. V.; Han, S. Hydrogenation of CO₂ to formic acid in the presence of the Wilkinson complex. *Russ. Chem. Bull., Int. Ed.* **2002**, *51*, 2165-2169.
- (114) Graf, E.; Leitner, W. Direct Formation of Formic-Acid from Carbon-Dioxide and Dihydrogen Using the [(Rh(Cod)Cl)₂]Ph₂P(CH₂)₄PPh₂ Catalyst System. *J. Chem. Soc., Chem. Commun.* **1992**, 623-624.
- (115) Gassner, F.; Leitner, W. CO₂-Activation .3. Hydrogenation of Carbon-Dioxide to Formic-Acid Using Water-Soluble Rhodium Catalysts. *J. Chem. Soc., Chem. Commun.* **1993**, 1465-1466.
- (116) Zhao, G.; Joó, F. Free formic acid by hydrogenation of carbon dioxide in sodium formate solutions. *Catalysis Communications* **2011**, *14*, 74-76.
- (117) Jessop, P. G.; Ikariya, T.; Noyori, R. Homogeneous Catalytic-Hydrogenation of Supercritical Carbon-Dioxide. *Nature* **1994**, *368*, 231-233.
- (118) Munshi, P.; Main, A. D.; Linehan, J. C.; Tai, C. C.; Jessop, P. G. Hydrogenation of carbon dioxide catalyzed by ruthenium trimethylphosphine complexes: The accelerating effect of certain alcohols and amines. *J. Am. Chem. Soc.* **2002**, *124*, 7963-7971.
- (119) Elek, J.; Nadasdi, L.; Papp, G.; Laurenczy, G.; Joó, F. Homogeneous hydrogenation of carbon dioxide and bicarbonate in aqueous solution catalyzed by water-soluble ruthenium(II) phosphine complexes. *Appl. Catal. A* **2003**, *255*, 59-67.
- (120) Laurenczy, G.; Joó, F.; Nadasdi, L. Formation and characterization of water-soluble hydrido-ruthenium(II) complexes of 1,3,5-triaza-7-phosphaadamantane and their catalytic activity in hydrogenation of CO₂ and HCO₃⁻ in aqueous solution. *Inorg. Chem.* **2000**, *39*, 5083-5088.
- (121) Federsel, C.; Jackstell, R.; Boddien, A.; Laurenczy, G.; Beller, M. Ruthenium-Catalyzed Hydrogenation of Bicarbonate in Water. *ChemSusChem* **2010**, *3*, 1048-1050.
- (122) Federsel, C.; Boddien, A.; Jackstell, R.; Jennerjahn, R.; Dyson, P. J.; Scopelliti, R.; Laurenczy, G.; Beller, M. A Well-Defined Iron Catalyst for the Reduction of Bicarbonates and Carbon Dioxide to Formates, Alkyl Formates, and Formamides. *Angew. Chem. Int. Ed.* **2010**, *49*, 9777-9780.
- (123) Federsel, C.; Ziebart, C.; Jackstell, R.; Baumann, W.; Beller, M. Catalytic hydrogenation of carbon dioxide and bicarbonates with a well-defined cobalt dihydrogen complex. *Chem.-Eur. J.* **2012**, *18*, 72-75.
- (124) Tanaka, R.; Yamashita, M.; Nozaki, K. Catalytic Hydrogenation of Carbon Dioxide Using Ir(III)-Pincer Complexes. *J. Am. Chem. Soc.* **2009**, *131*, 14168-14169.
- (125) Tanaka, R.; Yamashita, M.; Chung, L. W.; Morokuma, K.; Nozaki, K. Mechanistic Studies on the Reversible Hydrogenation of Carbon Dioxide Catalyzed by an Ir-PNP Complex. *Organometallics* **2011**, *30*, 6742-6750.
- (126) Langer, R.; Diskin-Posner, Y.; Leitner, G.; Shimon, L. J. W.; Ben-David, Y.; Milstein, D. Low-Pressure Hydrogenation of Carbon Dioxide Catalyzed by an Iron Pincer Complex Exhibiting Noble Metal Activity. *Angew. Chem. Int. Ed.* **2011**, *50*, 9948-9952.

- (127) Schmeier, T. J.; Dobereiner, G. E.; Crabtree, R. H.; Hazari, N. Secondary Coordination Sphere Interactions Facilitate the Insertion Step in an Iridium(III) CO₂ Reduction Catalyst. *J. Am. Chem. Soc.* **2011**, *133*, 9274-9277.
- (128) Hsu, S.-F.; Rommel, S.; Eversfield, P.; Muller, K.; Klemm, E.; Thiel, W. R.; Plietker, B. A Rechargeable Hydrogen Battery Based on Ru Catalysis. *Angew. Chem. Int. Ed.* **2014**, *53*, 7074-7078.
- (129) Jeletic, M. S.; Mock, M. T.; Appel, A. M.; Linehan, J. C. A Cobalt-Based Catalyst for the Hydrogenation of CO₂ under Ambient Conditions. *J. Am. Chem. Soc.* **2013**, *135*, 11533-11536.
- (130) Bays, J. T.; Priyadarshani, N.; Jeletic, M. S.; Hulley, E. B.; Miller, D. L.; Linehan, J. C.; Shaw, W. J. The Influence of the Second and Outer Coordination Spheres on Rh(diphosphine)₂ CO₂ Hydrogenation Catalysts. *ACS Catal.* **2014**, *4*, 3663-3670.
- (131) Filonenko, G. A.; Hensen, E. J. M.; Pidko, E. A. Mechanism of CO₂ hydrogenation to formates by homogeneous Ru-PNP pincer catalyst: from a theoretical description to performance optimization. *Catal. Sci. Technol.* **2014**, *4*, 3474-3485.
- (132) Filonenko, G. A.; van Putten, R.; Schulpen, E. N.; Hensen, E. J. M.; Pidko, E. A. Highly Efficient Reversible Hydrogenation of Carbon Dioxide to Formates Using a Ruthenium PNP-Pincer Catalyst. *ChemCatChem* **2014**, *6*, 1526-1530.
- (133) Huff, C. A.; Sanford, M. S. Catalytic CO₂ Hydrogenation to Formate by a Ruthenium Pincer Complex. *ACS Catal.* **2013**, *3*, 2412-2416.
- (134) Muller, K.; Sun, Y.; Heimermann, A.; Menges, F.; Niedner-Schatteburg, G.; van Wullen, C.; Thiel, W. R. Structure-reactivity relationships in the hydrogenation of carbon dioxide with ruthenium complexes bearing pyridinylazoloto ligands. *Chem.-Eur. J.* **2013**, *19*, 7825-7834.
- (135) Wesselbaum, S.; Hintermair, U.; Leitner, W. Continuous-Flow Hydrogenation of Carbon Dioxide to Pure Formic Acid using an Integrated scCO₂ Process with Immobilized Catalyst and Base. *Angew. Chem. Int. Ed.* **2012**, *51*, 8585-8588.
- (136) Muller, K.; Sun, Y.; Thiel, W. R. Ruthenium(II) Phosphite Complexes as Catalysts for the Hydrogenation of Carbon Dioxide. *ChemCatChem* **2013**, *5*, 1340-1343.
- (137) Moret, S.; Dyson, P. J.; Laurency, G. Direct synthesis of formic acid from carbon dioxide by hydrogenation in acidic media. *Nat. Commun.* **2014**, *5*, doi: 10.1038/ncomms5017.
- (138) Khan, M. M. T.; Halligudi, S. B.; Shukla, S. Reduction of CO₂ by Molecular-Hydrogen to Formic-Acid and Formaldehyde and Their Decomposition to CO and H₂O. *J. Mol. Catal.* **1989**, *57*, 47-60.
- (139) Lau, C. P.; Chen, Y. Z. Hydrogenation of Carbon Dioxide to Formic-Acid Using a 6,6'-Dichloro-2,2'-Bipyridine Complex of Ruthenium, Cis-[Ru(6,6'-Cl₂bpy)₂(H₂O)₂](CF₃SO₃)₂. *J. Mol. Catal. A* **1995**, *101*, 33-36.
- (140) Himeda, Y.; Onozawa-Komatsuzaki, N.; Sugihara, H.; Kasuga, K. Simultaneous tuning of activity and water solubility of complex catalysts by acid-base equilibrium of ligands for conversion of carbon dioxide. *Organometallics* **2007**, *26*, 702-712.
- (141) Himeda, Y.; Miyazawa, S.; Hirose, T. Interconversion between Formic Acid and H₂/CO₂ using Rhodium and Ruthenium Catalysts for CO₂ Fixation and H₂ Storage. *ChemSusChem* **2011**, *4*, 487-493.
- (142) Hull, J. F.; Himeda, Y.; Wang, W.-H.; Hashiguchi, B.; Periana, R.; Szalda, D. J.; Muckerman, J. T.; Fujita, E. Reversible hydrogen storage using CO₂ and a proton-

- switchable iridium catalyst in aqueous media under mild temperatures and pressures. *Nat. Chem.* **2012**, *4*, 383-388.
- (143) Wang, W.-H.; Hull, J. F.; Muckerman, J. T.; Fujita, E.; Himeda, Y. Second-coordination-sphere and electronic effects enhance iridium(III)-catalyzed homogeneous hydrogenation of carbon dioxide in water near ambient temperature and pressure. *Energy Environ. Sci.* **2012**, *5*, 7923-7926.
- (144) Suna, Y.; Ertem, M. Z.; Wang, W.-H.; Kambayashi, H.; Manaka, Y.; Muckerman, J. T.; Fujita, E.; Himeda, Y. Positional Effects of Hydroxy Groups on Catalytic Activity of Proton-Responsive Half-Sandwich Cp*Iridium(III) Complexes. *Organometallics* **2014**, *33*, 6519-6530.
- (145) Maenaka, Y.; Suenobu, T.; Fukuzumi, S. Catalytic interconversion between hydrogen and formic acid at ambient temperature and pressure. *Energy Environ. Sci.* **2012**, *5*, 7360-7367.
- (146) Wang, W.-H.; Muckerman, J. T.; Fujita, E.; Himeda, Y. Mechanistic Insight through Factors Controlling Effective Hydrogenation of CO₂ Catalyzed by Bioinspired Proton-Responsive Iridium(III) Complexes. *ACS Catal.* **2013**, *3*, 856-860.
- (147) Onishi, N.; Xu, S.; Manaka, Y.; Suna, Y.; Wang, W.-H.; Muckerman, J. T.; Fujita, E.; Himeda, Y. CO₂ Hydrogenation Catalyzed by Iridium Complexes with a Proton-responsive Ligand. *Inorg. Chem.* **2015**, *54*, 5114-5123.
- (148) Azua, A.; Sanz, S.; Peris, E. Water-Soluble Ir(III) N-Heterocyclic Carbene Based Catalysts for the Reduction of CO₂ to Formate by Transfer Hydrogenation and the Deuteration of Aryl Amines in Water. *Chem.-Eur. J.* **2011**, *17*, 3963-3967.
- (149) Jessop, P. G.; Hsiao, Y.; Ikariya, T.; Noyori, R. Homogeneous catalysis in supercritical fluids: Hydrogenation of supercritical carbon dioxide to formic acid, alkyl formates, and formamides. *J. Am. Chem. Soc.* **1996**, *118*, 344-355.
- (150) Tsai, J. C.; Nicholas, K. M. Rhodium-Catalyzed Hydrogenation of Carbon-Dioxide to Formic-Acid. *J. Am. Chem. Soc.* **1992**, *114*, 5117-5124.
- (151) Federsel, C.; Jackstell, R.; Beller, M. State-of-the-Art Catalysts for Hydrogenation of Carbon Dioxide. *Angew. Chem. Int. Ed.* **2010**, *49*, 6254-6257.
- (152) Jozsai, I.; Joó, F. Hydrogenation of aqueous mixtures of calcium carbonate and carbon dioxide using a water-soluble rhodium(I)-tertiary phosphine complex catalyst. *J. Mol. Catal. A* **2004**, *224*, 87-91.
- (153) Katho, A.; Opre, Z.; Laurency, G.; Joó, F. Water-soluble analogs of [RuCl₃(NO)(PPh₃)₂] and their catalytic activity in the hydrogenation of carbon dioxide and bicarbonate in aqueous solution. *J. Mol. Catal. A* **2003**, *204*, 143-148.
- (154) Joó, F.; Laurency, G.; Karady, P.; Elek, J.; Nadasdi, L.; Roulet, R. Homogeneous hydrogenation of aqueous hydrogen carbonate to formate under mild conditions with water soluble rhodium(I)- and ruthenium(II)-phosphine catalysts. *Appl. Organomet. Chem.* **2000**, *14*, 857-859.
- (155) Joó, F.; Laurency, G.; Nadasdi, L.; Elek, J. Homogeneous hydrogenation of aqueous hydrogen carbonate to formate under exceedingly mild conditions - a novel possibility of carbon dioxide activation. *Chem. Commun.* **1999**, 971-972.
- (156) Horvath, H.; Laurency, G.; Katho, A. Water-soluble (η^6 -arene)ruthenium(II)-phosphine complexes and their catalytic activity in the hydrogenation of bicarbonate in aqueous solution. *J. Organometal. Chem.* **2004**, *689*, 1036-1045.
- (157) Erlandsson, M.; Landaeta, V. R.; Gonsalvi, L.; Peruzzini, M.; Phillips, A. D.; Dyson, P. J.;

- Laurenczy, G. (Pentamethylcyclopentadienyl)iridium-PTA (PTA=1,3,5-triaza-7-phosphaadamantane) complexes and their application in catalytic water phase carbon dioxide hydrogenation. *Eur. J. Inorg. Chem.* **2008**, 620-627.
- (158) Laurenczy, G.; Jedner, S.; Alessio, E.; Dyson, P. J. In situ NMR characterisation of an intermediate in the catalytic hydrogenation of CO₂ and HCO₃⁻ in aqueous solution. *Inorg. Chem. Commun.* **2007**, *10*, 558-562.
- (159) Ziebart, C.; Federsel, C.; Anbarasan, P.; Jackstell, R.; Baumann, W.; Spannenberg, A.; Beller, M. Well-defined iron catalyst for improved hydrogenation of carbon dioxide and bicarbonate. *J. Am. Chem. Soc.* **2012**, *134*, 20701-20704.
- (160) Kisanga, P. B.; Verkade, J. G.; Schwesinger, R. pK_a Measurements of P(RNCH₂CH₃)₃N. *J. Org. Chem.* **2000**, *65*, 5431-5432.
- (161) Kumar, N.; Camaioni, D. M.; Dupuis, M.; Raugei, S.; Appel, A. M. Mechanistic insights into hydride transfer for catalytic hydrogenation of CO₂ with cobalt complexes. *Dalton Trans.* **2014**, *43*, 11803-11806.
- (162) Urakawa, A.; Jutz, F.; Laurenczy, G.; Baiker, A. Carbon dioxide hydrogenation catalyzed by a ruthenium dihydride: a DFT and high-pressure spectroscopic investigation. *Chem.-Eur. J.* **2007**, *13*, 3886-3899.
- (163) Drake, J. L.; Manna, C. M.; Byers, J. A. Enhanced Carbon Dioxide Hydrogenation Facilitated by Catalytic Quantities of Bicarbonate and Other Inorganic Salts. *Organometallics* **2013**, *32*, 6891-6894.
- (164) Li, Y.-N.; He, L.-N.; Liu, A.-H.; Lang, X.-D.; Yang, Z.-Z.; Yu, B.; Luan, C.-R. In situ hydrogenation of captured CO₂ to formate with polyethyleneimine and Rh/monophosphine system. *Green Chem.* **2013**, *15*, 2825-2829.
- (165) Xu, Z.; McNamara, N. D.; Neumann, G. T.; Schneider, W. F.; Hicks, J. C. Catalytic Hydrogenation of CO₂ to Formic Acid with Silica-Tethered Iridium Catalysts. *ChemCatChem* **2013**, *5*, 1769-1771.
- (166) Yang, X. Z. Hydrogenation of Carbon Dioxide Catalyzed by PNP Pincer Iridium, Iron, and Cobalt Complexes: A Computational Design of Base Metal Catalysts. *ACS Catal.* **2011**, *1*, 849-854.
- (167) Suh, H.-W.; Schmeier, T. J.; Hazari, N.; Kemp, R. A.; Takase, M. K. Experimental and Computational Studies of the Reaction of Carbon Dioxide with Pincer-Supported Nickel and Palladium Hydrides. *Organometallics* **2012**, *31*, 8225-8236.
- (168) Lubitz, W.; Ogata, H.; Ruediger, O.; Reijerse, E. Hydrogenases. *Chem. Rev.* **2014**, *114*, 4081-4148.
- (169) Nicolet, Y.; de Lacey, A. L.; Vernede, X.; Fernandez, V. M.; Hatchikian, E. C.; Fontecilla-Camps, J. C. Crystallographic and FTIR spectroscopic evidence of changes in Fe coordination upon reduction of the active site of the Fe-only hydrogenase from *Desulfovibrio desulfuricans*. *J. Am. Chem. Soc.* **2001**, *123*, 1596-1601.
- (170) Rakowski DuBois, M.; DuBois, D. L. The roles of the first and second coordination spheres in the design of molecular catalysts for H₂ production and oxidation. *Chem. Soc. Rev.* **2009**, *38*, 62-72.
- (171) Helm, M. L.; Stewart, M. P.; Bullock, R. M.; DuBois, M. R.; DuBois, D. L. A Synthetic Nickel Electrocatalyst with a Turnover Frequency Above 100,000 s⁻¹ for H₂ Production. *Science* **2011**, *333*, 863-866.
- (172) Horvath, S.; Fernandez, L. E.; Soudackov, A. V.; Hammes-Schiffer, S. Insights into proton-coupled electron transfer mechanisms of electrocatalytic H₂ oxidation and

- production. *Proc. Nat. Acad. Sci. U.S.A.* **2012**, *109*, 15663-15668.
- (173) Zhao, M.; Wang, H.-B.; Ji, L.-N.; Mao, Z.-W. Insights into metalloenzyme microenvironments: biomimetic metal complexes with a functional second coordination sphere. *Chem. Soc. Rev.* **2013**, *42*, 8360-8375.
- (174) Crabtree, R. H. Multifunctional ligands in transition metal catalysis. *New J. Chem.* **2011**, *35*, 18-23.
- (175) Milstein, D. Discovery of Environmentally Benign Catalytic Reactions of Alcohols Catalyzed by Pyridine-Based Pincer Ru Complexes, Based on Metal-Ligand Cooperation. *Top. Catal.* **2010**, *53*, 915-923.
- (176) Conley, B. L.; Pennington-Boggio, M. K.; Boz, E.; Williams, T. J. Discovery, Applications, and Catalytic Mechanisms of Shvo's Catalyst. *Chem. Rev.* **2010**, *110*, 2294-2312.
- (177) Grutzmacher, H. Cooperating ligands in catalysis. *Angew. Chem. Int. Ed.* **2008**, *47*, 1814-1818.
- (178) Vogt, M.; Gargir, M.; Iron, M. A.; Diskin-Posner, Y.; Ben-David, Y.; Milstein, D. A New Mode of Activation of CO₂ by Metal-Ligand Cooperation with Reversible C-C and M-O Bond Formation at Ambient Temperature. *Chem.-Eur. J.* **2012**, *18*, 9194-9197.
- (179) Huff, C. A.; Kampf, J. W.; Sanford, M. S. Role of a Noninnocent Pincer Ligand in the Activation of CO₂ at (PNN)Ru(H)(CO). *Organometallics* **2012**, *31*, 4643-4645.
- (180) Zhang, J.; Leitus, G.; Ben-David, Y.; Milstein, D. Efficient homogeneous catalytic hydrogenation of esters to alcohols. *Angew. Chem. Int. Ed.* **2006**, *45*, 1113-1115.
- (181) Praneeth, V. K. K.; Ringenberg, M. R.; Ward, T. R. Redox-Active Ligands in Catalysis. *Angew. Chem. Int. Ed.* **2012**, *51*, 10228-10234.
- (182) Gunanathan, C.; Milstein, D. Metal-Ligand Cooperation by Aromatization-Deaomatization: A New Paradigm in Bond Activation and "Green" Catalysis. *Acc. Chem. Res.* **2011**, *44*, 588-602.
- (183) Kang, P.; Cheng, C.; Chen, Z.; Schauer, C. K.; Meyer, T. J.; Brookhart, M. Selective electrocatalytic reduction of CO₂ to formate by water-stable iridium dihydride pincer complexes. *J. Am. Chem. Soc.* **2012**, *134*, 5500-5503.
- (184) Kang, P.; Meyer, T. J.; Brookhart, M. Selective electrocatalytic reduction of carbon dioxide to formate by a water-soluble iridium pincer catalyst. *Chem. Sci.* **2013**, *4*, 3497-3502.
- (185) Bernskoetter, W. H.; Hazari, N. A Computational Investigation of the Insertion of Carbon Dioxide into Four- and Five-Coordinate Iridium Hydrides. *Eur. J. Inorg. Chem.* **2013**, *2013*, 4032-4041.
- (186) Filonenko, G. A.; Conley, M. P.; Coperet, C.; Lutz, M.; Hensen, E. J. M.; Pidko, E. A. The impact of Metal-Ligand Cooperation in Hydrogenation of Carbon Dioxide Catalyzed by Ruthenium PNP Pincer. *ACS Catal.* **2013**, *3*, 2522-2526.
- (187) Sanz, S.; Benitez, M.; Peris, E. A New Approach to the Reduction of Carbon Dioxide: CO₂ Reduction to Formate by Transfer Hydrogenation in *i*PrOH. *Organometallics* **2010**, *29*, 275-277.
- (188) Sanz, S.; Azua, A.; Peris, E. '(η^6 -arene)Ru(bis-NHC)' complexes for the reduction of CO₂ to formate with hydrogen and by transfer hydrogenation with *i*PrOH. *Dalton Trans.* **2010**, *39*, 6339-6343.
- (189) Bolinger, C. M.; Sullivan, B. P.; Conrad, D.; Gilbert, J. A.; Story, N.; Meyer, T. J. Electrocatalytic Reduction of CO₂ Based on Polypyridyl Complexes of Rhodium and

- Ruthenium. *J. Chem. Soc., Chem. Commun.* **1985**, 796-797.
- (190) Caix, C.; ChardonNoblat, S.; Deronzier, A. Electrocatalytic reduction of CO₂ into formate with [(η⁵-Me₅C₅)M(L)Cl]⁺ complexes (L = 2,2'-bipyridine ligands; M = Rh(III) and Ir(III)). *J. Electroanal. Chem.* **1997**, *434*, 163-170.
- (191) Hayashi, H.; Ogo, S.; Abura, T.; Fukuzumi, S. Accelerating effect of a proton on the reduction of CO₂ dissolved in water under acidic conditions. Isolation, crystal structure, and reducing ability of a water-soluble ruthenium hydride complex. *J. Am. Chem. Soc.* **2003**, *125*, 14266-14267.
- (192) Wang, W.-H.; Ertem, M. Z.; Xu, S.; Onishi, N.; Manaka, Y.; Suna, Y.; Kambayashi, H.; Muckerman, J. T.; Fujita, E.; Himeda, Y. Highly Robust Hydrogen Generation by Bio-Inspired Ir Complexes for Dehydrogenation of Formic Acid in Water: Experimental and Theoretical Mechanistic Investigations at Different pH. *ACS Catal.* **2015**, in revision.
- (193) Himeda, Y.; Onozawa-Komatsuzaki, N.; Sugihara, H.; Arakawa, H.; Kasuga, K. Transfer hydrogenation of a variety of ketones catalyzed by rhodium complexes in aqueous solution and their application to asymmetric reduction using chiral Schiff base ligands. *J. Mol. Catal. A* **2003**, *195*, 95-100.
- (194) Tai, C. C.; Pitts, J.; Linehan, J. C.; Main, A. D.; Munshi, P.; Jessop, P. G. In situ formation of ruthenium catalysts for the homogeneous hydrogenation of carbon dioxide. *Inorg. Chem.* **2002**, *41*, 1606-1614.
- (195) Ohnishi, Y. Y.; Matsunaga, T.; Nakao, Y.; Sato, H.; Sakaki, S. Ruthenium(II)-catalyzed hydrogenation of carbon dioxide to formic acid. Theoretical study of real catalyst, ligand effects, and solvation effects. *J. Am. Chem. Soc.* **2005**, *127*, 4021-4032.
- (196) Himeda, Y.; Onozawa-Komatsuzaki, N.; Sugihara, H.; Kasuga, K. Highly efficient conversion of carbon dioxide catalyzed by half-sandwich complexes with pyridinol ligand: The electronic effect of oxyanion. *J. Photochem. Photobio. A* **2006**, *182*, 306-309.
- (197) Hansch, C.; Leo, A.; Taft, R. W. A Survey of Hammett Substituent Constants and Resonance and Field Parameters. *Chem. Rev.* **1991**, *91*, 165-195.
- (198) Askevold, B.; Roesky, H. W.; Schneider, S. Learning from the Neighbors: Improving Homogeneous Catalysts with Functional Ligands Motivated by Heterogeneous and Biocatalysis. *ChemCatChem* **2012**, *4*, 307-320.
- (199) Shima, S.; Lyon, E. J.; Sordel-Klippert, M. S.; Kauss, M.; Kahnt, J.; Thauer, R. K.; Steinbach, K.; Xie, X. L.; Verdier, L.; Griesinger, C. The cofactor of the iron-sulfur cluster free hydrogenase Hmd: Structure of the light-inactivation product. *Angew. Chem. Int. Ed.* **2004**, *43*, 2547-2551.
- (200) Shima, S.; Pilak, O.; Vogt, S.; Schick, M.; Stagni, M. S.; Meyer-Klaucke, W.; Warkentin, E.; Thauer, R. K.; Ermler, U. The crystal structure of Fe -hydrogenase reveals the geometry of the active site. *Science* **2008**, *321*, 572-575.
- (201) Shima, S.; Ermler, U. Structure and Function of Fe -Hydrogenase and its Iron-Guanylylpyridinol (FeGP) Cofactor. *Eur. J. Inorg. Chem.* **2011**, 963-972.
- (202) Yang, X.; Hall, M. B. Monoiron Hydrogenase Catalysis: Hydrogen Activation with the Formation of a Dihydrogen, Fe-H^{δ-}...H^{δ+}-O, Bond and Methenyl-H₄MPT⁺ Triggered Hydride Transfer. *J. Am. Chem. Soc.* **2009**, *131*, 10901-10908.
- (203) Fujita, K.-i.; Tanino, N.; Yamaguchi, R. Ligand-promoted dehydrogenation of alcohols catalyzed by Cp*Ir complexes. A new catalytic system for oxidant-free oxidation of alcohols. *Org. Lett.* **2007**, *9*, 109-111.
- (204) Yamaguchi, R.; Ikeda, C.; Takahashi, Y.; Fujita, K.-i. Homogeneous Catalytic System for

- Reversible Dehydrogenation-Hydrogenation Reactions of Nitrogen Heterocycles with Reversible Interconversion of Catalytic Species. *J. Am. Chem. Soc.* **2009**, *131*, 8410-8412.
- (205) Fujita, K.-i.; Yoshida, T.; Imori, Y.; Yamaguchi, R. Dehydrogenative Oxidation of Primary and Secondary Alcohols Catalyzed by a Cp*Ir Complex Having a Functional C,N-Chelate Ligand. *Org. Lett.* **2011**, *13*, 2278-2281.
- (206) Kawahara, R.; Fujita, K.-i.; Yamaguchi, R. Dehydrogenative Oxidation of Alcohols in Aqueous Media Using Water-Soluble and Reusable Cp*Ir Catalysts Bearing a Functional Bipyridine Ligand. *J. Am. Chem. Soc.* **2012**, *134*, 3643-3646.
- (207) Kelson, E. P.; Phengsy, P. P. Synthesis and structure of a ruthenium(II) complex incorporating kappa N bound 2-pyridonato ligands; a new catalytic system for transfer hydrogenation of ketones. *J. Chem. Soc., Dalton Trans.* **2000**, 4023-4024.
- (208) Himeda, Y.; Onozawa-Komatsuzaki, N.; Sugihara, H.; Arakawa, H.; Kasuga, K. Half-sandwich complexes with 4,7-dihydroxy-1,10-phenanthroline: Water-soluble, highly efficient catalysts for hydrogenation of bicarbonate attributable to the generation of an oxyanion on the catalyst ligand. *Organometallics* **2004**, *23*, 1480-1483.
- (209) Himeda, Y.; Onozawa-Komatsuzaki, N.; Sugihara, H.; Kasuga, K. Recyclable catalyst for conversion of carbon dioxide into formate attributable to an oxyanion on the catalyst ligand. *J. Am. Chem. Soc.* **2005**, *127*, 13118-13119.
- (210) Manaka, Y.; Wang, W.-H.; Suna, Y.; Kambayashi, H.; Muckerman, J. T.; Fujita, E.; Himeda, Y. Efficient H₂ generation from formic acid using azole complexes in water. *Catal. Sci. Technol.* **2014**, *4*, 34-37.
- (211) Wang, W.-H.; Xu, S.; Manaka, Y.; Suna, Y.; Kambayashi, H.; Muckerman, J. T.; Fujita, E.; Himeda, Y. Formic Acid Dehydrogenation with Bioinspired Iridium Complexes: A Kinetic Isotope Effect Study and Mechanistic Insight. *ChemSusChem* **2014**, *7*, 1976-1983.
- (212) Ogo, S.; Kabe, R.; Hayashi, H.; Harada, R.; Fukuzumi, S. Mechanistic investigation of CO₂ hydrogenation by Ru(II) and Ir(III) aqua complexes under acidic conditions: two catalytic systems differing in the nature of the rate determining step. *Dalton Trans.* **2006**, 4657-4663.
- (213) Hou, C.; Jiang, J.; Zhang, S.; Wang, G.; Zhang, Z.; Ke, Z.; Zhao, C. Hydrogenation of Carbon Dioxide using Half-Sandwich Cobalt, Rhodium, and Iridium Complexes: DFT Study on the Mechanism and Metal Effect. *ACS Catal.* **2014**, *4*, 2990-2997.
- (214) Xi, Z.; Zhou, N.; Sun, Y.; Li, K. Reaction-controlled phase-transfer catalysis for propylene epoxidation to propylene oxide. *Science* **2001**, *292*, 1139-1141.
- (215) Wang, W.; Zhang, G.; Lang, R.; Xia, C.; Li, F. pH-Responsive N-heterocyclic carbene copper(I) complexes: syntheses and recoverable applications in the carboxylation of arylboronic esters and benzoxazole with carbon dioxide. *Green Chem.* **2013**, *15*, 635-640.
- (216) Williams, R.; Crandall, R. S.; Bloom, A. Use of carbon dioxide in energy storage *Appl. Phys. Lett.* **1978**, *33*, 381-383.
- (217) Bi, Q.-Y.; Lin, J.-D.; Liu, Y.-M.; Du, X.-L.; Wang, J.-Q.; He, H.-Y.; Cao, Y. An Aqueous Rechargeable Formate-Based Hydrogen Battery Driven by Heterogeneous Pd Catalysis. *Angewandte Chemie International Edition* **2014**, *53*, 13583-13587.
- (218) Zhu, Q.-L.; Tsumori, N.; Xu, Q. Sodium hydroxide-assisted growth of uniform Pd nanoparticles on nanoporous carbon MSC-30 for efficient and complete dehydrogenation of formic acid under ambient conditions *Chem. Sci.* **2014**, *5*, 195-199.
- (219) Tedsree, K.; Li, T.; Jones, S.; Chan, C. W. A.; Yu, K. M. K.; Bagot, P. A. J.; Marquis, E. A.; Smith, G. D. W.; Tsang, S. C. E. Hydrogen production from formic acid

- decomposition at room temperature using a Ag-Pd core-shell nanocatalyst *Nature Nanotech.* **2011**, *6*, 302-307.
- (220) Noyori, R.; Hashiguchi, S. Asymmetric transfer hydrogenation catalyzed by chiral ruthenium complexes. *Acc. Chem. Res.* **1997**, *30*, 97-102.
- (221) Ikariya, T.; Blacker, A. J. Asymmetric Transfer Hydrogenation of Ketones with Bifunctional Transition Metal-Based Molecular Catalysts. *Accounts of Chemical Research* **2007**, *40*, 1300-1308.
- (222) Wei, Y.; Wu, X.; Wang, C.; Xiao, J. Transfer hydrogenation in aqueous media. *Catalysis Today* **2015**, *247*, 104-116.
- (223) Joó, F. Breakthroughs in Hydrogen Storage: Formic Acid as a Sustainable Storage Material for Hydrogen. *ChemSusChem* **2008**, *1*, 805-808.
- (224) Enthaler, S.; von Langermann, J.; Schmidt, T. Carbon dioxide and formic acid-the couple for environmental-friendly hydrogen storage? *Energy Environ. Sci.* **2010**, *3*, 1207-1217.
- (225) Grasemann, M.; Laurency, G. Formic acid as a hydrogen source – recent developments and future trends. *Energy Environ. Sci.* **2012**, *5*, 8171-8181.
- (226) Johnson, T. C.; Morris, D. J.; Wills, M. Hydrogen generation from formic acid and alcohols using homogeneous catalysts. *Chem. Soc. Rev.* **2010**, *39*, 81-88.
- (227) Coffey, R. S. A catalyst for the homogeneous hydrogenation of aldehydes under mild conditions. *J. Chem. Soc., Chem. Commun.* **1967**, 923b.
- (228) Loges, B.; Boddien, A.; Junge, H.; Beller, M. Controlled generation of hydrogen from formic acid amine adducts at room temperature and application in H₂/O₂ fuel cells. *Angew. Chem. Int. Ed.* **2008**, *47*, 3962-3965.
- (229) Fellay, C.; Dyson, P. J.; Laurency, G. A viable hydrogen-storage system based on selective formic acid decomposition with a ruthenium catalyst. *Angew. Chem. Int. Ed.* **2008**, *47*, 3966-3968.
- (230) Fellay, C.; Yan, N.; Dyson, P. J.; Laurency, G. Selective Formic Acid Decomposition for High-Pressure Hydrogen Generation: A Mechanistic Study. *Chem.-Eur. J.* **2009**, *15*, 3752-3760.
- (231) Majewski, A.; Morris, D. J.; Kendall, K.; Wills, M. A Continuous-Flow Method for the Generation of Hydrogen from Formic Acid. *ChemSusChem* **2010**, *3*, 431-434.
- (232) Morris, D. J.; Clarkson, G. J.; Wills, M. Insights into Hydrogen Generation from Formic Acid Using Ruthenium Complexes. *Organometallics* **2009**, *28*, 4133-4140.
- (233) Boddien, A.; Mellmann, D.; Gartner, F.; Jackstell, R.; Junge, H.; Dyson, P. J.; Laurency, G.; Ludwig, R.; Beller, M. Efficient dehydrogenation of formic acid using an iron catalyst. *Science* **2011**, *333*, 1733-1736.
- (234) Bielinski, E. A.; Lagaditis, P. O.; Zhang, Y.; Mercado, B. Q.; Wuertele, C.; Bernskoetter, W. H.; Hazari, N.; Schneider, S. Lewis Acid-Assisted Formic Acid Dehydrogenation Using a Pincer-Supported Iron Catalyst. *J. Am. Chem. Soc.* **2014**, *136*, 10234-10237.
- (235) Zell, T.; Butschke, B.; Ben-David, Y.; Milstein, D. Efficient hydrogen liberation from formic acid catalyzed by a well-defined iron pincer complex under mild conditions. *Chem.-Eur. J.* **2013**, *19*, 8068-8072.
- (236) Myers, T. W.; Berben, L. A. Aluminium-ligand cooperation promotes selective dehydrogenation of formic acid to H₂ and CO₂. *Chem. Sci.* **2014**, *5*, 2771-2777.
- (237) Boddien, A.; Loges, B.; Junge, H.; Gartner, F.; Noyes, J. R.; Beller, M. Continuous Hydrogen Generation from Formic Acid: Highly Active and Stable Ruthenium Catalysts. *Adv. Synth. Catal.* **2009**, *351*, 2517-2520.

- (238) Sponholz, P.; Mellmann, D.; Junge, H.; Beller, M. Towards a practical setup for hydrogen production from formic acid. *ChemSusChem* **2013**, *6*, 1172-1176.
- (239) Czaun, M.; Goepfert, A.; Kothandaraman, J.; May, R. B.; Haiges, R.; Prakash, G. K. S.; Olah, G. A. Formic Acid As a Hydrogen Storage Medium: Ruthenium-Catalyzed Generation of Hydrogen from Formic Acid in Emulsions. *ACS Catal.* **2014**, *4*, 311-320.
- (240) Oldenhof, S.; de Bruin, B.; Lutz, M.; Siegler, M. A.; Patureau, F. W.; van der Vlugt, J. I.; Reek, J. N. Base-free production of H₂ by dehydrogenation of formic acid using an iridium-bismetamorphos complex. *Chem.-Eur. J.* **2013**, *19*, 11507-11511.
- (241) Mellone, I.; Peruzzini, M.; Rosi, L.; Mellmann, D.; Junge, H.; Beller, M.; Gonsalvi, L. Formic acid dehydrogenation catalysed by ruthenium complexes bearing the tripodal ligands triphos and NP₃. *Dalton Trans.* **2013**, *42*, 2495-2501.
- (242) Barnard, J. H.; Wang, C.; Berry, N. G.; Xiao, J. Long-range metal-ligand bifunctional catalysis: cyclometallated iridium catalysts for the mild and rapid dehydrogenation of formic acid. *Chem. Sci.* **2013**, *4*, 1234-1244.
- (243) Fukuzumi, S.; Kobayashi, T.; Suenobu, T. Unusually Large Tunneling Effect on Highly Efficient Generation of Hydrogen and Hydrogen Isotopes in pH-Selective Decomposition of Formic Acid Catalyzed by a Heterodinuclear Iridium-Ruthenium Complex in Water. *J. Am. Chem. Soc.* **2010**, *132*, 1496-1497.
- (244) Himeda, Y. Highly efficient hydrogen evolution by decomposition of formic acid using an iridium catalyst with 4,4'-dihydroxy-2,2'-bipyridine. *Green Chem.* **2009**, *11*, 2018-2022.
- (245) Kothandaraman, J.; Czaun, M.; Goepfert, A.; Haiges, R.; Jones, J.-P.; May, R. B.; Prakash, G. K. S.; Olah, G. A. Amine-Free Reversible Hydrogen Storage in Formate Salts Catalyzed by Ruthenium Pincer Complex without pH Control or Solvent Change. *ChemSusChem* **2015**, *8*, 1442-1451.
- (246) Strauss, S. H.; Whitmire, K. H.; Shriver, D. F. Rhodium(I) catalyzed decomposition of formic acid. *J. Organometal. Chem.* **1979**, *174*, C59-C62.
- (247) Gao, Y.; Kuncheria, J. K.; Jenkins, H. A.; Puddephatt, R. J.; Yap, G. P. A. The interconversion of formic acid and hydrogen/carbon dioxide using a binuclear ruthenium complex catalyst. *J. Chem. Soc., Chem. Commun.* **2000**, 3212-3217.
- (248) Man, M. L.; Zhou, Z. Y.; Ng, S. M.; Lau, C. P. Synthesis, characterization and reactivity of heterobimetallic complexes (η^5 -C₅R₅)Ru(CO)(μ -dppm)M(CO)₂(η^5 -C₅H₅) (R = H, CH₃; M = Mo, W). Interconversion of hydrogen/carbon dioxide and formic acid by these complexes. *Dalton Trans.* **2003**, 3727-3735.
- (249) Yoshida, T.; Ueda, Y.; Otsuka, S. Activation of water molecule. 1. Intermediates bearing on water gas shift reaction catalyzed by platinum(0) complexes. *J. Am. Chem. Soc.* **1978**, *100*, 3941-3942.
- (250) Paonessa, R. S.; Trogler, W. C. Solvent-dependent reactions of carbon dioxide with a platinum(II) dihydride: Reversible formation of a platinum(II) formatehydride and a cationic platinum(II) dimer, [Pt₂H₃(PEt₃)₄][HCO₂]. *J. Am. Chem. Soc.* **1982**, *104*, 3529-3530.
- (251) Leitner, W.; Dinjus, E.; Gassner, F. Activation of Carbon Dioxide 4. Rhodium-Catalyzes Hydrogenation of Carbon Dioxide to Formic Acid. *J. Organometal. Chem.* **1994**, *475*, 257-266.
- (252) Boddien, A.; Loges, B.; Junge, H.; Beller, M. Hydrogen Generation at Ambient Conditions: Application in Fuel Cells. *ChemSusChem* **2008**, *1*, 751-758.

- (253) Manca, G.; Mellone, I.; Bertini, F.; Peruzzini, M.; Rosi, L.; Mellmann, D.; Junge, H.; Beller, M.; Ienco, A.; Gonsalvi, L. Inner- versus Outer-Sphere Ru-Catalyzed Formic Acid Dehydrogenation: A Computational Study. *Organometallics* **2013**, *32*, 7053-7064.
- (254) Sordakis, K.; Beller, M.; Laurenczy, G. Chemical Equilibria in Formic Acid/Amine-CO₂Cycles under Isochoric Conditions using a Ruthenium(II) 1,2-Bis(diphenylphosphino)ethane Catalyst. *ChemCatChem* **2014**, *6*, 96-99.
- (255) Oldenhof, S.; Lutz, M.; de Bruin, B.; van der Vlugt, J. I.; Reek, J. N. Dehydrogenation of formic acid by Ir-bismetamorphos complexes: experimental and computational insight into the role of a cooperative ligand *Chem. Sci.* **2015**, *6*, 1027-1034.
- (256) Enthaler, S.; Junge, H.; Fischer, A.; Kammer, A.; Krackl, S.; Epping, J. D. Dual functionality of formamidine polymers, as ligands and as bases, in ruthenium-catalysed hydrogen evolution from formic acid. *Polym. Chem.* **2013**, *4*, 2741-2746.
- (257) Thevenon, A.; Frost-Pennington, E.; Weijia, G.; Dalebrook, A. F.; Laurenczy, G. Formic Acid Dehydrogenation Catalysed by Tris(TPPTS) Ruthenium Species: Mechanism of the Initial "Fast" Cycle. *ChemCatChem* **2014**, *6*, 3146-3152.
- (258) Mazzone, G.; Alberto, M. E.; Sicilia, E. Theoretical mechanistic study of the formic acid decomposition assisted by a Ru(II)-phosphine catalyst. *J. Mol. Model.* **2014**, *20*, 2250-2257.
- (259) Gan, W.; Snelders, D. J. M.; Dyson, P. J.; Laurenczy, G. Ruthenium(II)-Catalyzed Hydrogen Generation from Formic Acid using Cationic, Ammoniomethyl-Substituted Triarylphosphine Ligands. *ChemCatChem* **2013**, *5*, 1126-1132.
- (260) Guerriero, A.; Bricout, H.; Sordakis, K.; Peruzzini, M.; Monflier, E.; Hapiot, F.; Laurenczy, G.; Gonsalvi, L. Hydrogen Production by Selective Dehydrogenation of HCOOH Catalyzed by Ru-Biaryl Sulfonated Phosphines in Aqueous Solution. *ACS Catal.* **2014**, *4*, 3002-3012.
- (261) Czaun, M.; Goepfert, A.; May, R.; Haiges, R.; Prakash, G. K.; Olah, G. A. Hydrogen generation from formic acid decomposition by ruthenium carbonyl complexes. Tetraruthenium dodecacarbonyl tetrahydride as an active intermediate. *ChemSusChem* **2011**, *4*, 1241-1248.
- (262) Horváth, H.; Kathó, Á.; Udvardy, A.; Papp, G.; Szikszai, D.; Joó, F. New Water-Soluble Iridium(I)-N-Heterocyclic Carbene-Tertiary Phosphine Mixed-Ligand Complexes as Catalysts of Hydrogenation and Redox Isomerization. *Organometallics* **2014**, *33*, 6330-6340.
- (263) Vogt, M.; Nerush, A.; Diskin-Posner, Y.; Ben-David, Y.; Milstein, D. Reversible CO₂ binding triggered by metal-ligand cooperation in a rhenium(I) PNP pincer-type complex and the reaction with dihydrogen. *Chem. Sci.* **2014**, *5*, 2043-2051.
- (264) Fukuzumi, S.; Kobayashi, T.; Suenobu, T. Efficient Catalytic Decomposition of Formic Acid for the Selective Generation of H₂ and H/D Exchange with a Water-Soluble Rhodium Complex in Aqueous Solution. *ChemSusChem* **2008**, *1*, 827-834.
- (265) Keller, S. G.; Ringenberg, M. R.; Häussinger, D.; Ward, T. R. Evaluation of the Formate Dehydrogenase Activity of Three-Legged Pianostool Complexes in Dilute Aqueous Solution. *Eur. J. Inorg. Chem.* **2014**, *2014*, 5860-5864.
- (266) Wang, W.-H.; Hull, J. F.; Muckerman, J. T.; Fujita, E.; Hirose, T.; Himeda, Y. Highly Efficient D₂ Generation by Dehydrogenation of Formic Acid in D₂O through H⁺/D⁺ Exchange on an Iridium Catalyst: Application to the Synthesis of Deuterated Compounds by Transfer Deuterogenation. *Chem.-Eur. J.* **2012**, *18*, 9397-9404.

- (267) Boddien, A.; Loges, B.; Gartner, F.; Torborg, C.; Fumino, K.; Junge, H.; Ludwig, R.; Beller, M. Iron-Catalyzed Hydrogen Production from Formic Acid. *J. Am. Chem. Soc.* **2010**, *132*, 8924-8934.
- (268) Boddien, A.; Gartner, F.; Jackstell, R.; Junge, H.; Spannenberg, A.; Baumann, W.; Ludwig, R.; Beller, M. ortho-Metalation of Iron(0) Tribenzylphosphine Complexes: Homogeneous Catalysts for the Generation of Hydrogen from Formic Acid. *Angew. Chem. Int. Ed.* **2010**, *49*, 8993-8996.
- (269) Mellmann, D.; Barsch, E.; Bauer, M.; Grabow, K.; Boddien, A.; Kammer, A.; Sponholz, P.; Bentrup, U.; Jackstell, R.; Junge, H.; Laurenczy, G.; Ludwig, R.; Beller, M. Base-Free Non-Noble-Metal-Catalyzed Hydrogen Generation from Formic Acid: Scope and Mechanistic Insights. *Chem.-Eur. J.* **2014**, *20*, 13589-13602.
- (270) Yang, L.; Wang, H.; Zhang, N.; Hong, S. The reduction of carbon dioxide in iron biocatalyst catalytic hydrogenation reaction: a theoretical study. *Dalton Trans.* **2013**, *42*, 11186-11193.
- (271) Sanchez-de-Armas, R.; Xue, L.; Ahlquist, M. S. One Site Is Enough: A Theoretical Investigation of Iron-Catalyzed Dehydrogenation of Formic Acid. *Chem.-Eur. J.* **2013**, *19*, 11869-11873.
- (272) Gao, Y.; Kuncheria, J.; J. Puddephatt, R.; P. A. Yap, G. An efficient binuclear catalyst for decomposition of formic acid. *Chem. Commun.* **1998**, 2365-2366.
- (273) Boddien, A.; Gartner, F.; Federsel, C.; Sponholz, P.; Mellmann, D.; Jackstell, R.; Junge, H.; Beller, M. CO₂-"Neutral" Hydrogen Storage Based on Bicarbonates and Formates. *Angew. Chem. Int. Ed.* **2011**, *50*, 6411-6414.
- (274) Papp, G.; Csorba, J.; Laurenczy, G.; Joó, F. A Charge/Discharge Device for Chemical Hydrogen Storage and Generation. *Angew. Chem. Int. Ed.* **2011**, *50*, 10433-10435.
- (275) Preti, D.; Squarcialupi, S.; Fachinetti, G. Production of HCOOH/NEt₃ Adducts by CO₂/H₂ Incorporation into Neat NEt₃. *Angew. Chem. Int. Ed.* **2010**, *49*, 2581-2584.
- (276) Boddien, A.; Federsel, C.; Sponholz, P.; Mellmann, D.; Jackstell, R.; Junge, H.; Laurenczy, G.; Beller, M. Towards the development of a hydrogen battery. *Energy Environ. Sci.* **2012**, *5*, 8907-8911.
- (277) Enthaler, S.; Brück, A.; Kammer, A.; Junge, H.; Irran, E.; Gülak, S. Exploring the Reactivity of Nickel Pincer Complexes in the Decomposition of Formic Acid to CO₂/H₂ and the Hydrogenation of NaHCO to HCOONa. *ChemCatChem* **2015**, *7*, 65-69.
- (278) Balaraman, E.; Gunanathan, C.; Zhang, J.; Shimon, L. J. W.; Milstein, D. Efficient hydrogenation of organic carbonates, carbamates and formates indicates alternative routes to methanol based on CO₂ and CO. *Nat. Chem.* **2011**, *3*, 609-614.
- (279) Schlögl, R. Chemistry's Role in Regenerative Energy. *Angewandte Chemie International Edition* **2011**, *50*, 6424-6426.
- (280) Olah, G. A. Towards Oil Independence Through Renewable Methanol Chemistry. *Angewandte Chemie International Edition* **2013**, *52*, 104-107.
- (281) Waugh, K. C. Methanol Synthesis. *Catalysis Today* **1992**, *15*, 51-75.
- (282) Behrens, M.; Studt, F.; Kasatkin, I.; Kühl, S.; Hävecker, M.; Abild-Pedersen, F.; Zander, S.; Girgsdies, F.; Kurr, P.; Knief, B.-L.; Tovar, M.; Fischer, R. W.; Nørskov, J. K.; Schlögl, R. The Active Site of Methanol Synthesis over Cu/ZnO/Al₂O₃ Industrial Catalysts. *Science* **2012**, *336*, 893-897.
- (283) Balaraman, E.; Ben-David, Y.; Milstein, D. Unprecedented Catalytic Hydrogenation of Urea Derivatives to Amines and Methanol. *Angew. Chem. Int. Ed.* **2011**, *50*, 11702-11705.

- (284) Yang, X. Metal Hydride and Ligand Proton Transfer Mechanism for the Hydrogenation of Dimethyl Carbonate to Methanol Catalyzed by a Pincer Ruthenium Complex. *ACS Catal.* **2012**, *2*, 964-970.
- (285) Han, Z.; Rong, L.; Wu, J.; Zhang, L.; Wang, Z.; Ding, K. Catalytic Hydrogenation of Cyclic Carbonates: A Practical Approach from CO₂ and Epoxides to Methanol and Diols. *Angew. Chem. Int. Ed.* **2012**, *51*, 13041-13045.
- (286) Miller, A. J. M.; Heinekey, D. M.; Mayer, J. M.; Goldberg, K. I. Catalytic Disproportionation of Formic Acid to Generate Methanol. *Angew. Chem. Int. Ed.* **2013**, *52*, 3981-3984.
- (287) Savourey, S.; Lefevre, G.; Berthet, J.-C.; Thuery, P.; Genre, C.; Cantat, T. Efficient Disproportionation of Formic Acid to Methanol Using Molecular Ruthenium Catalysts. *Angew. Chem. Int. Ed.* **2014**, *53*, 10466-10470.
- (288) Huff, C. A.; Sanford, M. S. Cascade Catalysis for the Homogeneous Hydrogenation of CO₂ to Methanol. *J. Am. Chem. Soc.* **2011**, *133*, 18122-18125.
- (289) Krocher, O.; Koppel, R.; Baiker, A. Highly active ruthenium complexes with bidentate phosphine ligands for the solvent-free catalytic synthesis of N,N-dimethylformamide and methyl formate. *Chemical Communications* **1997**, 453-454.
- (290) Wesselbaum, S.; Moha, V.; Meuresch, M.; Brosinski, S.; Thenert, K. M.; Kothe, J.; Stein, T. v.; Englert, U.; Holscher, M.; Klankermayer, J.; Leitner, W. Hydrogenation of carbon dioxide to methanol using a homogeneous ruthenium-triphos catalyst: from mechanistic investigations to multiphase catalysis. *Chem. Sci.* **2015**, *6*, 693-704.

TOC Graphic

